UNCLASSIFIED

MARTIN MARIETTA ENERGY SYSTEMS LIBRARIES
3 4456 0360844 2

ORNL 952
Series A
PHYSICS
8A

SHORT-LIVED ISOMERIC STATES OF NUCLEI

FRANCIS K. MCGOWEN

OAK RIDGE NATIONAL LABORATORY
CENTRAL RESEARCH LIBRARY
DOCUMENT COLLECTION
LIBRARY LOAN COPY
DO NOT TRANSFER TO ANOTHER PERSON
If you wish someone else to see this document, send in name with document and the library will arrange a loan.
UCN-7969
(3 3-67)

OAK RIDGE NATIONAL LABORATORY
OPERATED BY
CARBIDE AND CARBON CHEMICALS DIVISION
UNION CARBIDE AND CARBON CORPORATION
UCC
POST OFFICE BOX P
OAK RIDGE, TENNESSEE

UNCLASSIFIED

UNCLASSIFIED

ORNL-952

Physics
This document consists of
134 pages.
Copy 8 of 210 Series A

Contract No. W-7405, eng. 26

Physics Division

SHORT-LIVED ISOMERIC STATES OF NUCLEI*

by

Francis K. McGowan

Date Issued:

MAR 13 1951

OAK RIDGE NATIONAL LABORATORY
operated by
CARBIDE AND CARBON CHEMICALS DIVISION
Union Carbide and Carbon Corporation
Post Office Box P
Oak Ridge, Tennessee

*Submitted in partial fulfillment of the requirements for the degree of Doctor of Philosophy at the University of Tennessee.

UNCLASSIFIED

MARTIN MARIETTA ENERGY SYSTEMS LIBRARIES
3 4456 0360844 2

ORNL-952
Physics

INTERNAL DISTRIBUTION

1. G. T. Felbeck (C&CCD)
2-3. Chemistry Library
4. Physics Library
5. Biology Library
6. Health Physics Library
7. Metallurgy Library
8-9. Training School Library
10-13. Central Files
14. C. E. Center
15. C. E. Larson
16. W. B. Humes (K-25)
17. W. D. Lavers (Y-12)
18. A. M. Weinberg
19. J. A. Swartout
20. E. D. Shipley
21. E. J. Murphy
22. F. C. VonderLage
23. A. H. Snell
24. E. H. Taylor
25. A. Hollaender
26. K. Z. Morgan
27. F. L. Steahly
28. M. T. Kelley
29. W. H. Pennington
30. E. O. Wollan
31. D. W. Cardwell
32. A. S. Householder
33. L. D. Roberts
34. J. A. Lane
35. M. M. Mann
36. R. N. Lyon
37. W. C. Koehler
38. W. K. Ergen
39. E. P. Blizard
40. M. E. Rose
41. F. K. McGowan
42. M. J. Skinner
43-44. Central Files (O.P.)

EXTERNAL DISTRIBUTION

45-56. Argonne National Laboratory
57. Armed Forces Special Weapons Project
58-63. Atomic Energy Commission, Washington
64. Battelle Memorial Institute
65. Brush Beryllium Company
66-69. Brookhaven National Laboratory
70. Bureau of Medicine and Surgery
71. Bureau of Ships
72-75. Carbide and Carbon Chemicals Division (K-25 Plant)
76. Columbia University (J. R. Dunning)
77. Columbia University (G. Failla)
78-82. E. I. du Pont de Nemours and Company
83-86. General Electric, Richland
87-90. Idaho Operations Office
91-92. Iowa State College
93. Kansas City Operations Branch
94. Kellex Corporation
95-96. Kirtland Air Force Base
97-100. Knolls Atomic Power Laboratory
101-103. Los Alamos Scientific Laboratory
104. Mallinckrodt Chemical Works
105. Massachusetts Institute of Technology (A. Gaudin)
106. Massachusetts Institute of Technology (A. R. Kaufmann)
107-109. Mound Laboratory
110. National Advisory Committee for Aeronautics
111. National Bureau of Standards (R. D. Huntoon)
112. Naval Medical Research Institute
113-114. Naval Radiological Defense Laboratory
115. New Brunswick Laboratory

116-118. New York Operations Office
119. North American Aviation, Inc.
120-123. Carbide and Carbon Chemicals Division (Y-12)
124. Patent Branch, Washington
125. RAND Corporation
126. Sandia Corporation
127. Santa Fe Operations Office
128-142. Technical Information Service, Oak Ridge
143-145. USAF, NEPA Office
146-147. U. S. Geological Survey (T. B. Nolan)
148-149. U. S. Public Health Service
150. University of California at Los Angeles
151-155. University of California Radiation Laboratory
156-157. University of Rochester
158. University of Washington
159. Savannah River Operations Office (Wilmington)
160. Western Reserve University
161-164. Westinghouse Electric Corporation
165. Yale University
166-169. Atomic Energy Project, Chalk River
170. Chief of Naval Research
171. H. K. Ferguson Company
172. Harshaw Chemical Company
173. Isotopes Division (Mr. McCormick)
174-175. Library of Congress, Acquisition Department (J. W. Cormn)
176. National Bureau of Standards
177. National Research Council, Ottawa
178. Naval Research Laboratory
179-180. Nevis Cyclotron Laboratories
181. Nucleonics
182-183. Oak Ridge Institute of Nuclear Studies
184-193. United Kingdom Scientific Mission (M. Greenhill)
194. USAF, Eglin Air Force Base (Technical Library)
195. USAF, Wright-Patterson Air Force Base (Rodney Nudenberg)
196-200. USAF, Wright-Patterson Air Force Base (CADO)
201. U. S. Army, Army Field Forces (Captain James Kerr)
202. U. S. Army, Atomic Energy Branch (Lt. Col. A. W. Betts)
203. U. S. Army, Director of Operations Research (Dr. Ellis Johnson)
204. U. S. Army, Office, Chief of Ordnance (Col. A. R. Del Campo)
205-206. U. S. Army, Office of the Chief Signal Officer (Curtis T. Clayton thru Major George C. Hunt)
207-209. U. S. Army, Technical Command (Col. J. H. Rothschild Attn: Technical Library)
210. UT-AEC Agricultural Research Program (Charles S. Hobbs)

UNCLASSIFIED

ACKNOWLEDGMENTS

The author wishes to express his gratitude to Professor S. De Benedetti, now at the Carnegie Institute of Technology, who directed the initial search for short-lived isomers of nuclei performed at Oak Ridge National Laboratory and later gave advice and encouragement as a consultant to the research problem.

It is a pleasure for the author to acknowledge his appreciation to Mr. P. R. Bell and Dr. W. H. Jordan for constant advice on the development of the apparatus and for numerous stimulating discussions concerning the results. In particular, their development of the scintillation detector and scintillation spectrometer for measuring beta- and gamma-ray spectra has made it possible to extend the method of delayed coincidences to measure half-lives in the millimicrosecond region.

I am indebted to Mr. J. E. Francis, Jr., for assisting in the construction and the testing of the apparatus during the initial stages of development and to members of the Chemistry Division of Oak Ridge National Laboratory for supplying many pure samples of the rare earth elements.

Finally, I wish to thank Drs. M. E. Rose, A. H. Snell and E. O. Wollan for their interest and support of this problem.

TABLE OF CONTENTS

CHAPTER		PAGE
I.	INTRODUCTION	1
	Review of Previous Investigations	1
	Statement of the Problem	3
II.	ISOMERISM	5
	Classical Theory of Radiation	5
	Quantum Mechanical Aspects of a Radiating System	9
	Internal Conversion as a Competing Process	11
III.	APPARATUS	16
	Description of Scintillation Detectors	16
	Self-Delayed Coincidence Circuit	19
	Delayed Coincidence Apparatus 10^{-6} to 10^{-7} Sec.	21
	Delayed Coincidence Apparatus $\lesssim 10^{-8}$ Sec.	24
	Delayed Coincidence Scintillation Spectrometer	26
IV.	DISCUSSION OF THE METHOD	31
V.	NEGATIVE RESULTS	37
VI.	POSITIVE RESULTS	51
	$_{71}Lu^{177*}$ (1.3×10^{-7} sec.)	51
	Au^{197*} (7×10^{-9} sec.)	56
	$_{77}Ir^{191*}$ (5.7×10^{-9} sec.)	64
	Cd^{111*} (8×10^{-8} sec.)	74
	Ta^{181*} (10^{-8} sec. and 2.2×10^{-5} sec.)	80
	$_{32}Ge^{72*}$ (2.9×10^{-7} sec.)	90
	Re^{187*} (5.5×10^{-7} sec.)	91

CHAPTER PAGE

VI. (continued)

Tm^{169*} (7.0×10^{-7} sec.) 94

Hg^{198*}? 98

VII. DISCUSSION OF RESULTS 103

Comparison of Experimental Lifetimes with the Predicted Estimates 103

Prevalence of Short-Lived Isomers in Odd Mass Nuclei with Z Odd 109

Correlation of Negative Results with Nuclear Shell Structure 114

VIII. CONCLUSIONS 117

BIBLIOGRAPHY 120

LIST OF TABLES

TABLE		PAGE
I.	Lowest Allowed Transitions for Given Spin and Parity Changes	12
II.	Nuclei Investigated for Short-Lived Isomers	38
III.	Nuclei Investigated for Short-Lived Isomers	40
IV.	Experimental Conditions for 10^{-6} to 10^{-3} Sec. Range	41
V.	Data for the Short-Lived Isomers	104
VI.	Isomers for $(Z \text{ or } N)_{odd} = 63$ to 81	111

LIST OF FIGURES

FIGURE PAGE

1. Geometrical Arrangement of the Detectors 16
2. Block Diagram of the Self-Delayed Coincidence Apparatus . . 20
3. Circuit Diagram of the 10^{-6} to 10^{-3} Sec. Delayed Coincidence Apparatus 22
4. Block Diagram of the Delayed Coincidence Apparatus 23
5. Circuit Diagram of the 10^{-7} to 10^{-6} Sec. Delayed Coincidence Apparatus 25
6. Circuit Diagram of the Delayed Coincidence Scintillation Spectrometer 27
7. Delayed Coincidence Scintillation Spectrometer 29
8. Number of Coincidences as a Function of Delay Time from Au^{198} 43
9. Number of Coincidences as a Function of Delay Time from Hg^{203} 44
10. Decay of Lu^{177*} 52
11. Calibration of Pulse Height Dial in Energy Units 54
12. Spectrum of Lu^{177*} 55
13. Decay of Au^{197*} 57
14. Spectrum of $Hg^{197} \longrightarrow Au^{197}$ 59
15. Spectrum of Preceding Radiation for Au^{197*} 61
16. Spectrum of Au^{197*} 62
17. Decay of Ir^{191*} 66
18. Spectrum of Ir^{191*} 67

FIGURE PAGE

19. β-Spectrum of Os^{191} 69

20. Fermi-Kurie Plot of Os^{191} β-Spectrum 70

21. Decay of Cd^{111**} 75

22. Cd^{111*} Spectrum 77

23. Cd^{111} Decay Scheme 78

24. Level Schemes for Ta^{181} 82

25. Spectrum of Ta^{181*} (22 μsec.) 84

26. Radiation Preceding Ta^{181*} (10^{-8} Sec.). 85

27. Spectrum of Ta^{181*} (10^{-8} Sec.) below 150 kev 86

28. Spectrum of Ta^{181*} above 100 kev 88

29. Spectrum of Re^{187*} (5.5×10^{-7} Sec.). 93

30. Spectrum of the Radiation Preceding Tm^{169*}. 96

31. Spectrum of Tm^{169*}. 97

32. Disintegration Scheme for Tm^{169} 99

33. Resolution Curve of β-γ Coincidences from Au^{198} 101

34. Values of Log τ_γ as a Function of Log W 105

35. Values of Log ($\tau_\gamma \rho^{2\ell}$) as a Function of Log W 107

CHAPTER I

INTRODUCTION

A nuclear isomeric state may be defined as an excited state of a nucleus which exists for a measurable length of time ($\tau_\gamma \geqslant 10^{-10}$ sec.). Generally excited states of nuclei decay with a half-life too short to be directly measurable. However, there exist numerous examples (~ 60) of metastable states that decay to another state in the same nucleus with a half-life long enough to be measured with the stop watch.[1,2] These transitions have been classified on the basis of forbiddenness $\ell = 4$ and 5,[3] and they correspond to a change of angular momentum of 3, 4, or 5 units of $\hbar$ depending on the electric and magnetic character of the radiation emitted. It is therefore reasonable to assume that a number of metastable states of intermediate but directly measurable half-life (short-lived isomers) should exist for transitions corresponding to forbiddenness $\ell = 2$ and 3.

Review of Previous Investigations

Prior to 1949 investigations for the existence of short-lived isomers yielded five cases. Using the method of delayed coincidences

---

[1] W. Bothe and W. Gentner, Naturwiss 25, 284 (1937).

[2] Emilio Segrè and A. C. Helmholz, Rev. Mod. Phys. 21, 271 (1949).

[3] P. Axel and S. M. Dancoff, Phys. Rev. 76, 892 (1949).

between two Geiger counters, DeBenedetti and McGowan[4] performed a systematic search for the occurrence of nuclear excited states decaying with half-lives between 10^{-6} and 10^{-3} sec. A short-lived isomer is detected by the measurement of the time lapsed between β-decay and γ - (or internal conversion electron) emission. Out of 60 nuclei investigated, four short-lived isomeric states were found. These were Ta^{181*} (22 μsec.), Re^{187*} (0.65 μsec.), Tm^{169*} (1 μsec.), and Tm^{171*} (2.5 μsec.). Bowe et al.[5] observed an isomeric state in Ge^{72} (0.5 μsec.) by the same method.

From these results one cannot escape the impression that low energy transitions from 25 to 500 kev, involving changes of angular momentum of 2 or 3 units of $\hbar$, occur less frequently than changes of 4 or 5 units of $\hbar$. One must keep in mind, however, that the method used in the previous investigations cannot be expected to detect all the isomeric states of the nuclei studied. The requirements for a positive result were that the metastable state must be reached as a product of β-disintegration and the radiation resulting from the decay of the isomeric state must be strongly internally converted. The electric multipole internal conversion coefficient for the K shell increases approximately as $Z^3 (2\ mc^2/E)^{\ell+5/2}$ for $Z < 40$ and $E \ll mc^2$. Therefore the method of delayed coincidences between two Geiger counters is most sensitive for low energy and high multipole order transitions in nuclei of high atomic number. For the detection of high energy isomeric transitions in nuclei

---

[4] S. DeBenedetti and F. K. McGowan, Phys. Rev. 74, 728 (1948).

[5] J. C. Bowe, M. Goldhaber, R. D. Hill, W. E. Meyerhof, and O. Sala, Phys. Rev. 73, 1219 (1948).

of low atomic number, it would be advantageous to measure β-γ delayed coincidences. The scintillation detector, which is a method of detecting ionizing radiations by photoelectric measurement of the fluorescent light quanta emitted by certain organic and inorganic phosphors, is particularly suitable because of its high efficiency for the detection of γ-rays.

Finally, the efficiency of detection of delayed radiation from the decay of metastable states was not constant over the whole time range explored but increased for shorter periods. Although this disadvantage is inherent in the method of delayed coincidences, Geiger counters involve the disadvantage of the variation of the time lag between ionization and discharge which prevented measurement of time intervals less than one microsecond. Scintillation detectors, which have a time lag spread $\lesssim 10^{-8}$ sec., are therefore suitable for measurement of shorter time intervals.

Statement of the Problem

This paper summarizes the extension of the method of delayed coincidences between scintillation detectors to measure shorter time intervals and the systematic search for the occurrence of nuclear excited states decaying with half-lives between 5×10^{-9} and 10^{-4} sec.

During the course of the survey a delayed coincidence scintillation spectrometer was developed. This instrument has increased the sensitivity of the method and has permitted a measure of the energy and type of radiation announcing the formation of an isomeric state, the

energy of the radiation following the decay of a metastable state, the ratio of K shell internal conversion to L shell internal conversion of γ-rays, and the position of the isomeric state in the disintegration scheme.

CHAPTER II

ISOMERISM

In order to facilitate the discussion of results in Chapter VII, a semiquantitative theory for the decay of isomeric states will be reviewed in this chapter. Most of the material is taken from a series of lectures on nuclear isomerism presented by Professor Dancoff[1] at the Clinton National Laboratories Training School during 1947.

Classical Theory of Radiation

Since most nuclear excited states decay with half-lives $\tau < 10^{-10}$ sec., isomeric states must be characterized by having only highly forbidden transitions. Weizsacker[2] first explained this forbiddenness by postulating that each transition had a large angular momentum change associated with it. Therefore, only quanta of high multipole order could be emitted. At the present it is impossible to calculate quantum mechanically the life-time of isomeric states due to the lack of knowledge of the nuclear wave functions. One proceeds in a relatively crude manner using classical theory of radiation from a set of moving charges or currents.

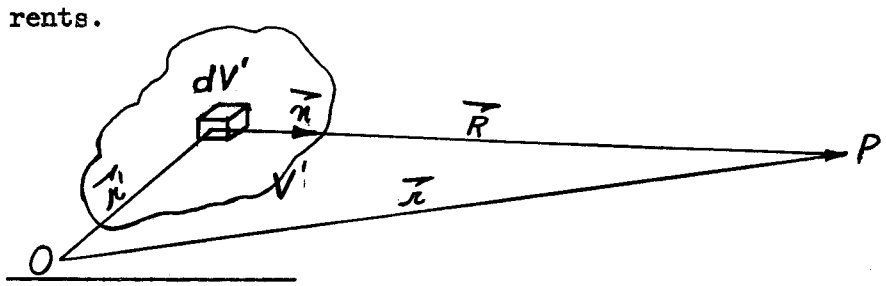

[1] M. E. Rose, Theoretical Nuclear Physics Lecture Notes, 148 (1947).

[2] C. F. von Weizsacker, Naturwiss. 24, 813 (1936).

In the general case the rate of radiation[3] $R(\vec{r})d\Omega$ is given by

$$R(\vec{r})d\Omega = |\vec{S}| \; r^2 \, d\Omega \; , \tag{1}$$

where $\vec{S}$ is the Poynting vector

$$|\vec{S}| = \frac{c}{4\pi} \; |\vec{E} \times \vec{H}| \tag{2}$$

and in vacuo

$$|\vec{S}| = \frac{c}{4\pi} \; |\vec{H}|^2 .$$

But $\vec{H}$ is given by the general electrodynamic vector potential

$$\vec{H} = \vec{\nabla}_r \times \vec{A}(\vec{r},t),$$

where

$$\vec{A}(\vec{r},t) = \frac{1}{c} \int_{V'} \frac{\vec{j}(\vec{r}',t - R/c)}{R} \, dV' . \tag{3}$$

For the wave zone approximation $|\vec{r}| \gg |\vec{r}'|$ and for monochromatic radiation $\vec{j} = \vec{j}_o(\vec{r}') \; e^{i\omega(t - R/c)}$, one has

$$\vec{\nabla}_R \times \vec{A}(\vec{r},t) = - \frac{i\omega}{c^2} \; e^{i\omega t} \int_{V'} \frac{e^{-i\omega R/c}}{R} \; \vec{n} \times \vec{j}_o(\vec{r}') \, dV' .$$

Using the wave zone approximation again to replace R by r in the denominator but not in the exponential because λ is not necessarily large compared to the linear dimensions of V', one has

---

[3] Julius Adams Stratton, Electromagnetic Theory (New York and London: McGraw-Hill Book Company, 1941), p. 424.

$$\vec{\nabla}_R \times \vec{A}(\vec{r},t) = -\frac{i\omega}{c^2}\,\frac{e}{r}\,e^{i\omega(t-\frac{\vec{n}\cdot\vec{r}}{c})}\int_{V'} \vec{n}\times\vec{j}_o(\vec{r}\,')\,e^{i\frac{\omega\vec{n}\cdot\vec{r}\,'}{c}}\,dV'.$$

The average power radiated per unit solid angle is

$$R_{av}(\vec{r}\,')d\Omega = \frac{\omega^2}{8\pi c^3}\,d\Omega\left|\int_{V'} \vec{n}\times\vec{j}_o(\vec{r}\,')\,e^{\frac{i\omega\vec{n}\cdot\vec{r}\,'}{c}}\,dV'\right|^2, \quad (4)$$

where $\vec{n}$ is the unit vector in the direction of propagation and $\vec{j}_o(\vec{r}\,')$ is the time independent part of the current density. Equation (4) is an exact classical formula for the rate of radiation from a system in which all charges and currents are contained within a volume element V' and holds at distances from the volume V' large compared with the linear dimensions of V' (wave zone approximation).

The factor $e^{i\frac{\omega\vec{n}\cdot\vec{r}\,'}{c}}$ arises from the finite velocity of light and corresponds to the phase difference of the radiation from various points of the radiating system, arriving simultaneously at the point of observation. This effect is the retardation and may be neglected for systems with $\frac{\omega r'}{c} \ll 1$. In the more general case an expansion of the retardation term yields

$$e^{i\frac{\omega\vec{n}\cdot\vec{r}\,'}{c}} = 1 + \frac{i\omega\,\vec{n}\;\vec{r}\,'}{c} + \cdots + \left(\frac{i\omega}{c}\,\vec{n}\cdot\vec{r}\,'\right)^{\ell-1}\frac{1}{(\ell-1)!}$$

The first term corresponds to electric dipole radiation, the second to magnetic dipole and electric quadrupole radiation, and so forth. Thus,

the integral in equation (4) may be broken into a sum of terms using the expansion of the retardation. The total rate of radiation, R_{av}, is given by

$$R_{av} = (R_{E_1}) + (R_{M_1} + R_{E_2}) + (R_{M_2} + R_{E_3}) + \cdots , \qquad (5)$$

where R_{E_i} is the rate of electric 2^i-pole radiation and R_{M_i} is the rate of magnetic 2^i-pole radiation. The individual contributions which are of the same order of magnitude are bracketed into terms. Successive terms decrease rapidly if the dimension of the oscillator is small compared to the radiated wave length. The first contributing term essentially determines the total probability of radiation and a high forbiddenness corresponds to the vanishing of all lower terms. It is convenient to designate this forbiddenness by ℓ, the number of the first contributing term. A given ℓ value corresponds to either electric 2^{ℓ}- or magnetic $2^{\ell-1}$-pole radiation.

On using higher terms of the expansion of the retardation, one may obtain a rough estimate of the rate of radiation corresponding to the $\ell^{\underline{th}}$ term, assuming that for some reason the radiation from all lower terms in the expansion vanishes. The mean life of the state for γ-ray emission only is

$$\tau_\gamma \sim \frac{\hbar\omega}{\int R_{av}\, d\Omega} \sim \frac{3(\ell!)^2}{\rho^{2\ell}} \left(\frac{137}{W}\right)^{2\ell+1} \frac{\hbar}{mc^2} , \qquad (6)$$

where ρ = radius of the nucleus in units of e^2/mc^2 and $W = E_\gamma/mc^2$. The derivation of this relation involves a very crude approximation replacing lengths that enter the nuclear matrix element by the nuclear

radius. Other models[4-6] yield formulas agreeing as to the dependence of τ_γ on ρ and W but differing as to numerical factors of the same order of magnitude.

In order to explain long lived isomeric states all terms below $\ell = 4$ must vanish. Classically there is no mechanism to explain the vanishing of the lower terms in the expansion. However, from quantum mechanical aspects of a radiating system selection rules are obtained from the conservation of angular momentum and the parity of the wave functions.

Quantum Mechanical Aspects of a Radiating System

In general the electric or magnetic 2^L-pole radiation[7] behaves as if it has an angular momentum $L\hbar$. Also, the total angular momenta of the initial and final states are constants of the motion. From the principle of conservation of angular momentum selection rules for the emission of radiation of a definite multipole order are obtained. In order for a multipole of the order 2^L to be emitted in a transition from an initial state of angular momentum J_i to a final state of angular momentum J_f, the vector relation must hold

$$\overline{J_i} = \overline{J_f} + \overline{L}.$$

---

[4] H. A. Bethe, Rev. Mod. Phys. 9, 226 (1937).

[5] I. S. Lowen, Phys. Rev. 59, 835 (1941).

[6] M. Fierz, Helv. Phys. Acta 16, 365 (1943).

[7] W. Heitler, Proc. Camb. Phil. Soc. 32, 112 (1936).

This is equivalent to the scalar relation

$$\left| J_f - J_i \right| \leq L \leq J_f + J_i . \tag{7}$$

If no other selection rule exists, the most probable transition will correspond to the emission of electric 2^L-pole radiation, where $L = \Delta J$ has the lowest value permitted by equation (7). The magnetic radiation of the same multipole order is less probable, its probability being about the same as that of electric radiation of the next higher multipole.

The selection rule to be deduced from the behavior of the wave functions and the radiation term under an inversion of coordinates in the center of mass does not allow all the transitions that would occur in equation (7). Nuclear wave functions have the property with the origin of coordinates at the center of gravity of the nucleus

$$\psi(-\vec{r}_1, -\vec{r}_2, \cdots) = \pm \quad \psi(\vec{r}_1, \vec{r}_2, \cdots),$$

where the upper sign is said to correspond to even parity and the lower sign to odd parity. The matrix element occurring in the transition probability for electric dipole radiation is

$$\int_{\substack{\text{over all}\\ \text{space}}} \psi_i^* \sum_j e \, \vec{r}_j \, \psi_f \, d\tau$$

Since $\vec{r}_j$ is of odd parity, the product $\psi_i^* \sum_j \vec{r}_j \psi_f$ must be of even parity in order to have electric dipole radiation, which means that the parity of ψ_i^* must differ from that of ψ_f (i.e. must be a parity

change). On the other hand, since $\overline{r'} \times \overline{j_o}(\overline{r'})$ is an axial vector and is of even parity, magnetic dipole radiation is allowed if no parity change or ψ_i^* and ψ_f have the same parity. Likewise electric quadrupole radiation is allowed for no parity change.

Making use of the more general relation that electric 2^L-pole radiation has parity $(-1)^L$ and magnetic 2^L-pole radiation has parity $(-1)^{L+1}$, the following table of the lowest allowed transitions for given angular momentum and parity changes may be constructed. For case (A) the transition is termed parity allowed and the radiation is essentially electric in character. On the other hand, for case (B) the transition is termed parity forbidden and the radiation is a mixture with the relative amounts of electric and magnetic character unpredictable.

Internal Conversion as a Competing Process

There is another competing process which permits the nucleus to go from an excited state to a lower state with the simultaneous ejection of one of the orbital atomic electrons. This is known as internal conversion. The observed lifetime will be less than the estimated lifetime for γ-ray emission. The internal conversion coefficient is defined as $N_e/N_\gamma = \tau_\gamma/\tau_e$, where N_e is the number of electrons observed in unit time and N_γ the number of γ-rays observed in the same time. The observed lifetime is related to lifetime τ_γ by

$$\frac{1}{\tau_{exp}} = \frac{1}{\tau_\gamma} + \frac{1}{\tau_e}$$

TABLE I

LOWEST ALLOWED TRANSITIONS FOR GIVEN SPIN AND PARITY CHANGES

	Parity Change	Lowest Allowed Transitions	Forbiddenness
(A)	$(-1)^{\Delta J}$	el $2^{\Delta J}$	$\ell = \Delta J$
(B)	$(-1)^{\Delta J+1}$	el $2^{\Delta J+1}$ and mag $2^{\Delta J}$	$\ell = \Delta J+1$

or

$$\frac{1}{\tau_{exp}} = \frac{1}{\tau_\gamma} \left(1 + \frac{N_e}{N_\gamma}\right) = \frac{1}{\tau_\gamma} (1 + \alpha), \tag{8}$$

where α is the total internal conversion coefficient. If α is known, τ_γ may be determined from the experimental lifetime by equation (8) in order to compare theory and experiment.

Simple Transition Scheme That Indicates the Existence of an Isomeric State

To detect a short-lived isomeric state let us consider a simple transition scheme as follows:

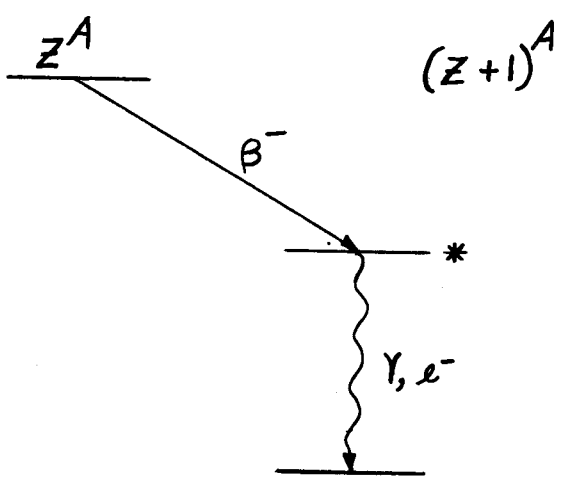

The metastable state marked with an asterisk must be reached as a product of a radioactive disintegration. Assuming now that the excited state is metastable, there will be a time interval between the rays of the radioactive disintegration and the radiation emitted by the decay of the

metastable state. The β- and γ-rays will not be, as usual, coincident, but will give two signals in a detector shifted in time, one corresponding to the formation of the metastable state and the other to its decay. Experimentally the problem is to measure this time interval. For this purpose the method of delayed coincidences is used.

CHAPTER III

APPARATUS

Description of Scintillation Detectors

For the detection of the radiations scintillation counters were used. This detector presents the advantages of a high sensitivity for the detection of gamma radiation, a very short resolving time, and a measure of the energy of the radiation being detected.

The general geometrical arrangement of the detectors is shown in Fig. 1. In traversing the phosphor, the particle radiation to be detected loses its energy in exciting and ionizing the molecules of the crystal. These molecules then radiate energy in the form of light. In the case of gamma radiation traversing the phosphor, there will be Compton recoil electrons (low Z phosphor) which excite and ionize the molecules. Some of the light is collected on the photocathode of the multiplier tube. The multiplier tube consists of a photocathode on the inside surface of the glass envelope which converts a fraction ($\sim 10\%$) of the photons falling on it into photoelectrons. The elements of the type 1P21 multiplier are a series of ten dynodes, each at a higher potential than the preceding one. The electrons which strike each dynode produce many more electrons by secondary electron emission. The performance of the photomultiplier has been studied in considerable detail by Morton and Mitchell.[1] At an accelerating potential of approximately 100 volts

---

[1] G. A. Morton and J. A. Mitchell, Nucleonics 4, 16 (1949).

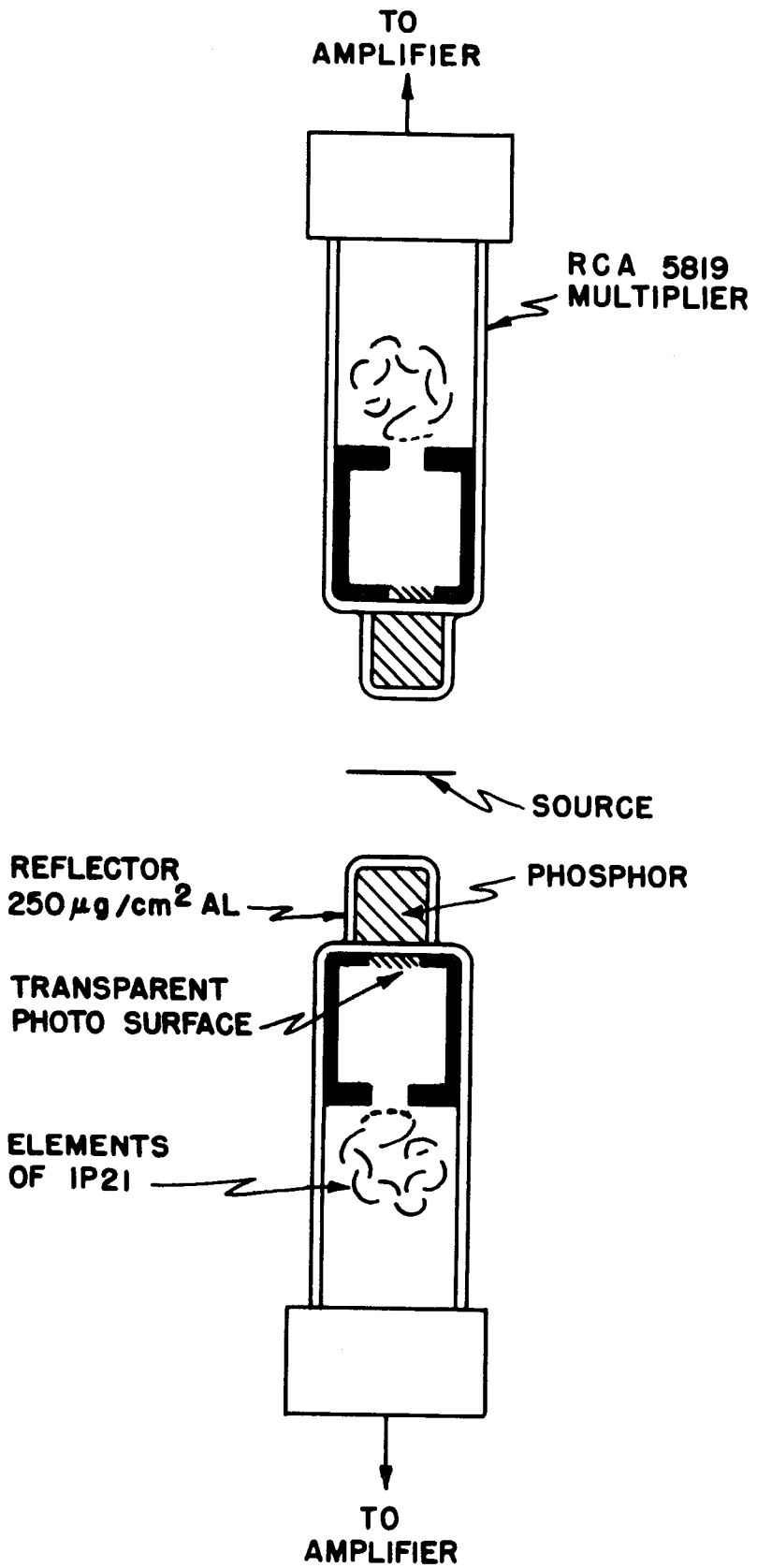

FIG. 1
GEOMETRICAL ARRANGEMENT OF THE DETECTORS

per stage, the gain of the tube is of the order 10^6. Actually the number of secondary electrons produced at each dynode will vary in a statistical manner, so that pulses obtained from a given number of photoelectrons are not all the same height. Morton's results indicate that the spread in pulse height is chiefly in the original number of photoelectrons produced. For this reason it is desirable to collect as much light as possible from the phosphor. The phosphor in the form of a crystal is cemented to the tube envelope with Canada balsam. This improves the optical path at the crystal-glass interface (i.e. makes the critical angle large in order that most of the light escapes from the phosphor on the first try). In addition the aluminum leaf reflector surrounding the crystal increases the light collection efficiency.

Anthracene and trans-stilbene have been used for the scintillating phosphor. The resolving time of the detector depends upon the time required for the light to be emitted by the phosphor, the energy of the radiation being detected, and the electron transit time spread in the multiplier. For this reason trans-stilbene is superior to anthracene for good coincidence resolution. The radiation lifetimes[2] of stilbene and anthracene are 8×10^{-9} sec. and 3.5×10^{-8} sec. respectively at room temperature. With regard to energy resolution anthracene is superior. The pulse height, which is essentially equivalent to the light energy emitted for a given ionizing event in the stilbene, is about 60% that obtained from anthracene. Morton has reported calculations and measurements of the transit time spread or rise time spread of about 5×10^{-9} sec. for

---

[2] G. G. Kelley, ORNL 366 (June, 1949).

the type 5819 tube under normal operating conditions ($\sim$ 100 volts per stage). For the moment the phosphors and photomultiplier tube have not limited the resolving time obtainable. Actually the limitation for coincidence resolution has been due to the amplifiers and other electronic circuits that follow the photomultiplier tubes.

Two different counter sets were used during the experiments. The first detector set used type 1P21 multiplier tubes. With this tube the problem of light collection is particularly difficult. The small photocathode being some distance from the glass envelope presents a relatively small solid angle at the phosphor compared to the type 5819 tube. In many experiments it was desirable to detect particle radiation below 100 kev and still have the noise background count low. This noise background in the multiplier is due to thermionic electrons emitted from photocathode and dynodes. In order to circumvent this difficulty the tubes were operated at dry-ice temperature. At a discrimination level of 75 kev the noise background from a good multiplier tube was about one count per second. When the type 5819 multiplier became available, a second counter set using these tubes was employed during the latter half of the survey. Because of the increased efficiency in light collection, this detector set is operated at room temperature with essentially the same noise background counting rate. However, radiation as low as 25 kev energy may be detected with the second set when anthracene is used.

Self-Delayed Coincidence Circuit

In general, if the detector or electronic circuits preceding the coincidence stage have a dead time, it is necessary to use two detectors, one for the detection of the radiation announcing the formation of the metastable state, the other for the detection of the delayed radiation. Since the dead time of the scintillation detector is very short, a single detector in principle should be sufficient for the method of delayed coincidences. It is possible to measure time intervals between two ionizing events by studying the distribution of pulses from a single detector provided the dead time of the detector is smaller than the interval to be measured.[3] Fig. 2 is a block diagram of the self-delayed coincidence apparatus. The method consists in recording the coincidences between the signals from two separate channels, both activated by the same detector pulse, but designed so that one channel produces an immediate signal of duration τ_1 and the other channel gives a signal of delay T and duration τ_2. Provided $T > 2\tau_1$, a count is recorded for detector pulses whose interval in time is between $T - \tau_1$ and $T + \tau_2$. Since multivibrators were used for delaying and shaping the signal in τ_2 channel, a gating signal from $T + \tau_2$ channel is necessary to render the channel insensitive during the "on time" of the circuit for recording a delayed coincidence count. The method of self-delayed coincidences has the advantage of requiring only one amplifier. With this arrangement the half-life of Ta^{181*} was measured in good agreement with previous

---

[3] S. DeBenedetti, F. K. McGowan, J. E. Francis, Phys. Rev. 73, 1404 (1948).

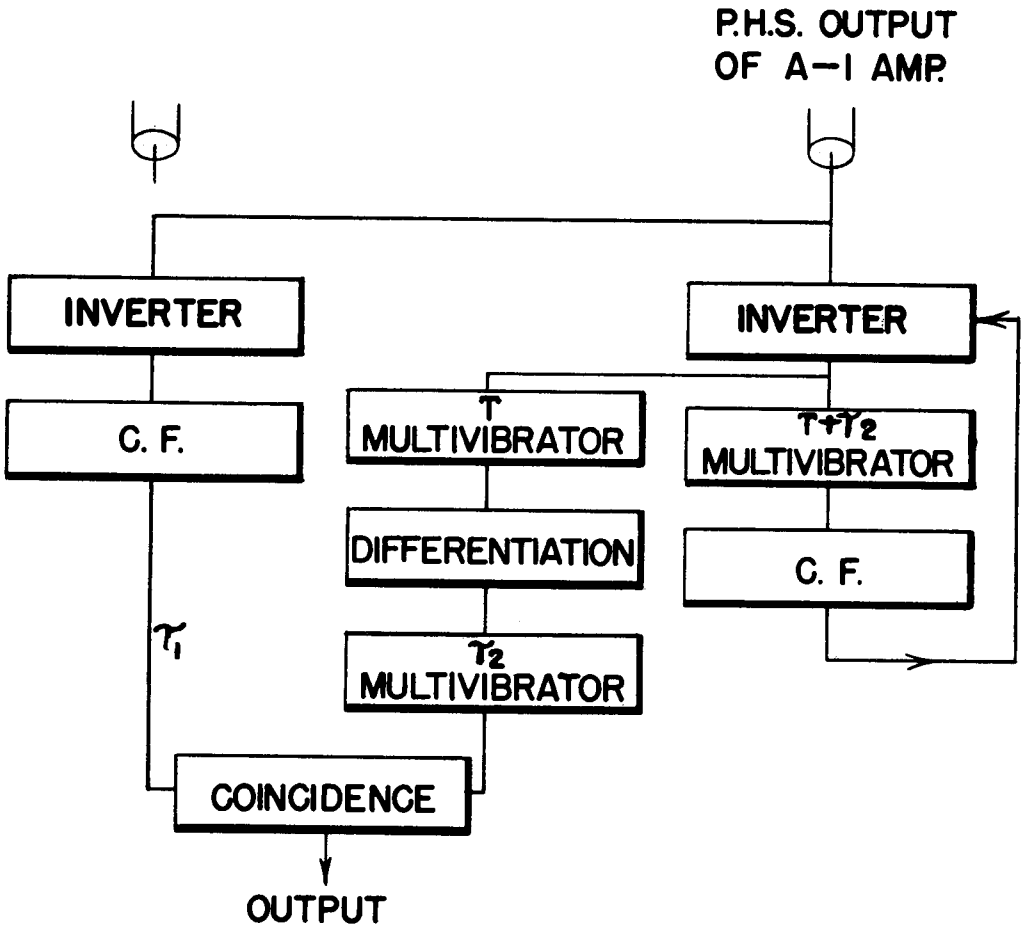

FIG. 2

BLOCK DIAGRAM OF THE SELF-DELAYED COINCIDENCE APPARATUS

measurements. In practice the method of self-delayed coincidences was limited to the measurement of time intervals $\geqslant 10^{-6}$ sec. with the linear amplifiers available. A circuit diagram of the self-delayed coincidence apparatus is shown in Fig. 3.

Delayed Coincidence Apparatus 10^{-6} to 10^{-7} Sec.

For the measurement of shorter time intervals it is easier to use two detectors rather than attempt to design an amplifier with a very short resolution time and no dead time when overloaded. In effect, the next step in instrumentation extended the method of delayed coincidences to measure time intervals in the region 10^{-6} to 10^{-7} sec. using the general purpose linear amplifier Model A-1.[4] Fig. 4 is a generalized block diagram of the apparatus. The pulses from two 1P21 or 5819 photomultipliers are supplied to linear amplifiers whose output signal has a rise time of approximately 1.5×10^{-7} sec. The output of a pulse height selector operating on this signal has a variation of delay from the original signal of about this amount. The delay is variable depending upon the amplitude of the original signal from the amplifier. This introduces an error in the measurement of time intervals $< 10^{-6}$ sec. In order to circumvent this variable delay the pulse height selectors were modified with additional circuits which minimize the variation in delay.[5] The maximum variation in delay was measured using pulses of different

---

[4] W. H. Jordan and P. R. Bell, Rev. Sci. Inst. 18, 703 (1947).

[5] P. R. Bell, S. DeBenedetti, J. E. Francis, Jr., Phys. Rev. 72, 160 (1947).

UNCLASSIFIED
DWG. 9855

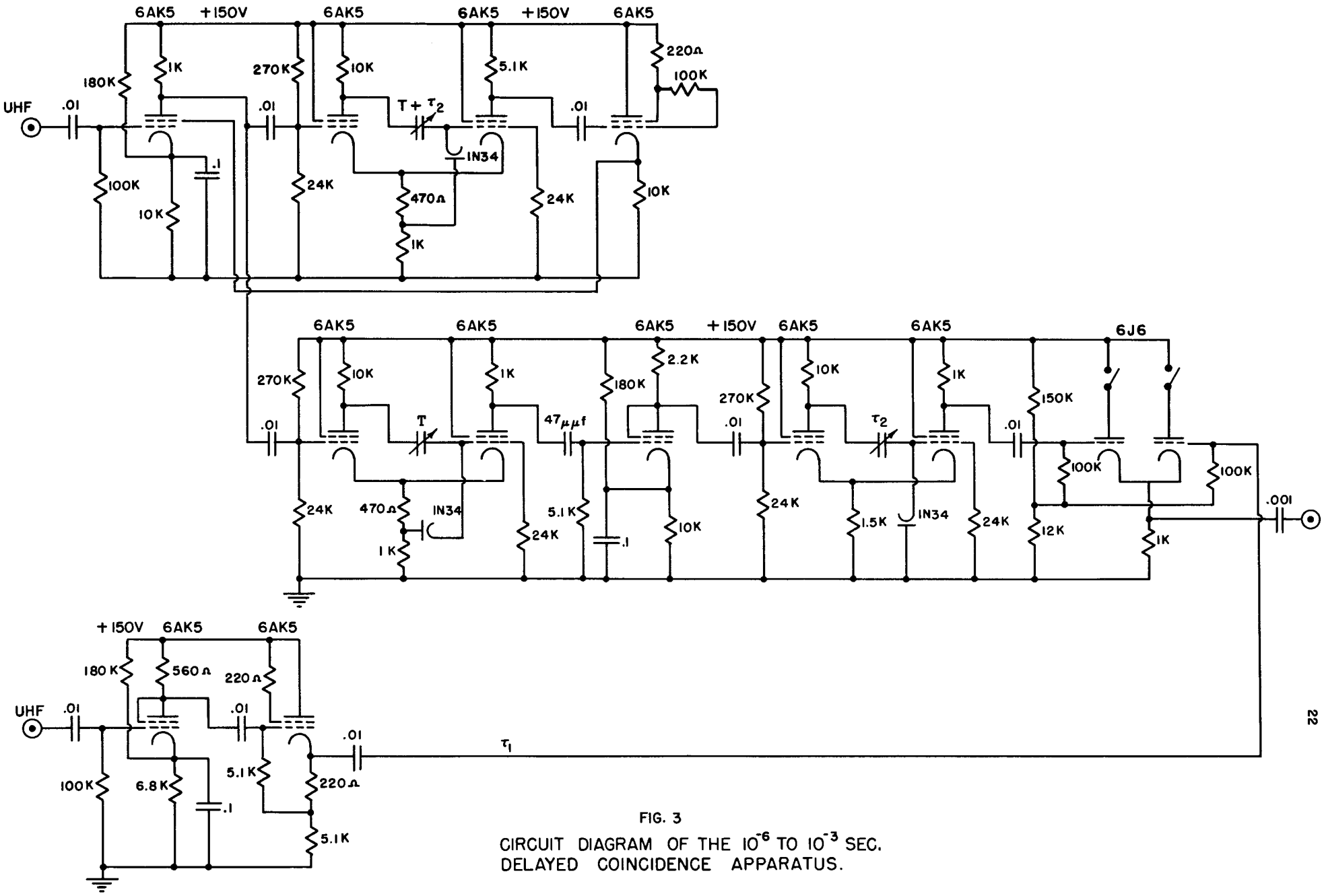

FIG. 3

CIRCUIT DIAGRAM OF THE 10^{-6} TO 10^{-3} SEC. DELAYED COINCIDENCE APPARATUS.

UNCLASSIFIED
DWG. 7690

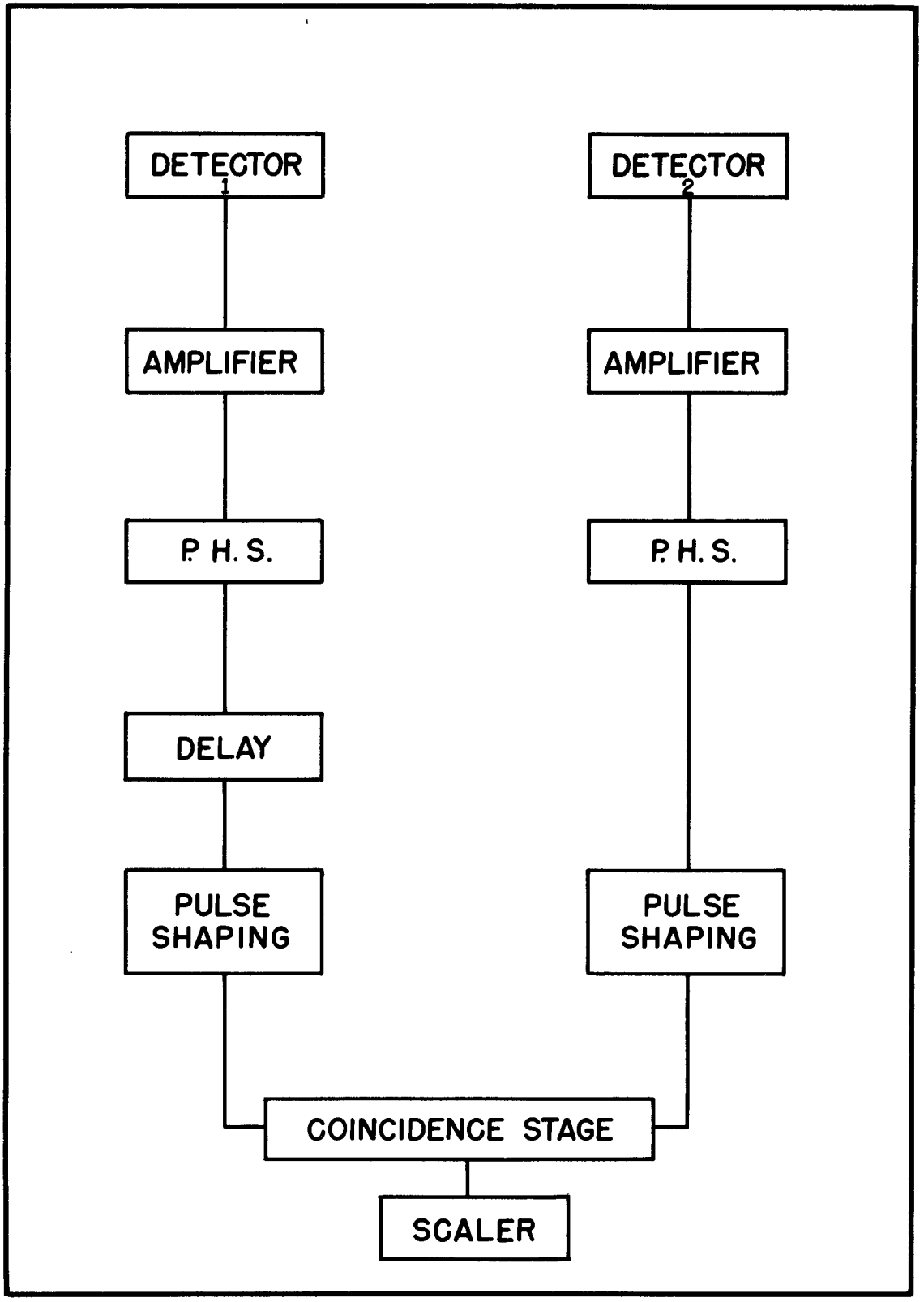

FIG. 4
BLOCK DIAGRAM OF THE DELAYED COINCIDENCE APPARATUS

heights from a signal generator and was found to be 8×10^{-8} sec. After pulse height selection, the pulses are fed to a pulse shaping circuit through terminated coaxial cables which introduce a delay of 1.0 μsec. per 24 feet of line length (RG 65/U; characteristic impedance 1000 ohms). The delay time can be varied from 0 to 2.0 μsec. in discontinuous steps of 2×10^{-8} sec. The dependence of delay time on line length was measured with a synchroscope. All delays were found to be linear with the length of the coaxial cable. The resolving time of the coincidence circuit is 7×10^{-8} sec. and is kept constant. A circuit diagram of the pulse shaping stage and coincidence stage is shown in Fig. 5. The clear anthracene crystals and the type 1P21 photomultiplier tubes are cooled to dry-ice temperature, and the tubes are operated at 60 volts per stage.

Delayed Coincidence Apparatus $\lesssim 10^{-8}$ Sec.

A third delayed coincidence unit was developed which extended the method to measurement of time intervals $\lesssim 10^{-8}$ sec. In order to reduce the variable delay introduced by a pulse height selector operating on signals of different amplitude with a finite rise time, the linear amplifiers were replaced by video amplifier sections with a rise time of approximately 10^{-8} sec. and a maximum gain of 240. Each channel consists of five tubes with gain using 6AK5 tubes with 560 ohm resistors and peaking coils in the plate circuit. The pulses may be delayed in discontinuous steps after the first stage of amplification by terminated coaxial cables (RG 7/U; characteristic impedance 100 ohms) in the plate circuit of a 6AK5 with no gain. This coaxial line does not introduce any

UNCLASSIFIED
DWG. 9856

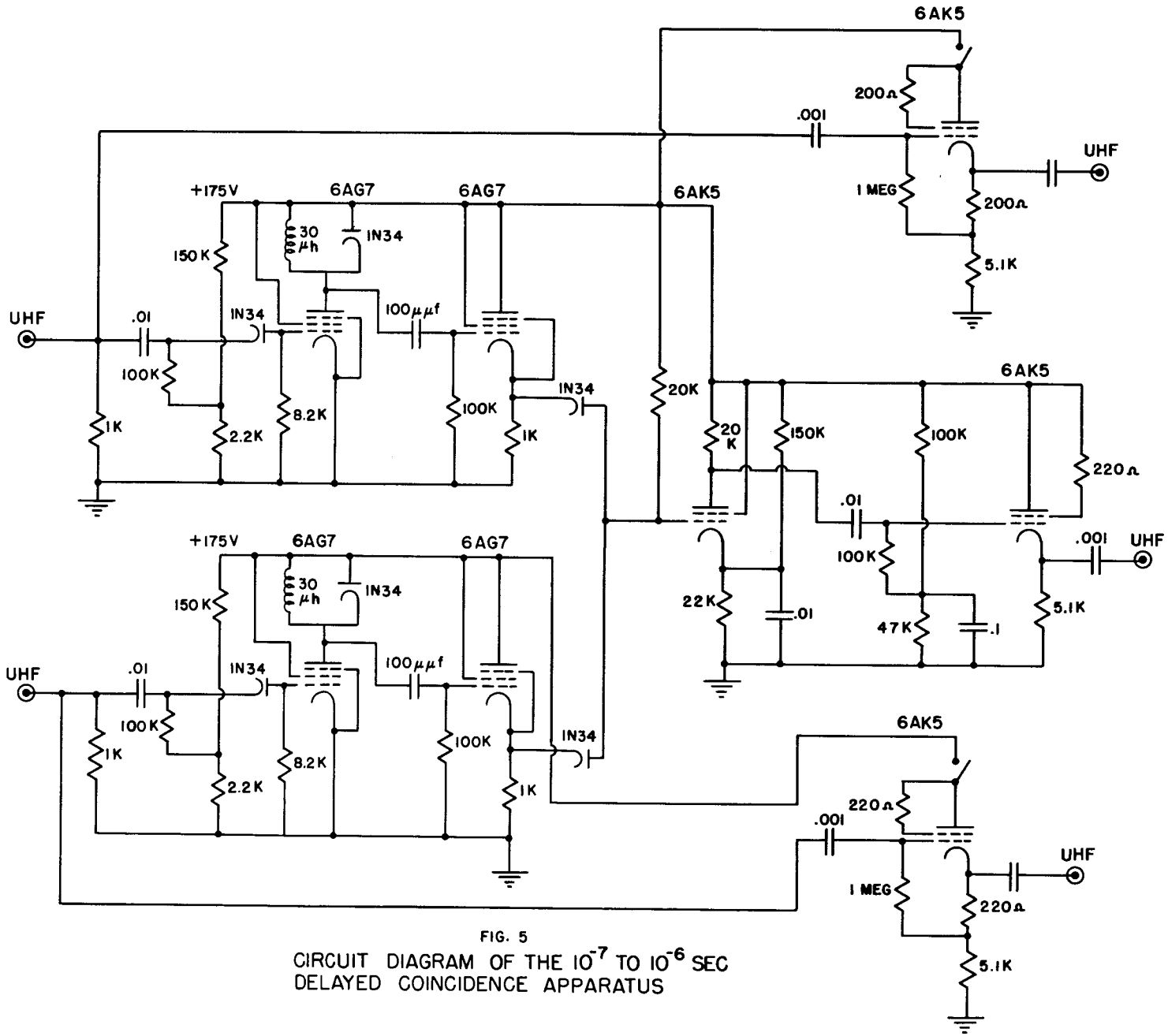

FIG. 5
CIRCUIT DIAGRAM OF THE 10^{-7} TO 10^{-6} SEC
DELAYED COINCIDENCE APPARATUS

observable distortion. When the photomultipliers are operated at approximately 80 volts per stage most of the pulses due to a scintillation saturate or nearly saturate the amplifier. These signals trigger a pulse forming tube which produces a pulse with a shape of half a sine wave whose width at the base is of the order of 2×10^{-8} sec. The formed pulse is fed directly to a coincidence stage consisting of two IN34 diodes. The coincidence pulse is lengthened to drive a scaler and pulse discrimination is done at the input to the scaler. The resolving time of the coincidence circuit is about 1.5×10^{-8} sec. as determined by counting delayed random coincidences. The coincidence resolution time will be discussed in more detail under the section on negative results. A circuit diagram of the delayed coincidence apparatus described is shown in Fig. 6.

Delayed Coincidence Scintillation Spectrometer

Another important use of the scintillation detector is the measurement of the amount of energy lost by ionizing particles penetrating the phosphor. This means that the amount of light emitted is proportional to the energy of the incident particle. Experimental evidence for this proportionality in the case of β particles and γ-rays will be presented under the section on results.

In order to obtain additional information on the nature of the isomeric transitions, the delayed coincidence method has been complemented with the scintillation spectrometer. P. R. Bell and W. H. Jordan have described in considerable detail the scintillation spectrometer for

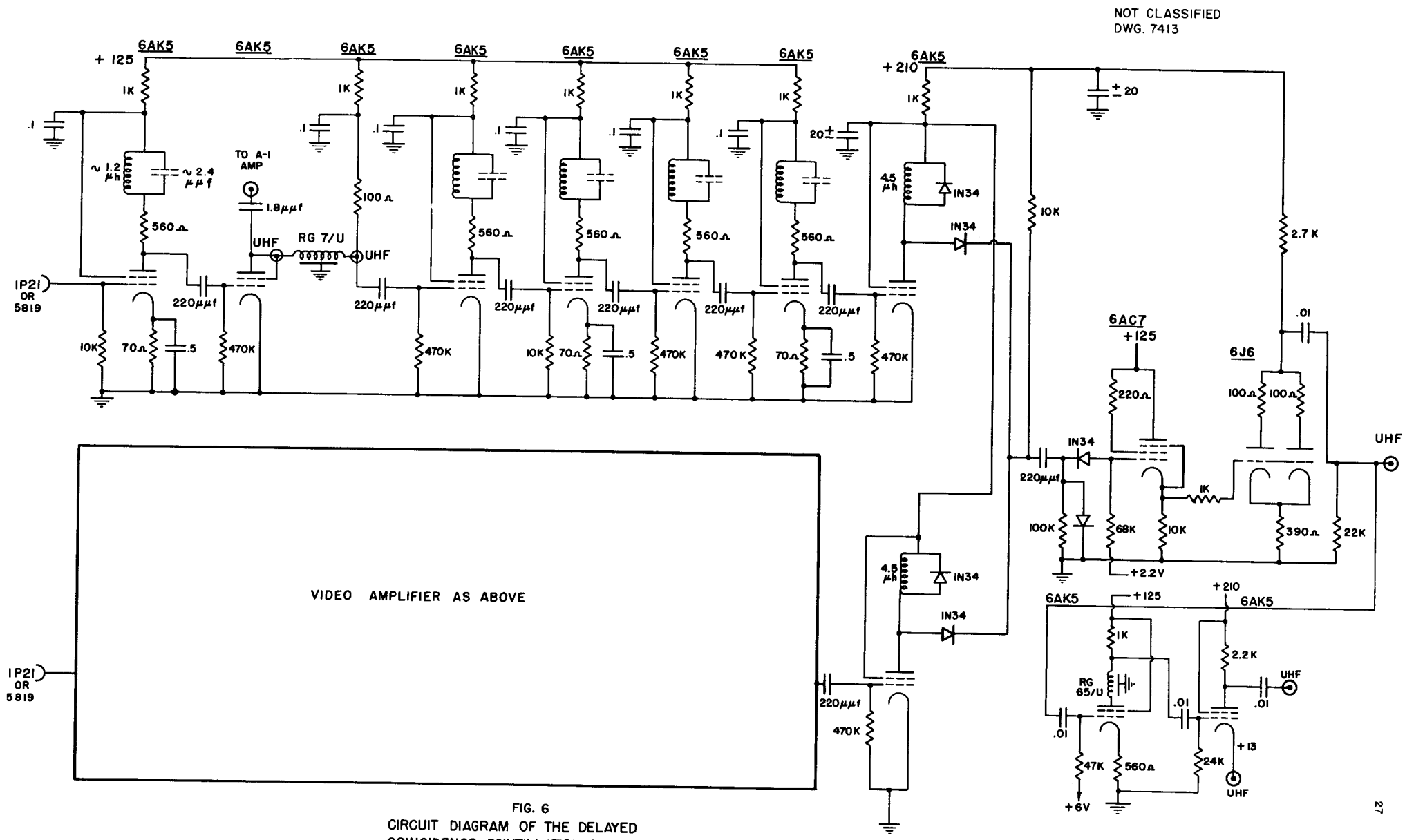

FIG. 6
CIRCUIT DIAGRAM OF THE DELAYED
COINCIDENCE SCINTILLATION SPECTROMETER

measuring beta- and gamma-ray spectra.[6] A delayed coincidence scintillation spectrometer has been developed and is proving to be a useful instrument. Fig. 7 is a block diagram of the equipment. Channels (1) and (2) represent the usual delayed coincidence circuit described above. Anthracene and type 5819 photomultipliers are used as detectors. A small portion of the signal from channel (2) is fed to a linear amplifier Model A-1. The differential pulse height selector selects all pulses whose amplitudes lie between H and H + ΔH. These signals are fed into a second coincidence stage. The fast coincidence pulses from the delayed coincidence apparatus are lengthened and delayed to match the delay introduced by the differential pulse height selector operating on a signal with a relatively long rise time before being fed to the other channel of the second coincidence stage. In this way only those delayed coincidences are selected corresponding to signals from detector (2) whose amplitude after suitable amplification falls within the gate of the differential pulse height selector. When detector (2) is used to detect the radiation announcing the formation of an isomeric state, a measurement of that spectrum is obtained. Similarly, when detector (2) is used to detect the delayed radiation, a measurement of its spectrum is obtained. The scale of the pulse height dial is calibrated in energy units using internal conversion lines of γ-rays whose energies are known from magnetic type spectrometer measurements. For most photomultiplier tubes used in these experiments, the optimum operating conditions for

---

[6] W. H. Jordan and P. R. Bell, Nucleonics 5, No. 4, 30 (1949).

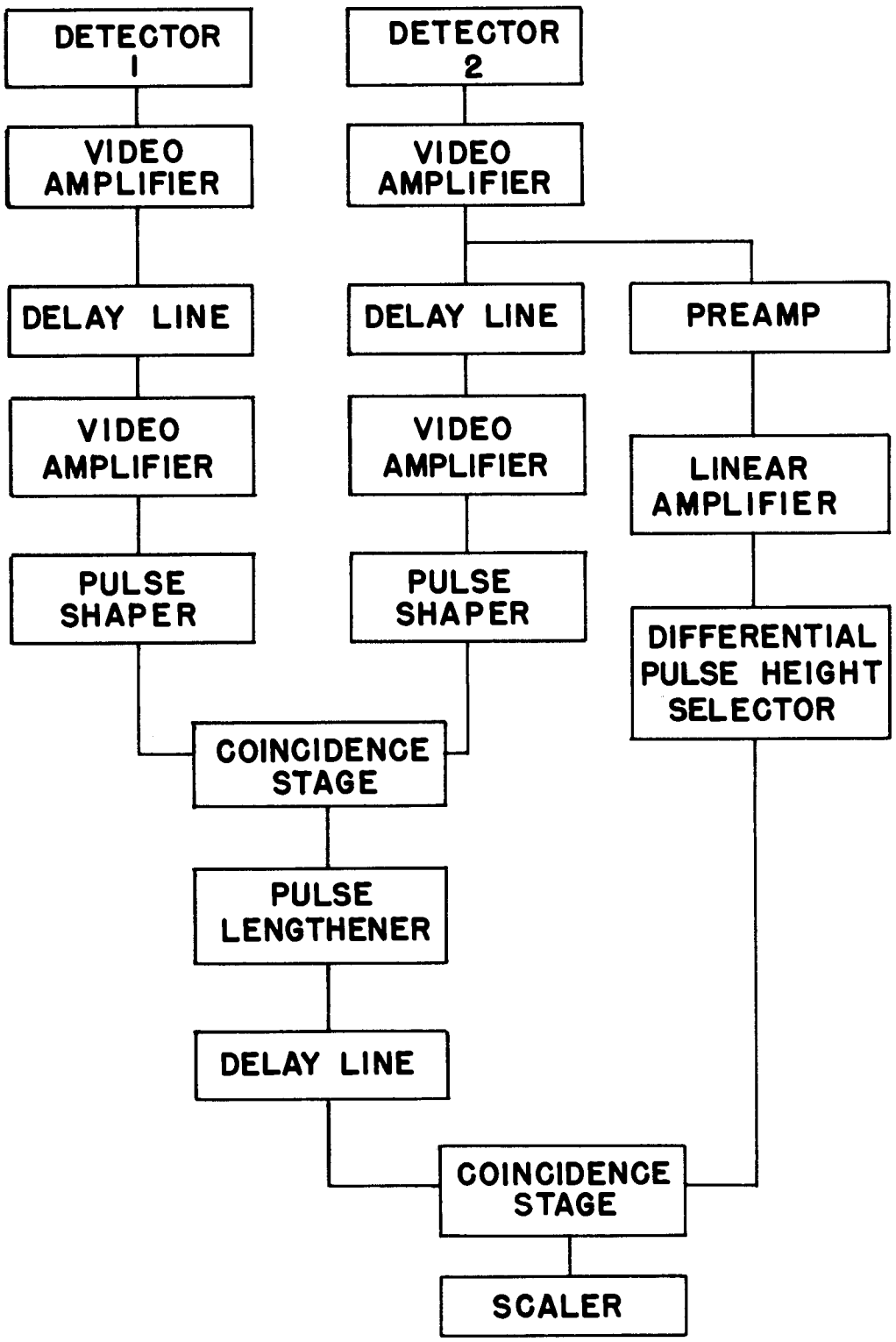

FIG. 7
DELAYED COINCIDENCE SCINTILLATION SPECTROMETER

energy resolution were 225 volts between the photocathode and the first dynode, 150 volts between the first dynode and the second dynode, and 75 volts between each of the remaining stages. For instance, a 30% decrease of the accelerating potentials decreased the energy resolution approximately 15%. Most of this decrease is probably due to the decrease of the collection efficiency of the photoelectrons and only a slight amount due to the decrease of the secondary electron emission coefficient of the dynodes.

CHAPTER IV

DISCUSSION OF THE METHOD

Let us consider a source disintegrating with the emission of β-rays and let N be the number of disintegrations per second of the source. In order to discuss the general case, let the preceding radiation be that part of the radiation of the source which announces the formation of the metastable state; delayed radiation, the radiation emitted by the decay of the metastable state; and parallel radiation, the radiation from the source which does not lead to the metastable state. The immediate radiation is then the sum of the preceding and parallel radiations. If a fraction k of these disintegrations lead to a short-lived metastable state and if α is the internal conversion coefficient, then there are $n_e = k\alpha/(1+\alpha)$ delayed electrons per disintegration, accompanied by the same number of atomic x-rays (provided the fluorescent yield is complete), and $n_\gamma = k/(1+\alpha)$ gamma-quanta per disintegration. The fraction of the disintegrations through parallel radiation is (1 - k). If ϵ_{1pr}, ϵ_{2pr} are the efficiencies (including geometric factors) of the detectors (1) and (2) for preceding rays as a whole, and if ϵ_{1d}, ϵ_{2d}, ϵ_{1par}, ϵ_{2par} are similarly defined, then

$$N_1 = N \left[k \ \epsilon_{1pr} + k \ \epsilon_{1d} + (1-k) \ \epsilon_{1par} \right] , \qquad (9)$$

where N_1 is the number of single counts per second in detector (1). If ϵ_{1pr} is large, then a large fraction of the preceding radiation will be recorded by either detector. Though the dead time of the scintillation

detector was smaller than the delay time, a considerable fraction of the delayed radiation will fail to be recorded because the associated circuits following the detectors have a dead time larger than the delay time $T \leq 10^{-6}$ sec. Thus, (9) becomes

$$N_1 = N \left[k \; \epsilon_{1pr} + k \; \epsilon_{1d} \, (1 - \epsilon_{1pr}) + (1 - k) \; \epsilon_{1par} \right] \tag{10}$$

The number of delayed coincidences per second is

$$D = N \; \epsilon_{1pr} \; \epsilon_{2d} \; k\lambda \int_{T - \tau_1}^{T + \tau_2} e^{-\lambda t} \, dt \; ,$$

$$= 2N \; \epsilon_{1pr} \; \epsilon_{2d} \; k \; e^{-\lambda T} \; \sinh \lambda \tau , \tag{11}$$

where λ is the disintegration constant of the metastable state and $\tau_1 = \tau_2 = \tau$. The efficiency ϵ_{2d} is generally complex and may be expressed as

$$\epsilon_{2d} = n_{Ke^-} \; \epsilon_{2Ke^-} + n_{Le^-} \; \epsilon_{2Le^-} + \cdots\cdots + n_\gamma \, \epsilon_{2\gamma}$$

$$+ n_{KX} \; \epsilon_{2KX} + n_{LX} \; \epsilon_{2LX} + \cdots\cdots ,$$

where n_{Ke^-} is the number of K shell conversion electrons per metastable state formed, ... n_γ is the number of γ-rays, n_{KX} is the number of K x-rays, ... , and the ϵ's are the efficiencies for the corresponding radiations. If other γ-ray transitions follow in cascade with the decay of the metastable state, the corresponding sums for these

radiations must be included in ϵ_{2d}. Equations (9) and (11) are, in general, too complicated to be of any use for the computation of k and α. However, they are important for a qualitative interpretation of the results.

The number of random coincidences per second is expressed by the usual formula

$$R = 2\tau N_1 N_2 , \tag{12}$$

where N_1 and N_2 are the single counts per second in each detector.

The number of immediate coincidences between the two detectors are due to the back scattering of particle radiation from one detector to the other, two Compton scatterings of a single γ-ray, or the eventual emission of simultaneous rays in the immediate radiation. Normally the immediate coincidences would not interfere with the counting of delayed coincidences if it were not for the effect of dead times in the instrument. When a short-lived isomer is present there is a definite correlation between the time of emission of a preceding and of a delayed ray, and this requires special corrections for delay times shorter than instrument dead time which is of the order 10^{-6} sec. One can easily see, for instance, that no delayed random coincidences can be expected if all the pulses with the two detectors are simultaneous and if the delay time is shorter than the dead time. Both the expressions for the number of delayed coincidences and random coincidences must be modified and equations (11) and (12) become

$$D = 2(N \epsilon_{1pr} - C) \ \epsilon_{2d} \ k \ e^{-\lambda T} \sinh \lambda \tau \tag{11'}$$

$$R = 2\tau(N_1 - C)(N_2 - C), \tag{12'}$$

where C is the number of simultaneous coincidences between the two detectors.

As a help in studying the disintegration scheme, the delayed coincidence method may be complemented by the scintillation spectrometer. These measurements can be done with the delayed coincidence scintillation spectrometer which was discussed in Chapter III. The spectrum of the preceding and delayed radiation is obtained separately by counting delayed coincidences at a given delay time as a function of the pulse height which is calibrated in energy units. Either spectrum may, in general, be a superposition of the particle (β^- particles or conversion electrons) spectrum and the spectrum of the γ-rays. By counting delayed coincidences as a function of the pulse height with a lucite absorber to stop the β^- particles and conversion electrons a spectrum of the γ-rays is obtained through the Compton recoil electron distribution. This distribution contains electrons of all energies up to a maximum kinetic energy given by

$$E = mc^2 \frac{2k_o^2}{1 + 2k_o} \tag{13}$$

where $k_o = E_\gamma/mc^2$ and mc^2 = self energy of the electron. The number of recoils reaches a maximum at the greatest energy, then sharply drops to zero. By measuring the energy at the point of maximum slope, equation (13) can be used to calculate the γ-ray energy E_γ. The difference between the "gross spectrum", obtained without the lucite absorber, and

the γ-ray spectrum, obtained with the lucite absorber, yields the spectrum of the particle radiation. With this instrument one obtains the group of β^- rays and/or γ-rays that are in the radiation preceding the formation of a metastable state. Likewise the spectrum of the delayed radiation yields those γ-rays following the decay of the metastable state. Besides measuring the energy of the radiation emitted in the decay of an isomeric transition, the internal conversion electron spectrum of the delayed radiation gives a value for the ratio of the number of K shell internal conversion electrons to the number of L shell internal conversion electrons (N_K/N_L).

In principle the delayed coincidence scintillation spectrometer should lend itself to the measurement of the total internal conversion coefficient which is defined as N_e/N_γ. The number of conversion electrons N_e may be obtained from the integral of the internal conversion electron spectrum appearing in the delayed radiation. The number of γ-rays N_γ may be obtained from the integral of the Compton recoil electron distribution provided the efficiency for the detection of the γ-ray is known. If both spectra are obtained with the same geometrical conditions, a knowledge of geometric factors that enter ϵ_{2d} is not needed. However, the energies of the isomeric transitions studied in the present survey were in the neighborhood of 150 kev or less. This means the maximum energy of Compton recoil electron is $\sim$ 50 kev or smaller, whereas, the minimum detectable energy under the most favorable conditions with the scintillation spectrometer is about 25 kev. Thus a large portion of the Compton recoil electron distribution was not directly measurable. Also, most of the isomers occurred in isotopes with $69 \leq Z \leq 79$ in which the

K x-rays resulting from internal conversion range in energy from 50 to 68 kev. Normally, the Compton recoil electron energy would be too small to be detectable if the x-ray quantum suffered only one Compton scattering. At these energies, however, the Compton scattering cross section is large enough so that some of the scattered quanta do not escape from the phosphor but instead suffer several Compton scatterings. For this reason the peculiar spectrum resulting from x-ray quanta appeared superimposed on the Compton electron distribution of the γ-rays. Therefore, measurements of the internal conversion coefficients were not feasible for the isomeric transitions studied with the scintillation spectrometer.

In addition to the spectra of the preceding radiation and of the delayed radiation, a measurement of the spectrum of the total radiation from the radioactive source is obtained by counting single counts as a function of pulse height under the same geometrical conditions. With these three spectra it might in some cases be possible to draw conclusions concerning the disintegration scheme.

CHAPTER V

NEGATIVE RESULTS

Sources of the 42 isotopes listed in the first column of Tables II and III were tested for delayed coincidences and found not to give any appreciable number of delayed coincidences above the expected random rate. The sources were prepared either by neutron activation in the Oak Ridge Pile or were obtained as products of uranium fission. Many of the extremely pure rare earth elements used in these experiments were prepared by G. E. Boyd and D. H. Harris of the Chemistry Division of the Oak Ridge National Laboratory. When necessary for the identification of the radioisotope, their decay was followed for a sufficient length of time. The active material was deposited on aluminum foil 1.5 mg/cm^2, with the thickness of the source never exceeding 1 mg/cm^2. In case of extremely low energy radiation the source was mounted on formvar of the order 100 $\mu g/cm^2$. The source mount was introduced between the scintillation detectors with the activity facing the detector which detected the delayed radiation.

For each isotope three different delayed coincidence units were used to cover the time region 5×10^{-9} to 10^{-3} sec. A typical set of experimental conditions for the range 10^{-6} to 10^{-3} sec. is shown in Table IV. The number of delayed random coincidences obtained in each experiment was compared with the expected delayed random coincidence rate computed by the use of the appropriate formula (12) or (12').

Many of the isotopes in Tables II and III were investigated for short-lived isomeric states with half-lives between 10^{-7} to 10^{-6} sec.

TABLE II

NUCLEI INVESTIGATED FOR SHORT-LIVED ISOMERS

Nucleus Odd Z or N	Spin (units of $\hbar$)	Energy E_γ kev	$T_{\frac{1}{2}} \times 10^{-8}$ sec.	Radioactive Source
$_{21}Sc^{45}$	7/2		< 0.5	Ca^{45} (180 da.)
$_{23}V^{51}$	7/2	267, 320	< 4	Cr^{51} (25 da.)
$_{27}Co^{59}$	7/2	1100, 1300	< 3	Fe^{59} (46 da.)
$_{33}As^{75}$	3/2	Many gammas	< 1	Se^{75} (127 da.)
$_{39}Y^{89}$	1/2		< 4	Sr^{89} (55 da.)
$_{41}Nb^{95}$		708	< 1	Zn^{95} (65 da.)
$_{45}Rh^{103}$		239, 312	< 3	Ru^{103} (42 da.)
$_{47}Ag^{109}$	1/2		< 0.5	Pd^{109} (13 hr.)
$_{49}In^{115}$	9/2		< 3	Cd^{115} (43 da.)
$_{51}Sb^{121}$	5/2		< 3	Sn^{121} (27 hr.)
$_{51}Sb^{123}$	7/2	153	< 5	Sn^{123} (40 min.)
$_{57}La^{139}$	7/2	165	< 4	Ba^{139} (1.5 hr.)
$_{59}Pr^{141}$	5/2	146, 315	< 3	Ce^{141} (38 da.)
$_{61}Pm^{147}$			< 0.5	Nd^{147} (11 da.)
$_{61}Pm^{149}$			< 0.5	Nd^{149} (1.7 hr.)
$_{63}Eu^{151}$	5/2		< 1	Sm^{151} (long)

TABLE II

NUCLEI INVESTIGATED FOR SHORT-LIVED ISOMERS (Continued)

Nucleus Odd Z or N	Spin (units of $\hbar$)	Energy E_γ kev	$T_{\frac{1}{2}} \times 10^{-8}$ sec.	Radioactive Source
$_{63}Eu^{153}$	5/2	69, 103	< 0.5	Sm^{153} (47 hr.)
$_{63}Eu^{153}$	5/2	103	< 0.5	Gd^{153} (225 da.)
$_{65}Tb^{159}$	3/2	380	< 0.4	Gd^{159} (18 hr.)
$_{67}Ho^{165}$	7/2	91, 370	< 0.4	Dy^{165} (2.4 hr.)
$_{67}Ho^{166}$			< 0.4	Dy^{166} (81 hr.)
$_{52}Te^{123}$	1/2	159	< 0.4	Te^{123} (100 da.)
$_{71}Lu^{175}$	7/2	Several gammas	< 0.4	Yb^{175} (4.2 da.)
$_{52}Te^{125}$	1/2	35	< 0.4	Te^{125} (60 da.)
$_{75}Re^{185}$	5/2		< 3	W^{185} (73 da.)
$_{77}Ir^{193}$	3/2	39, 129	> 10^{-3}	Os^{193} (15 da.)
$_{81}Tl^{203}$	1/2	279	< 0.2	Hg^{203} (46 da.)
$_{62}Sm^{149}$		250	< 0.5	Pm^{149} (47 hr.)
$_{72}Hf^{177}$	1/2 or 3/2	112, 206	< 0.4	Lu^{177} (6.8 da.)
$_{80}Hg^{199}$	1/2	156	< 0.5	Au^{199} (3.3 da.)

TABLE III

NUCLEI INVESTIGATED FOR SHORT-LIVED ISOMERS

Nucleus Even-Even	Energy E_γ kev	$T_{\frac{1}{2}} \times 10^{-8}$ sec.	Radioactive Source
$_{34}Se^{76}$	Several gammas	< 4	As^{76} (26 hr.)
$_{36}Kr^{82}$	Several gammas	< 4	Br^{82} (34 hr.)
$_{40}Zr^{90}$		< 4	Y^{90} (61 da.)
$_{48}Cd^{110}$	Many gammas	< 0.5	Ag^{110} (270 da.)
$_{52}Te^{124}$	Many gammas	< 0.5	Sb^{124} (60 da.)
$_{66}Dy^{160}$	85	< 0.5	Tb^{160} (73 da.)
$_{68}Er^{166}$	80	< 0.5	Ho^{166} (27 hr.)
$_{70}Yb^{170}$	84	< 0.5	Tm^{170} (129 da.)
$_{74}W^{182}$	Many gammas	< 0.5	Ta^{182} (117 da.)
$_{76}Os^{186}$	138	< 0.5	Re^{186} (92 hr.)
$_{72}Pt^{192}$	Many gammas	< 0.5	Ir^{192} (70 da.)
$_{80}Hg^{198}$	411	< 0.3	Au^{198} (2.7 da.)

TABLE IV

EXPERIMENTAL CONDITIONS FOR

10^{-6} TO 10^{-3} SEC. RANGE

Delay Time T	Resolving Time $\bar{\tau} = \frac{\tau_1 + \tau_2}{2}$, where $\tau_1 = 0.3$ μsec.	Single Counts $N_1 \approx N_2$	Expected Random Coincidences R
1.0 μsec.	.55 μsec.	7500 C/M	1.0 C/M
1.0	5.2	2500	1.1
1.0	44	900	1.2

using the second delayed coincidence apparatus described under instrumentation. Fig. 8 shows the number of coincidences as a function of delay time obtained with a source of Au^{198}. The majority of the radioisotopes tested gave similar curves exhibiting a sharp break at 1.5×10^{-7} sec. The coincidences observed for shorter delays are due to the scattering of particle radiation from one to the other detector and the emission of simultaneous immediate radiation from the source. The width of the peak is just equal to resolving time of the coincidence circuit (7×10^{-8} sec.) plus the variation in delay introduced by the pulse height selectors (8×10^{-8} sec.). For delays larger than 1.5×10^{-7} sec. the number of coincidences is constant and equal to the computed random coincidence rate given by formula (12').

The present observations with Au^{198} are difficult to reconcile with the reported half-life of (2 to 3) $\times 10^{-7}$ sec.[1] for the 411 kev excited state in Hg^{198} following the β-decay of Au^{198}.

On completion of the third delayed coincidence apparatus most of the isotopes in the first column of Tables II and III were investigated again for short-lived states with half-lives $\geqslant 5 \times 10^{-9}$ sec. Fig. 9 shows the number of coincidences as a function of delay time obtained with a source of Hg^{203}. This resolution curve is typical of a negative result. The majority of the radioisotopes investigated gave similar curves exhibiting a sharp break at a delay of 2 to 3×10^{-8} sec. As mentioned above the coincidences observed for shorter delays are due to simultaneous events and scattering particle radiation from one to the

---

[1] Leon Madansky and M. L. Wiedenbeck, Phys. Rev. 72, 185 (1947).

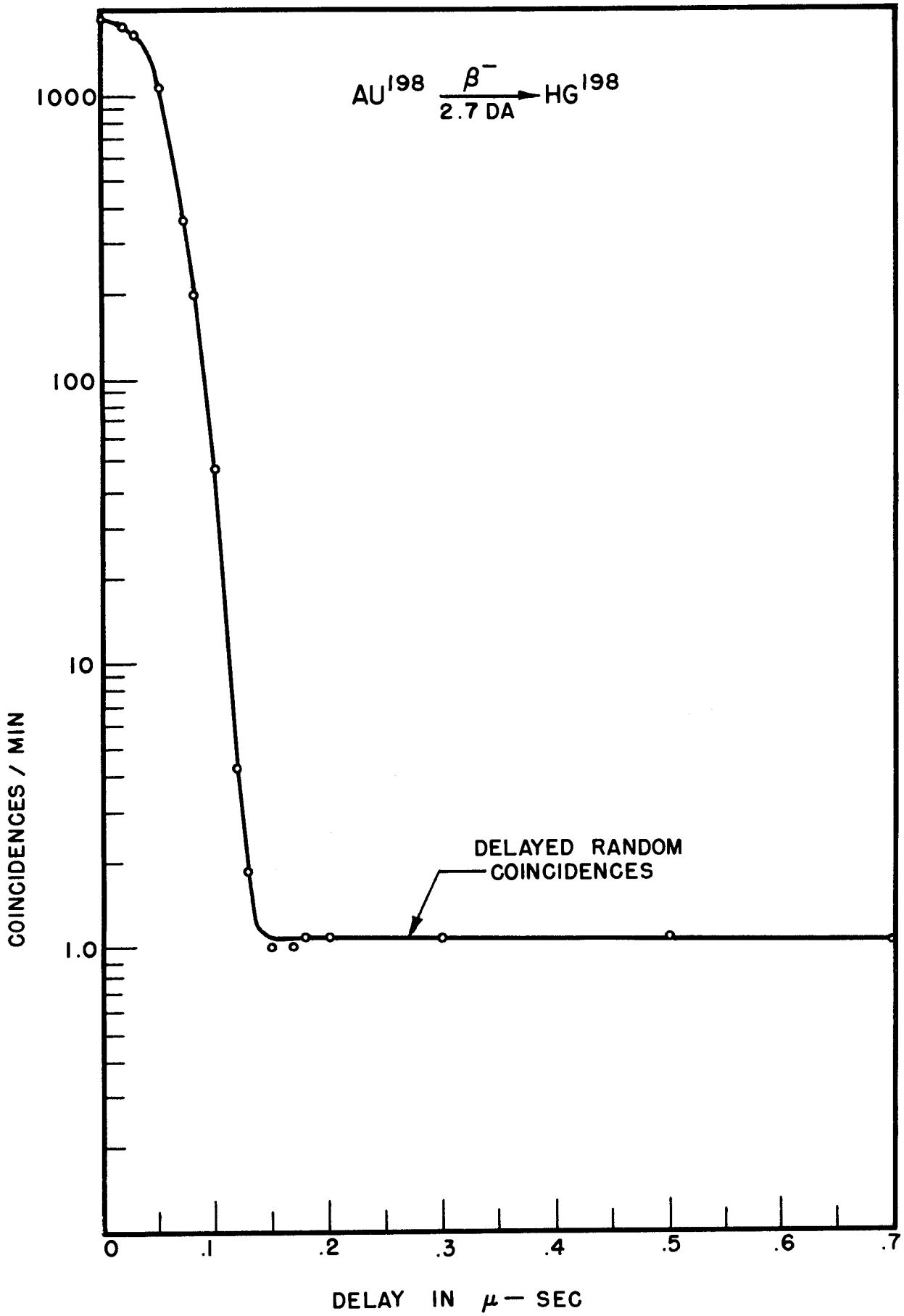

FIG. 8

THE NUMBER OF COINCIDENCES AS A FUNCTION OF DELAY TIME FROM Au^{198}

UNCLASSIFED
DWG. 8460

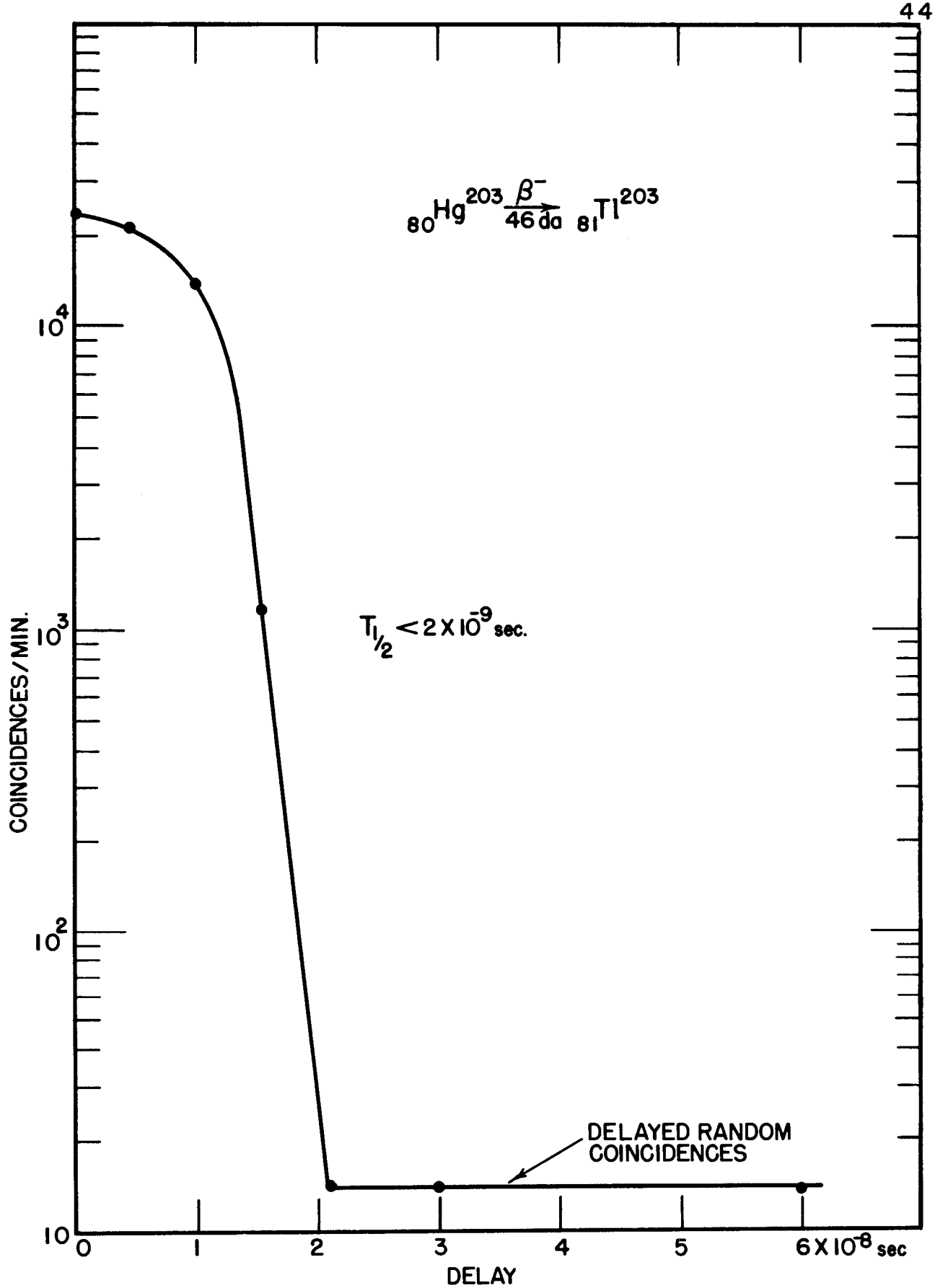

FIG. 9

THE NUMBER OF COINCIDENCES AS A FUNCTION OF DELAY TIME FROM Hg^{203}

other detector. For larger delays the coincidence rate is constant and equal to the random coincidence rate. The average resolving time of this coincidence circuit is 1.5×10^{-8} sec.

In principle the existence of an isomeric state is observed, within the limits of sensitivity of the given delayed coincidence apparatus, only if there is an excess of delayed coincidences above the random coincidence rate for $T \geqslant 2 \times 10^{-8}$ sec. For half-lives which are long compared to the resolving time of the coincidence circuit, the trailing edge of the delayed coincidence curve becomes an exponential decay whose slope is determined by the half-life of interest. For half-lives of the same order of magnitude as the resolving time ($\lesssim 10^{-8}$ sec.) of the coincidence circuit this statement is not useful. The form of the curve of coincidence counts versus delay for originally simultaneous events depends essentially upon the distribution of amplitude of the original pulses. In general this distribution is not known nor determined for most of the experiments which have been made. For example, if the pulses from the detector announcing the formation of an excited nuclear state are very large compared to the pulses from the detector detecting the decay of the excited state, the width of the resolution curve will increase according to the difference in amplitude of the originally simultaneous events. With the present instrument the slope of the "trailing" edge of the resolution curve for simultaneous events varies with a half-period from 1.0 to 2.5×10^{-9} sec. being a minimum for simultaneous events which give rise to pulses of equal or nearly equal amplitude. This exponential trailing edge is instrumental and generally occurs for 2 to 3 decades depending on the number of simultaneous events.

This instrumental effect is inherent in a coincidence system with amplifiers of finite rise time operating on pulses having more or less a continuous distribution in amplitude. In the general case for sources decaying by beta disintegration the energy distribution of the radiation incident on the phosphor will be a continuous distribution superimposed with a Compton recoil electron distribution of the γ-rays and the internal conversion electron lines. The response of the scintillation detector at each step further smears the distribution in amplitude of the pulses that arrive at the input to the amplifiers. This is easily seen by considering the individual steps of the response of the detector. The number of photons resulting from an ionizing event, the number of photoelectrons from the photocathode, and the number of secondary electrons produced at each dynode will vary in each case in a statistical manner, so that the pulses obtained from monochromatic radiation incident on the phosphor are not all the same height.

Furthermore, the rise time of the integral pulse will not be a fixed quantity for several reasons. The excited molecular states in the phosphor decay with the emission of photons according to the exponential law. Thus, for an individual ionizing event there are statistical fluctuations in the time of emission of the photons. Within the multiplier the resolving time is limited by the spread in transit time itself. Under normal operating conditions this is less than 5×10^{-9} sec.[2] according to measurements and calculations by Morton. Finally, there is the response rise time of the video amplifiers. The rise time of the

---

[2] W. H. Jordan and P. R. Bell, Nucleonics 5, No. 4, 30 (1949).

amplifiers used in the third delayed coincidence apparatus was 10^{-8} sec. The primary limitation on the resolving time of this coincidence apparatus was the rise time of the amplifiers. Any theoretical analysis of the performance of the coincidence circuit would mean treating a composite statistical problem which would be quite complicated. It should be mentioned that several workers[3,4] have made calculations for coincidence curves for both prompt events and delayed events based on some assumption concerning the time delays in the equipment and a knowledge of the resolving time. In particular Binder used a Gaussian distribution for the time delays. Comparison of Binder's theoretical resolution curve for prompt events with measured curves from this survey for short-lived isomers gave very poor agreement. This result is not surprising considering the assumption made concerning the time delays in the equipment.

The foregoing remarks pertained to the case in which both channels were excited by the parent (β-disintegration) radiation and daughter radiation (γ-radiation or conversion electrons). Most of the isotopes in Tables II and III were investigated in this manner for intensity reasons. In the event the resolution curve for an isotope was somewhat wider than the average resolution curve the experiment was repeated exciting one channel by both parent and daughter radiation and the other channel by daughter radiation. This is accomplished by placing a lucite absorber between the source and the detector of delayed

---

[3] F. W. Van Name, Phys. Rev. 75, 100 (1949).

[4] D. Binder, Phys. Rev. 76, 856 (1949).

radiation. If the daughter nucleus in an excited state is metastable with a measurable life time, the resolution curve for β-γ coincidences will not be symmetrical about the zero of delay time.

The β-γ coincidence resolution curve offers the advantage that the spurious simultaneous events due to scattering of particle radiation from one detector to the other are removed. For lifetimes that are comparable to the resolving time of the coincidence circuit it appears that the β-γ coincidence experiment is more sensitive for detection of metastable states with low intensity than the experiment where both channels are excited by parent and daughter radiation. This conclusion is certainly true for γ-ray transitions above 300 kev. However, from previous surveys[5] the isomeric transitions involved energies less than 200 kev. In this domain of energy and multipole order $el(2)^{3 \text{ or } 2}$ and $mag\ (2)^{2 \text{ or } 1}$ the internal conversion coefficients[6] become quite appreciable compared to the efficiency of detection of electromagnetic radiation ($\sim$ 5%). In this case it is advantageous to measure β-e and β-γ coincidences.

With the development of the delayed coincidence scintillation spectrometer the sensitivity for detection of metastable states with periods comparable to the resolving time ($\sim 10^{-8}$ sec.) has been increased appreciably. It is possible to select coincidences with the parent radiation exciting one channel and the daughter radiation exciting

---

[5] S. DeBenedetti and F. K. McGowan, Phys. Rev. 74, 728 (1948).

[6] M. E. Rose, G. H. Goertzel, B. I. Spinrad, J. Harr, and P. Strong, Phys. Rev. 76, 1883 (1949). Tables of K-shell internal conversion coefficients privately circulated.

the other channel in the presence of other parallel radiation giving rise also to coincidences. The merits of this method will be discussed in more detail under Chapter VI. Since the delayed coincidence scintillation spectrometer was developed towards the end of the present survey, only a few of the isotopes in Tables II and III have been re-investigated.

Finally, the upper limit set for $T_{\frac{1}{2}}$ in columns 4 and 3 of Tables II and III respectively for an excited state in the isotope of the first column assumes that the beta decay leads to the excited state in a large percentage of the disintegrations. If the excited state is reached in a low percentage branch of the beta decay, the lifetime limit should be increased by a factor of 3 or 4. The upper limit was chosen as twice the half-period of the trailing edge of the delayed coincidence resolution curve for each isotope.

In the case of Ir^{193} a lower limit is set for the half-life of the 127 kev transition following the beta decay of Os^{193}. The beta-spectrum of Os^{193} is known to consist of one component of 142 kev accompanied by two γ-ray transitions of energy 127 and 39 kev.[7] Saxon has shown also that $\alpha_K = .41$ and $N_K/N_L = 1.4$ for the 127 kev transition. The delayed coincidence resolution curve obtained with a source of Os^{193} indicated that the number of immediate coincidences was unusually low. To check this point the energy spectrum of the immediate coincidences was examined with the coincidence scintillation spectrometer. A comparison of this spectrum with the single count spectrum, which is the spectrum of the total radiation emitted in the decay of Os^{193}, showed clearly

---

[7] D. Saxon, Phys. Rev. 74, 1264A (1948).

that the 127 kev transition is not in coincidence with the beta ray. Since the measurements of Saxon showed all the conversion lines to decay with the 15 day period, the lifetime of either the 127 kev or the 39 kev transition must be less than 15 days but greater than 10^{-3} sec.

CHAPTER VI

POSITIVE RESULTS

Out of 50 nuclei investigated, three short-lived isomeric states were found. These are Lu^{177*} (1.3×10^{-7} sec.), Au^{197*} (7×10^{-9} sec.), and Ir^{191*} (5.7×10^{-9} sec.). Independently from this survey and essentially at the same time, Goldhaber at the University of Illinois, Deutsch at the Massachusetts Institute of Technology, and Barber at Stanford University have used the method of delayed coincidences for the study of short-lived isomers. These authors have reported metastable states in Ge^{72*} (5×10^{-7} sec.),[1] Cd^{111*} (8×10^{-8} sec.),[2] and Ta^{181*} (1.1×10^{-8} sec.).[3] The existence of these has been confirmed in this survey and the results will be included in this chapter. In addition the results of measurements with the delayed coincidence scintillation spectrometer on previously reported short-lived isomeric states will be presented.

${}_{71}Lu^{177*}$ (1.3×10^{-7} sec.)

An excited state in Lu^{177} with a half-life $(1.3 \pm 0.2) \times 10^{-7}$ sec.[4] was observed following the β-decay of Yb^{177} (1.8 hr.). In Fig. 10 the number of delayed coincidences after subtraction of random

---

[1] J. C. Bowe, M. Goldhaber, R. D. Hill, W. E. Meyerhof, and O. Sala, Phys. Rev. 73, 1219 (1948).

[2] Martin Deutsch and D. T. Stevenson, Phys. Rev. 76, 184 (1949).

[3] W. C. Barber, Phys. Rev. 80, 332 (1950).

[4] F. K. McGowan, Phys. Rev. 76, 1730 (1949).

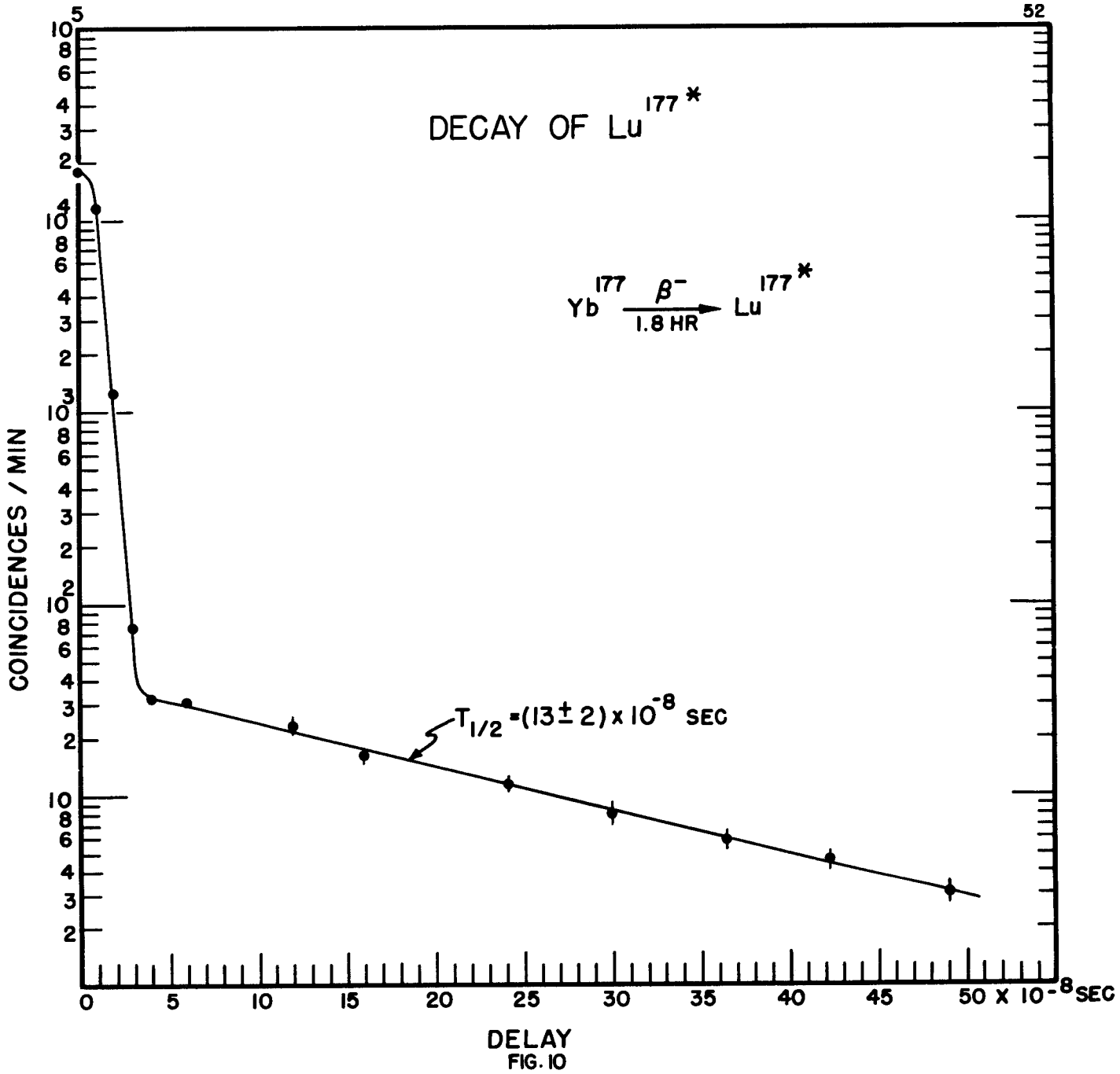

FIG. 10

THE NUMBER OF DELAYED COINCIDENCES AS A FUNCTION OF DELAY TIME

coincidences is plotted as a function of delay time. It appears from this curve that the disintegration of Yb^{177} leads to a metastable state Lu^{177*} which in turn decays to a state of lower energy.

In order to obtain additional information on the nature of this isomeric transition the delayed coincidence scintillation spectrometer was used to measure the energy of the radiation emitted in the decay of the isomeric state and the ratio N_K/N_L.

Experimental evidence for the proportionality between the energy lost by the ionizing particles penetrating the anthracene and the light emitted by the phosphor is shown in Fig. 11. This is a typical calibration curve of the pulse height as a function of energy. The monoenergetic electrons are obtained from internally converted γ-rays whose energies are known from magnetic spectrometer measurements. For example, Hg^{203} and Te^{125} emit K and L shell internal conversion electrons of energies 265, 195, 105, and 78 kev. The point at 35 kev corresponds to the complete absorption of a 35 kev γ-ray from Te^{125} in the anthracene by multiple Compton scatterings. For energies above 100 kev the pulse height versus energy is linear.

By plotting delayed coincidences in a small height interval against pulse height, a measurement of the spectrum of the delayed radiation was obtained. Fig. 12 shows the result of such a measurement. The scale of the pulse height dial was calibrated in energy units by using the K and L internal conversion lines of the 132 kev transition from the decay of the 22 μsec. metastable state of Ta^{181}. The solid curve is the internal conversion electron spectrum obtained after subtraction of the Compton electron distribution produced by the γ-rays and

UNCLASSIFIED
DWG. 8461

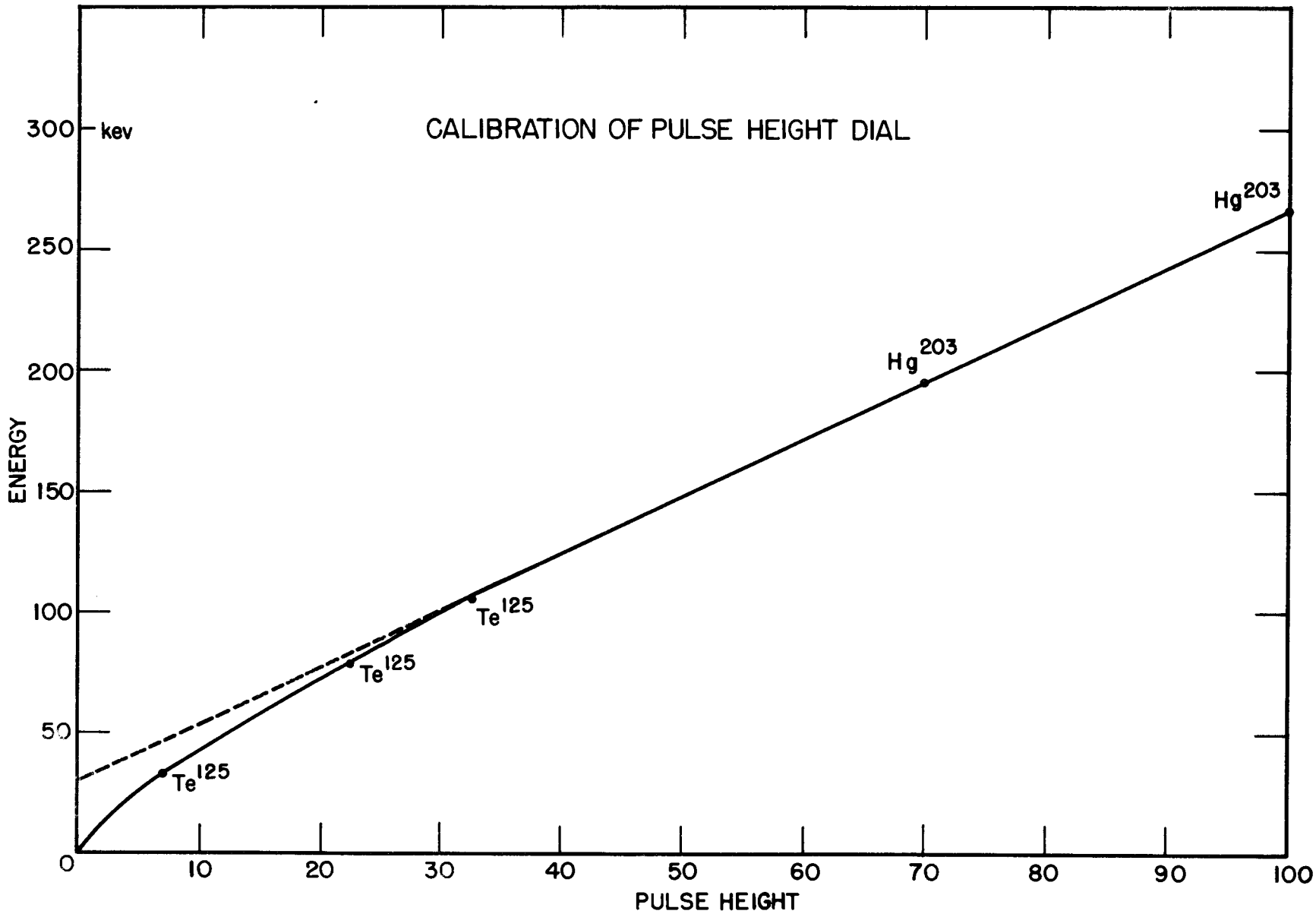

FIG. 11

PULSE HEIGHT RESPONSE OF THE ANTHRACENE SCINTILLATION DETECTOR AS A FUNCTION OF THE ELECTRON ENERGY

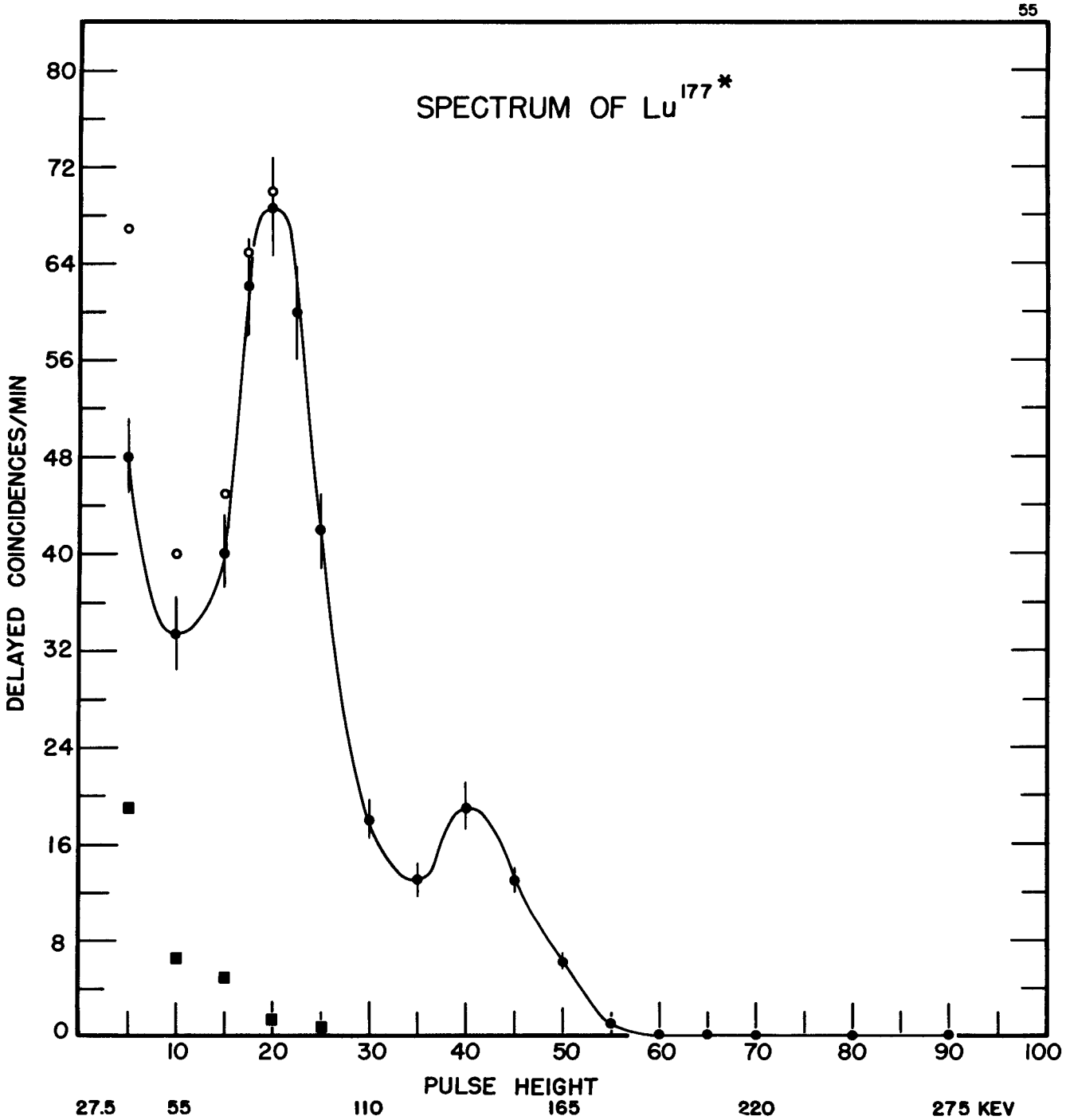

FIG. 12

DELAYED COINCIDENCE COUNTING RATE AS A FUNCTION OF PULSE HEIGHT

X-rays from the gross spectrum. The K and L internal conversion lines at 87 and 140 kev correspond to a (150 ± 10) kev transition. The ratio of K shell conversion to L shell conversion obtained from the area under the peaks is 3 ± 1. From the energy and half-life of this isomeric state the transition is probably electric octupole radiation or a combination of electric octupole and magnetic quadrupole radiation. Since the number of delayed coincidences is zero above 185 kev, it appears that no other γ-rays follow in cascade with the decay of Lu^{177*}.

The half-life of Yb^{177} as listed in the Table of Isotopes[5] ranges from 1.9 to 3.5 hours. A conventional half-life determination is complicated by the presence of the daughter activity Lu^{177} (6.9 da.) and the Yb^{175} (100 hr.) present in the source. By counting delayed coincidences at a fixed delay as a function of time, the coincidence counting rate decreases according to the decay of Yb^{177}. The decay was observed for six hours and the half-life of Yb^{177} appears to be (1.8 ± 0.1) hr.

Au^{197*} (7×10^{-9} sec.)

An excited state in Au^{197} with a half-life $(7.0 \pm 1.0) \times 10^{-9}$ sec.[6] was observed using sources of Hg^{197}. In Fig. 13 the number of delayed coincidences is plotted as a function of delay time. The portion of the solid curve for delays less than 3.5×10^{-8} sec. and points indicated by circles represent the gross data. After subtraction of random coincidences the solid curve for delay time $T \geqslant 3.5 \times 10^{-8}$ sec.

---

[5] G. T. Seaborg and I. Perlman, Rev. Mod. Phys. 20, 585 (1948).

[6] F. K. McGowan, Phys. Rev. 77, 138 (1950).

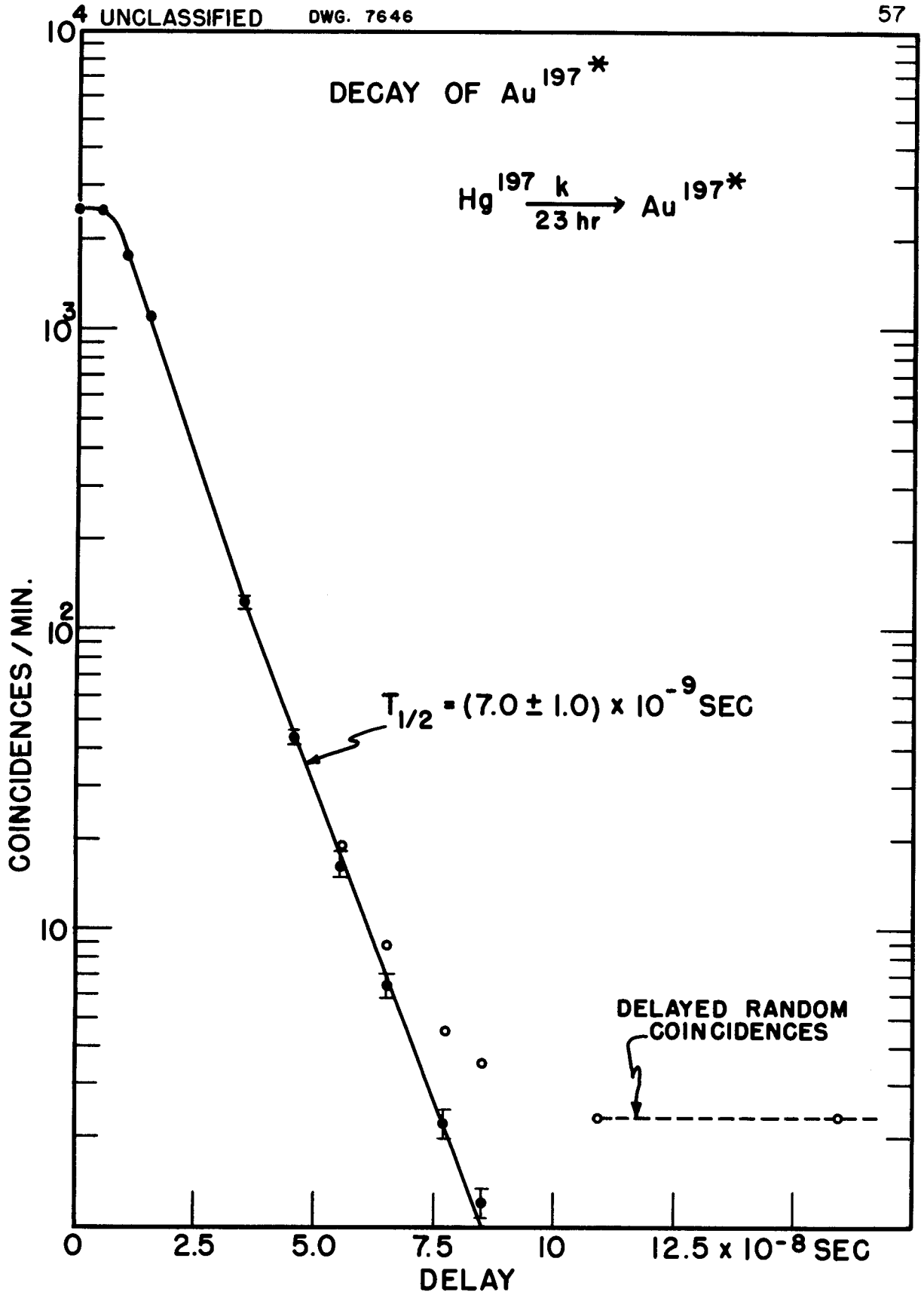

FIG. 13

THE NUMBER OF DELAYED COINCIDENCES AS A FUNCTION OF DELAY TIME

represents the decay of the short-lived isomeric state which has been produced by the K-capture decay of Hg^{197}. Hg^{197} as listed in the Table of Isotopes[7] is known to decay by K-capture with periods 23 and 65 hr. All points on the decay curve of Au^{197*} appeared to decay according to the 23 hr. period.

Using a high speed synchroscope developed by G. G. Kelley[8] photographs of the individual signals from the type 5819 multiplier showed the presence of delayed signals due to the decay of the isomeric state.

This isomeric state has been observed by Deutsch and Wright[9] independently and essentially at the same time.

Both the radiation announcing the formation of the isomeric state and radiation resulting from its decay have been measured with a delayed coincidence scintillation spectrometer. Previously, Huber et al.[10] have observed that 4% of the disintegrations of Hg^{197} (23 hr.) lead to a 7.5 sec. isomeric state in Au^{197} and 96% of the disintegrations are followed by γ-ray transitions corresponding to 135 and 165 kev which are strongly converted. They also observed a 77 kev γ-ray in the 65 hr. period and attributed the 7.5 sec. isomeric transition to a 273 kev γ-ray.

The gross spectrum is shown in Fig. 14 curve (1) obtained by

---

[7] G. T. Seaborg and I. Perlman, Rev. Mod. Phys. 20, 630 (1948).

[8] G. G. Kelley, Rev. Sci. Inst. 21, 71 (1950).

[9] Martin Deutsch and W. E. Wright, Phys. Rev. 77, 139 (1950).

[10] O. Huber, R. Steffen, F. Humbel, Helv. Phys. Acta 21, 192 (1948).

UNCLASSIFIED
Dwg. 8285

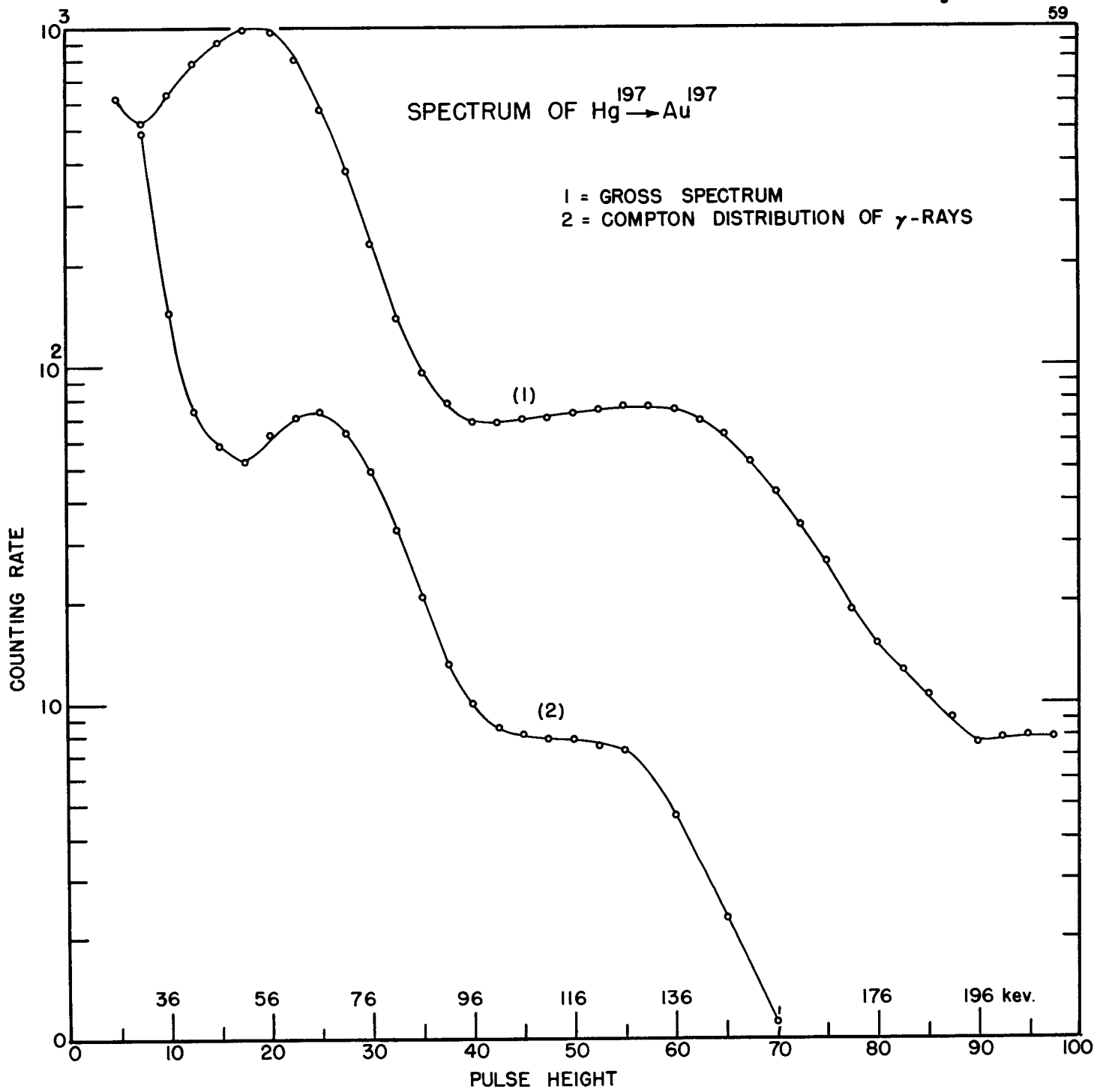

FIG. 14

PULSE HEIGHT DISTRIBUTION OF THE RADIATION FROM Hg^{197}

counting single counts. The first peak is essentially a superposition of unresolved lines from the 77 kev γ-ray and K internal conversion lines of the 135 and 165 kev γ-rays. The second peak is the L internal conversion lines which are not resolved. Beyond 200 kev there is a line at 250 kev (not shown in Fig. 14) which is probably due to the 273 kev γ-ray if the line corresponds to L shell internal conversion. Curve (2) is the Compton distribution of recoil electrons from γ-rays and x-rays taken with a much larger source. The peak at 68 kev is due to K x-rays which are totally absorbed in the anthracene by several Compton encounters. The second peak is attributed to the maximum of the Compton distribution for a 273 kev γ-ray.

The spectrum of the radiation announcing the formation of the isomeric state obtained by counting delayed coincidences as a function of energy is shown in Fig. 15. The K and (L + M) internal conversion lines correspond to the 165 kev transition. The ratio of K shell conversion to (L + M) shell conversion is ~ 0.1. It would appear that the initial state of the 165 kev transition may be metastable with a longer lifetime.

The spectrum of the radiation emitted in the decay of the metastable state is shown in Fig. 16. The K and (L + M) internal conversion lines correspond to the 135 kev transition. In this case the K to (L + M) ratio is $\lesssim 1$. On comparing the energy and half-life of the metastable state with the theoretical estimate of the lifetime for γ-ray emission, the transition corresponds to forbiddenness $\ell = 2$. The experimental K to L ratio cannot be compared with theory as the relativistic calculations for L shell internal conversion are not completed.

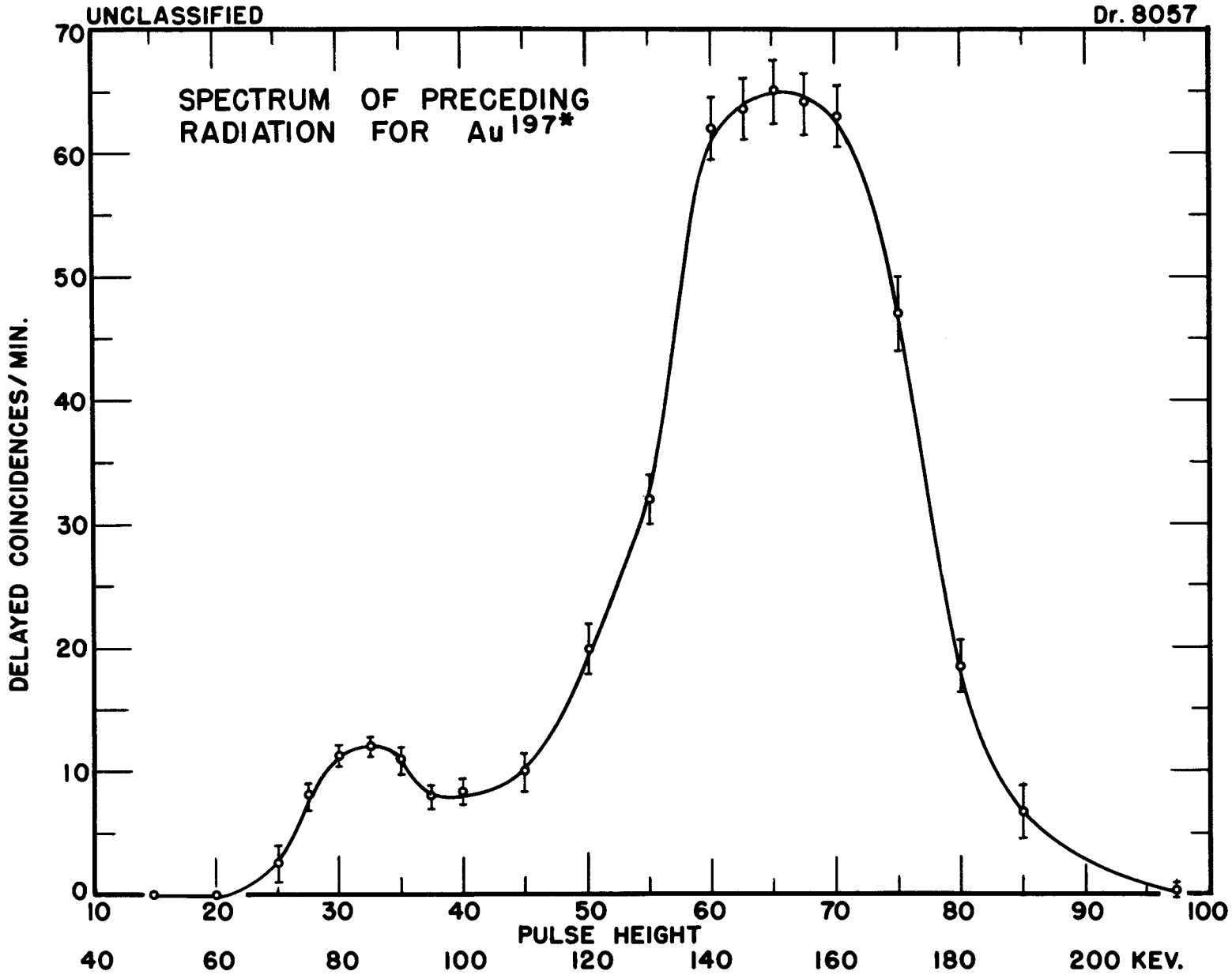

FIG. 15

DELAYED COINCIDENCE COUNTING RATE AS A FUNCTION OF PULSE HEIGHT

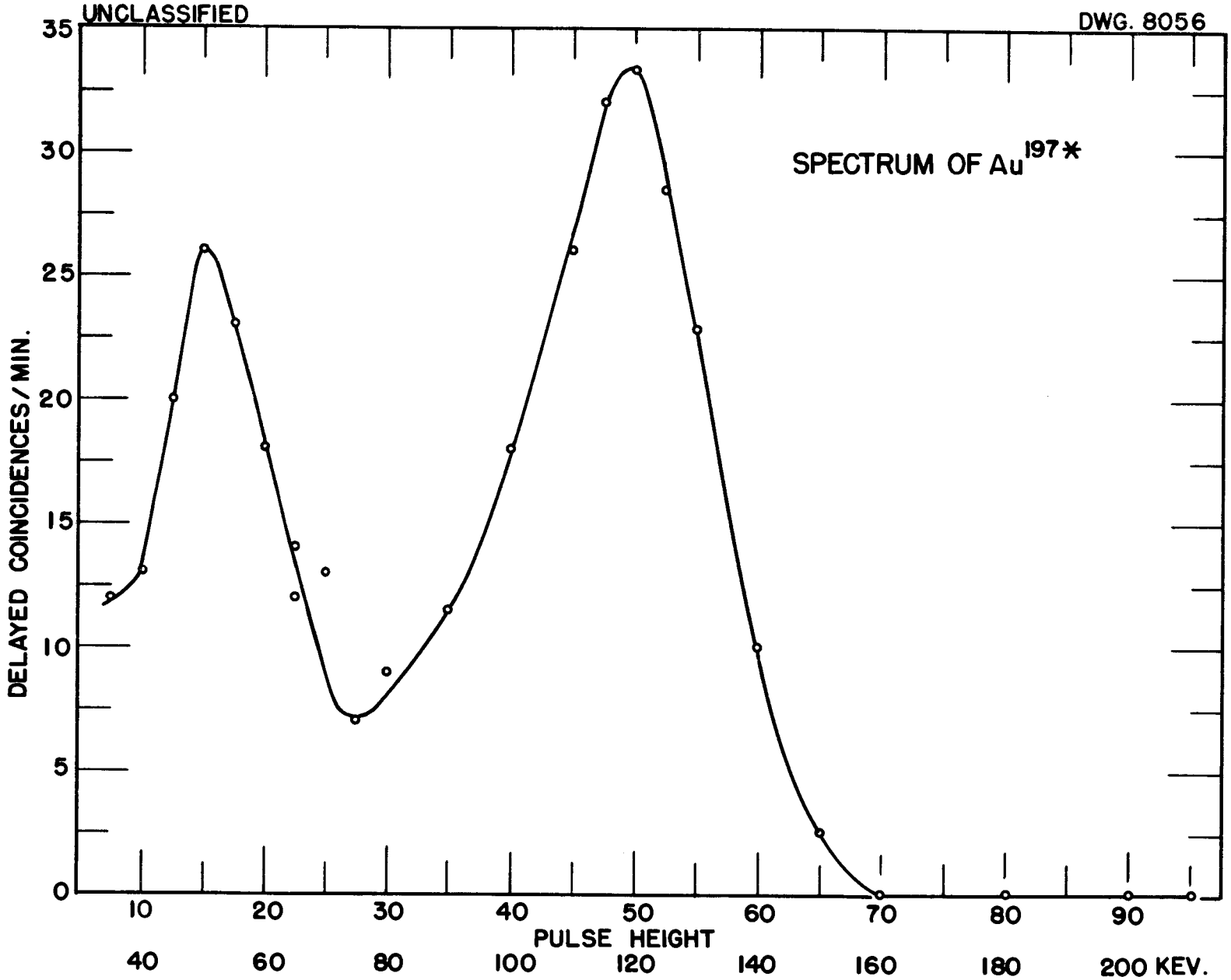

FIG. 16

DELAYED COINCIDENCE COUNTING RATE AS A FUNCTION OF PULSE HEIGHT

In the meantime one is tempted to use the approximate estimates for the K to L ratios, which are valid for $Z < 25$ and $E < 150$ kev,[11,12] as a guide to indicate the electric or magnetic character of the radiation. For instance, the $(N_K/N_L)_{el(2)^\ell}$ is of the same order of magnitude as $(N_K/N_L)_{mag(2)^{\ell+1}}$. For a given forbiddenness one is interested in the case of pure $el(2)^\ell$-pole or a combination of $el(2)^\ell$-pole and $mag(2)^{\ell-1}$-pole. Because of the large difference between electric and magnetic K to L ratios (i.e. $(N_K/N_L)_{el(2)^\ell\text{-pole}} \ll (N_K/N_L)_{mag(2)^{\ell-1}}$), it seems possible that one might draw a tentative conclusion on the character of radiation from experimental K to L ratios.

Recently a few relativistic calculations without screening for L_I shell internal conversion[13] have been completed for $Z = 92$, 84 and 49 and for electric and magnetic dipole and electric quadrupole radiation. For a gamma-ray energy of 134 kev and $Z = 84$ the ratios $(N_K/N_{L_I})_{el(2)^2}$ and $(N_K/N_{L_I})_{mag(2)^1}$ are 2.0 and 19 respectively. In the approximate theory by Tralli and Lowen the contribution by sub-shells L_{II} and L_{III} to the L shell internal conversion coefficient is small compared to L_I sub-shell for magnetic dipole and quadrupole radiation. In the electric case the relative contributions from L_{II} and L_{III} sub-shells are not known

---

[11] N. Tralli and I. S. Lowen, Phys. Rev. 76, 1541 (1949).

[12] M. H. Hebb and E. Nelson, Phys. Rev. 58, 486 (1940).

[13] H. Gellman, B. A. Griffith, and J. P. Stanley, Phys. Rev. 80, 866 (1950).

explicitly. In any event it appears that in the vicinity of Z = 84 and a gamma-ray energy of 134 kev the ratio $(N_K/N_L)_{el(2)^2\text{-pole}}$ is much smaller than the ratio $(N_K/N_L)_{mag(2)^1\text{-pole}}$. Measurements of the K to L ratios of other isomeric transitions with similar energy, Z, and lifetime have been as high as 6. Thus for Au^{197*}, where the K to (L + M) ratio is $\lesssim 1$, it would appear that electric quadrupole radiation occurs. Although the approximate K to L ratios may be in error by a factor as large as 3, this conclusion would still hold.

The above conclusions were based on a disintegration scheme proposed by Huber et al.[10] Recently Huber and coworkers have reported new measurements[14] on the radiations from Hg^{197} which contradict some of their previous measurements. They have remeasured the spectrum of the conversion lines of Hg^{197} with a magnetic lens spectrometer. From the accurately determined (K - L) and (K - M) differences of the conversion lines from the 164 and 133 kev transitions, they conclude that these γ-rays are converted in Hg and not, as previously assumed, in Au^{197}. Except for four per cent of the decays by K capture to Au^{197*} (7.5 sec.), the Hg^{197} (23 hr.) decays by an isomeric transition to Hg^{197} (65 hr.). The energy transition associated with the 23 hour period is the 164 kev γ-ray followed by the 133 kev γ-ray where the half-life of the intermediate state is 7×10^{-9} sec. The final state of the cascade decays by K capture to Au^{197} with a 65 hour half-life.

$$_{77}Ir^{191*} \ (5.7 \times 10^{-9} \text{ sec.})$$

---

[14] H. Frauenfelder, O. Huber, A. De-Shalit, and W. Zunti, Phys. Rev. 79, 1029 (1950).

An excited state in Ir^{191} with a half-life $(5.7 \pm 0.5) \times 10^{-9}$ sec.[15] was observed with the delayed coincidence scintillation spectrometer. In Fig. 17 the number of delayed coincidences is plotted as a function of delay time obtained with a source of Os^{191} (32 hr.). The solid portion of the curve for delay time $T \geqslant 2.5 \times 10^{-8}$ sec. represents the decay of the short-lived isomeric state which has been produced by the β-decay of Os^{191}.

Both the end point of the β-spectrum announcing the formation of the isomeric state and energy of the radiation emitted in the decay of the metastable state have been determined. Curve (1) in Fig. 18 is the spectrum of the radiation resulting from the decay of the short-lived isomer in Ir^{191} obtained by counting delayed coincidences in a small height interval and plotting against pulse height. The internal conversion electron peak corresponds to 52 kev. The scale of pulse height was calibrated in energy units using internal conversion electron lines of γ-rays whose energies are well known from magnetic spectrometer measurements. Curve (2) shows the internal conversion electron lines at 65 and 122 kev of the 132 kev transition from the decay of the 22 μsec. metastable state of Ta^{181} which announces the formation of the 1.1×10^{-8} sec.[3] metastable state of Ta^{181}. In addition, L internal conversion electrons of the 85 and 80 kev transitions following the β-decay of Tm^{170} and Ho^{166} respectively were used for calibration.

Measurements of the radiation of other isomeric transitions with similar energy and lifetime have shown that the amount of internal con-

---

[15] F. K. McGowan, Phys. Rev. 79, 404 (1950).

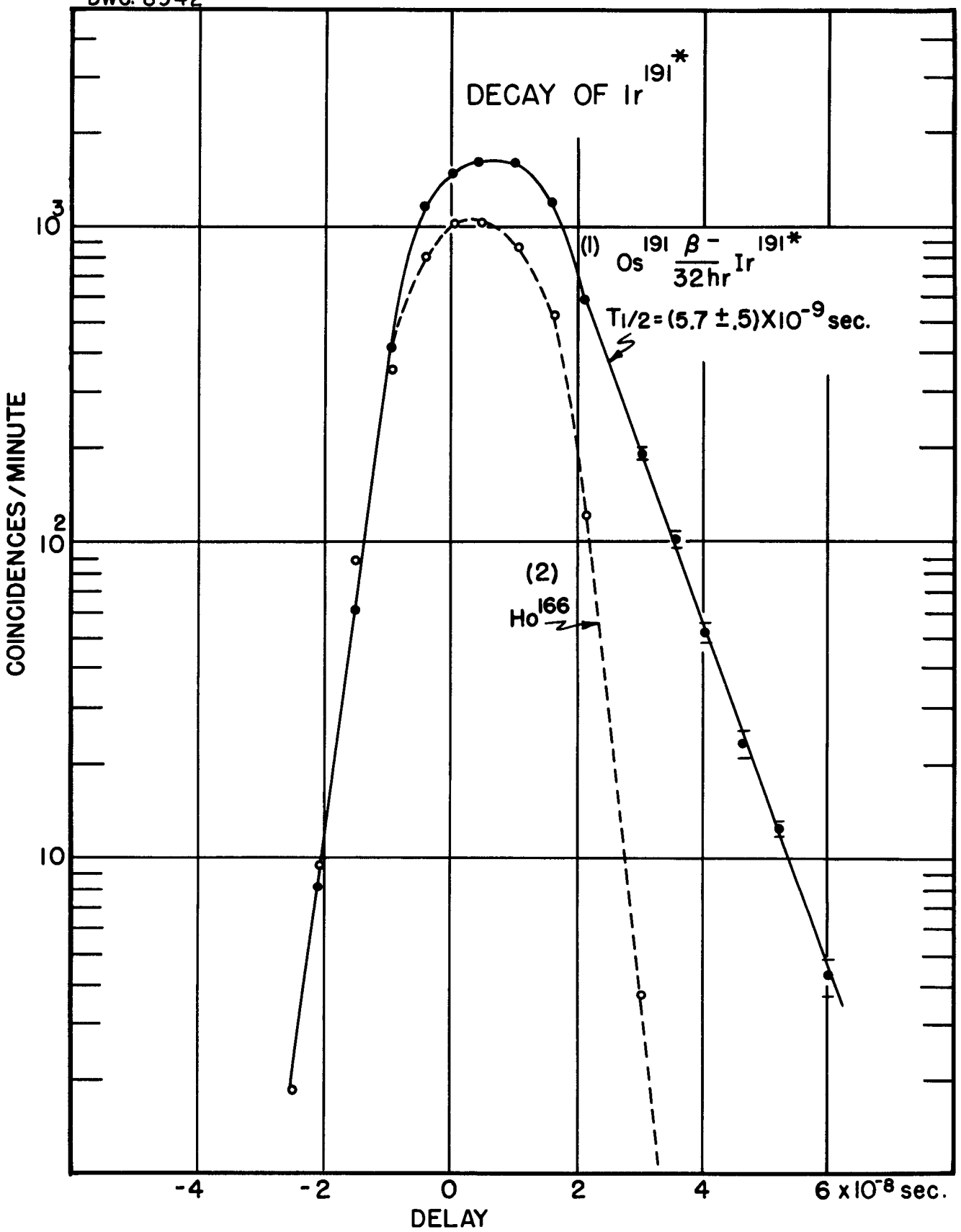

FIG. 17

THE NUMBER OF DELAYED COINCIDENCES AS A FUNCTION OF DELAY TIME

UNCLASSIFIED
DWG. 8941

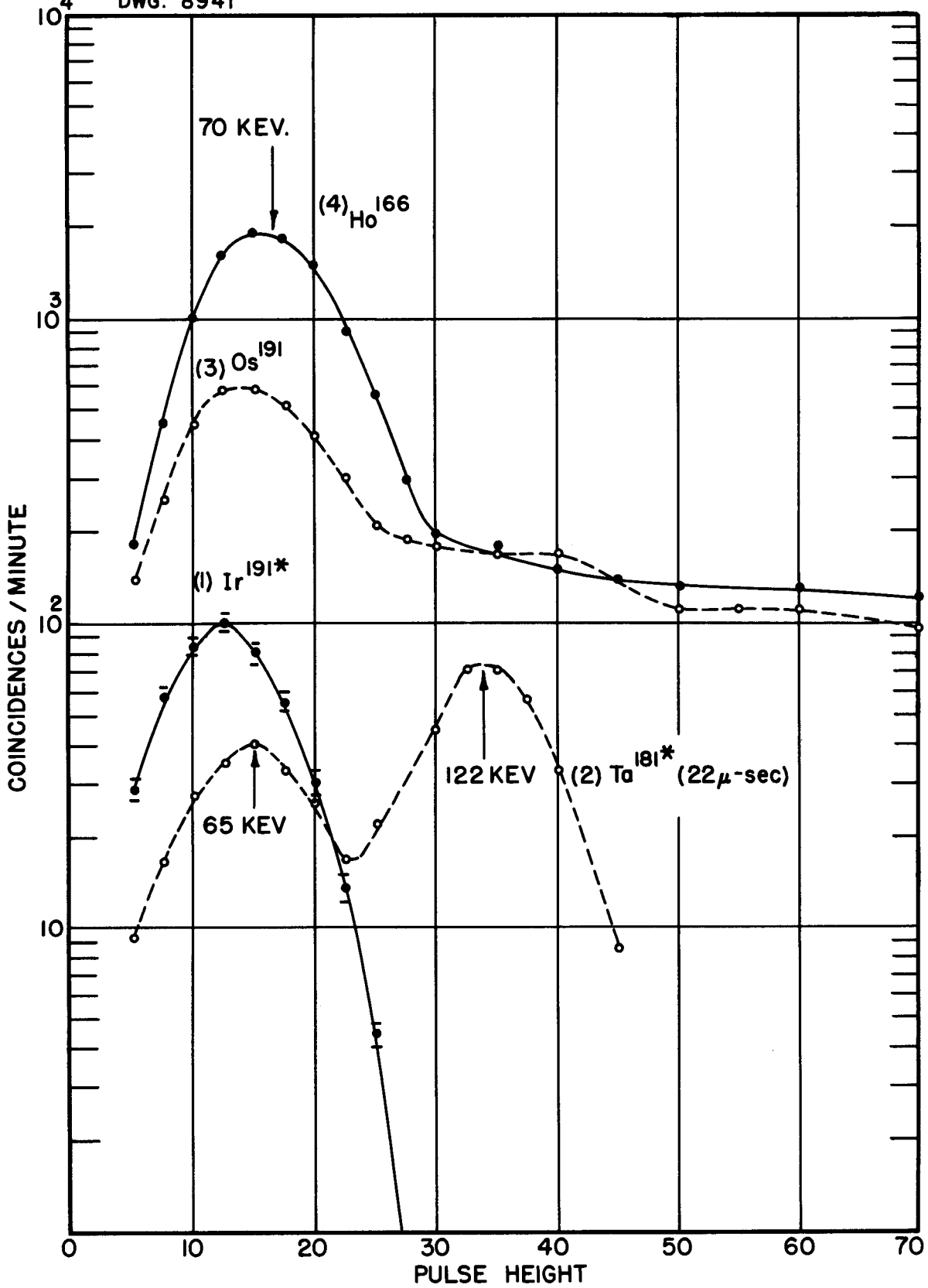

FIG. 18

COINCIDENCE COUNTING RATE AS A FUNCTION OF PULSE HEIGHT

version in the L shell is comparable to that in the K shell. Since only one internal conversion line appears in the spectrum of the decay of Ir^{191*}, the peak probably corresponds to L shell internal conversion. The energy of the transition is then (65 ± 5) kev which is less than the K shell electron binding energy (76 kev).

The spectrum of the radiation announcing the formation of the metastable state appears to be a single beta ray distribution. Fig. 19 is the spectrum of the total radiation from Os^{191} obtained by counting single counts. Since the "single count" distribution and the distribution obtained by counting delayed coincidences are alike for energies above 400 kev and more data are available from the "single count" spectrum, a Fermi-Kurie plot of the "single count" data above 300 kev was made. This is shown in Fig. 20 and the maximum energy of the beta spectrum is (1.05 ± 0.03) Mev. The ft-value of this β transition is 1.7×10^7 which places the transition in the first forbidden empirical classification on the basis of the Gamow-Teller selection rules[16] ($\Delta J = 0, \pm 1, \pm 2$ and parity change lead to first forbidden transitions). However, for Z large and $\Delta J = 0, \pm 1$ the spectrum is such that a first forbidden transition exhibits an allowed shape on a conventional Fermi-Kurie plot. That is, the correction factors for this case are relatively energy independent.[17] However, for $\Delta J = 2$ the conventional Fermi-Kurie plot will not yield a straight line but instead is concave to the

---

[16] Emil J. Konopinski, Rev. Mod. Phys. 15, 209 (1943).

[17] L. P. Langer, Phys. Rev. 77, 50 (1950).

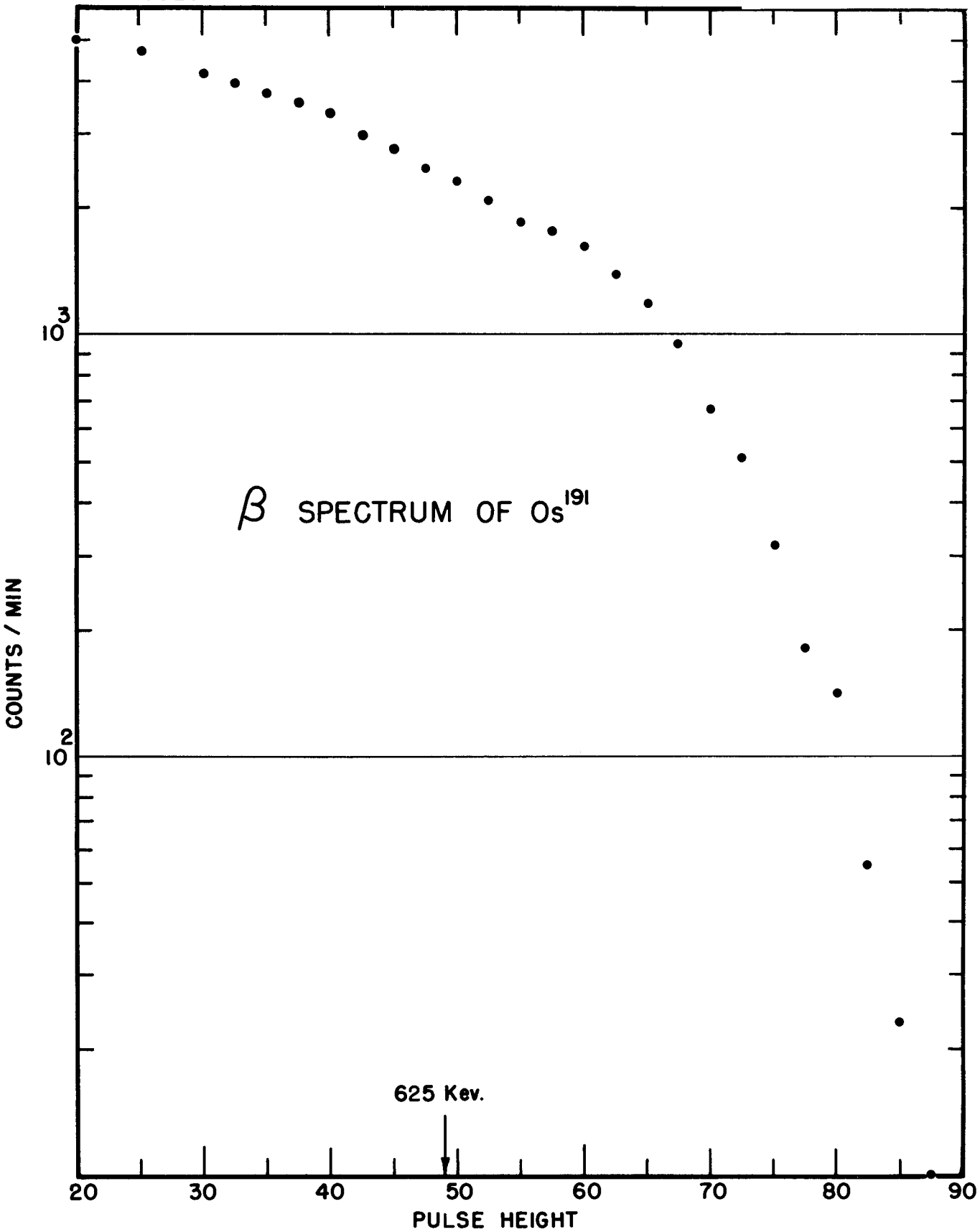

FIG. 19

PULSE HEIGHT DISTRIBUTION OF β-RADIATION FROM Os^{191}

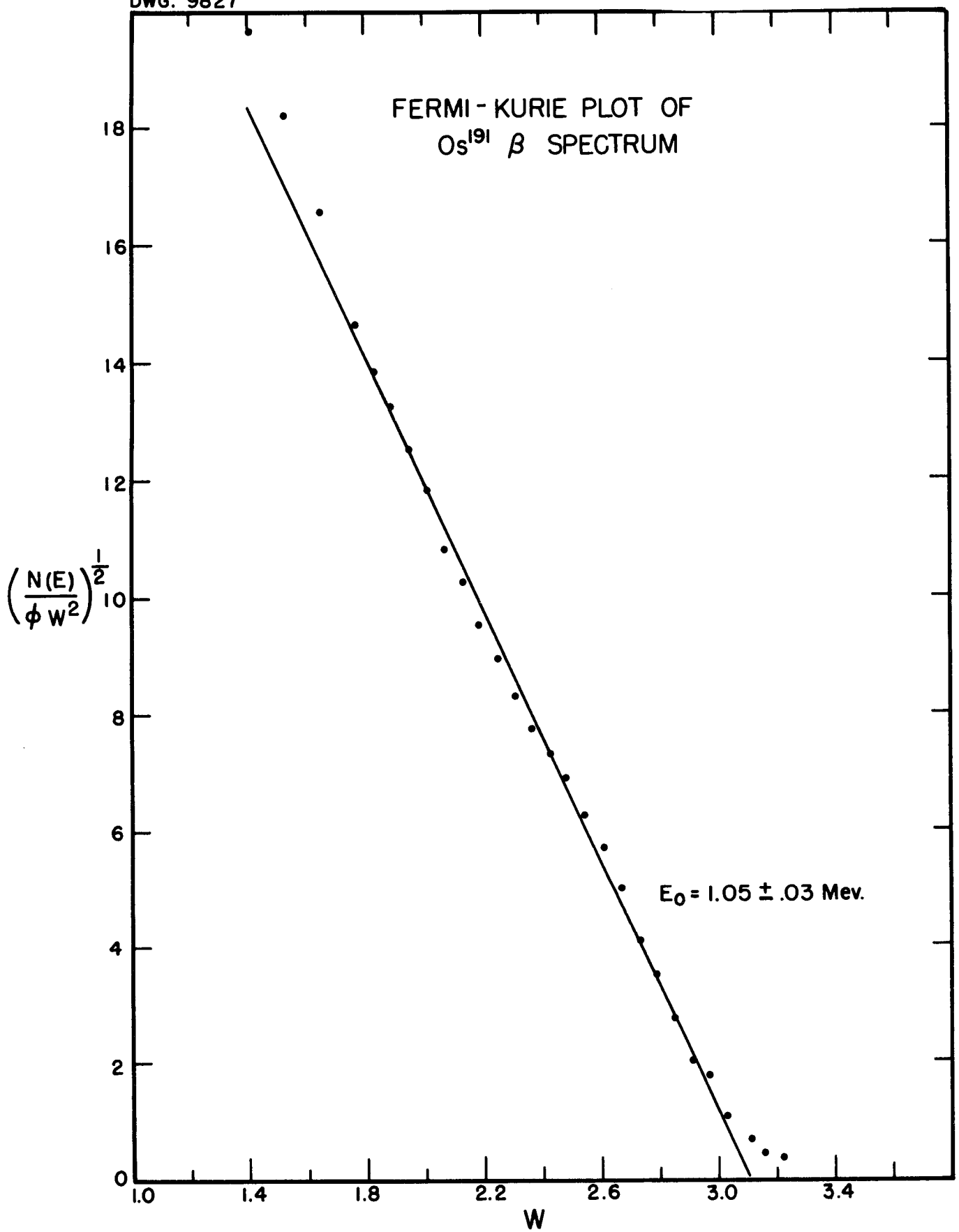

FIG. 20

FERMI-KURIE PLOT OF Os^{191} β SPECTRUM

energy axis at the higher energy end of the spectrum. Also recently, Nordheim[18] has pointed out that transitions for odd-A nuclei with change in parity and $\Delta J = \pm 2$ have log (ft) values mostly between 8 and 9. Transitions with change in parity and $\Delta J = 0, \pm 1$ are first forbidden with log (ft) mostly in the range 6.5 to 7.5. Thus, the above β-transition is probably first forbidden with $\Delta J = 0, \pm 1$ and change in parity.

The decay curve of Fig. 17 was obtained with the analyzer gate accepting only small pulses corresponding to the 65 kev transition while the other channel was excited by the high energy β-rays which gave rise to large pulses. Since the form of delayed coincidence resolution curves for originally simultaneous events depends essentially upon the distribution in amplitude of the original pulses, it is conceivable that the 65 kev transition is not metastable with respect to the β-ray event. In order to rule out this possible instrumental effect on the resolution curve obtained with a coincidence system using amplifiers of finite rise time, a number of other sources were tested; namely, the 1.84 Mev β-decay of Ho^{166} followed by a 80 kev internally converted γ-ray, the 900 kev β-decay of Tm^{170} followed by a 84 kev internally converted γ-ray, and the 1.076 Mev β-decay of Re^{186} followed by a 138 kev internally converted γ-ray. Curve (2) in Fig. 17 shows a typical resolution curve obtained with Ho^{166}. In each case the resolution curve obtained with analyzer accepting only the low energy internally converted γ-ray was was symmetrical with the leading and trailing edge being roughly

---

[18] L. W. Nordheim, Phys. Rev. 78, 294 (1950).

exponential over three decades corresponding to a half-period 2×10^{-9} sec. In Fig. 18 curves (3) and (4), which are the low energy portion of the spectra of simultaneous events from Os^{191} and Ho^{166} respectively, show clearly the similarity of the two distributions in amplitude of the original pulses from the scintillation detector.

As an additional check for validity of this isomeric state in Ir^{191} the delayed coincidence resolution curve of Fig. 17 was analyzed by a graphical method which is analogous to a method of analysis recently reported by Newton[19] and Bay.[20] For convenience and clarity Newton's notation will be used in the discussion here. Also, since Newton's analysis is not directly applicable to the resolution curves of Fig. 17, only the first two equations of his method will be considered to describe a graphical analysis of a delayed coincidence resolution curve.

In the ideal experiment, one desires to excite one channel of the apparatus by the parent radiation or the radiation announcing an excited state in a nucleus and to excite the other channel by radiation emitted in the decay of the excited state whose lifetime is to be measured. The ideal experiment is achieved by means of a delayed coincidence spectrometer. If the excited state has a lifetime much too short to be measured by the coincidence circuit, one obtains the "prompt coincidence resolution curve", $P(x)$, where x is the delay time introduced in the delayed coincidence apparatus. If there is a measurable lifetime, the

---

[19] T. D. Newton, Phys. Rev. 78, 490 (1950).

[20] Z. Bay, Phys. Rev. 77, 419 (1950).

daughter emission has a probability f(t) dt of occurring t seconds after the parent emission. From experiment one obtains in this case the "delayed coincidence resolution curve", F(x). If F(x), P(x), and f(t) are all normalized as differential probability distributions, then

$$F(x) = \int_{-\infty}^{\infty} f(t)\, P(x - t)\, dt. \tag{14}$$

If the excited state has a mean life $\tau = 1/\lambda$, then f(t) = 0 for t < 0 and $f(t) = \lambda e^{-\lambda t}$ for t > 0. Putting y = x - t, then (14) becomes

$$F(x) = \lambda e^{-\lambda x} \int_{-\infty}^{x} e^{+\lambda y}\, P(y)\, dy. \tag{15}$$

Since the energy resolution of the scintillation spectrometer is relatively poor compared to the best magnetic beta-ray spectrometers, the "delayed coincidence resolution curve" in Fig. 17 for $Os^{191} \longrightarrow Ir^{191}$ is F(x) plus possibly some prompt event counts not related to $Os^{191} \longrightarrow Ir^{191*}$ decay and prompt events due to scattering from one detector to the other as mentioned in the Chapter V. Prompt events due to scattering are, of course, greatly reduced in number when the delayed coincidence scintillation spectrometer is used, but there are still a few present to distort possibly the desired F(x) distribution.

"Delayed coincidence resolution curves" F(x) were calculated graphically using for P(x) curve (2) of Fig. 17 and using various values of λ equal to or near that to be obtained in the usual way from the slope of curve (1) at large positive delays. The prompt curve P(x) represents the response of the apparatus to simultaneous emission of particles of the same kind and energy that gave curve (1). The resulting

F(x) curves were normalized with respect to curve (1) at a large positive delay (5×10^{-8} sec.). The difference between curve (1) and F(x) should yield a "prompt curve" of the prompt events not related to $Os^{191} \longrightarrow Ir^{191*}$ and those due to scattering. The value of λ that led to a "residual prompt curve" with the leading and trailing edge symmetrical about zero delay was chosen as the best value for the decay constant of Ir^{191*}.

From the energy and lifetime of this isomeric state the transition corresponds to a forbiddenness $\ell = 2$ and is probably an electric quadrupole transition. It appears from the spectrum of delayed radiation in Fig. 18 curve (1) that no other γ-rays follow in cascade with the decay of Ir^{191*}. At least for the $Os^{191} \longrightarrow Ir^{191*}$ decay the disintegration is certainly a beta decay to the metastable state which decays directly to the ground state of Ir^{191}.

$$Cd^{111*} \ (8 \times 10^{-8} \text{ sec.})$$

The existence of the short-lived isomeric state in Cd^{111} $(8 \pm 1) \times 10^{-8}$ sec. was confirmed using sources of Cd^{111*} (48 min.) produced by (n,γ) reaction on a sample of enriched Cd^{110}. Deutsch and Stevenson observed the metastable state following the K capture decay of In^{111}. Fig. 21 shows the number of delayed coincidences plotted as a function of delay time obtained with a source of Cd^{111*} which decays predominately by internal conversion of a 148 kev γ-ray. This decay curve of the metastable state corresponds to a half-life of $(8 \pm 1) \times 10^{-8}$ sec. which is in good agreement with the originally reported value. Sources

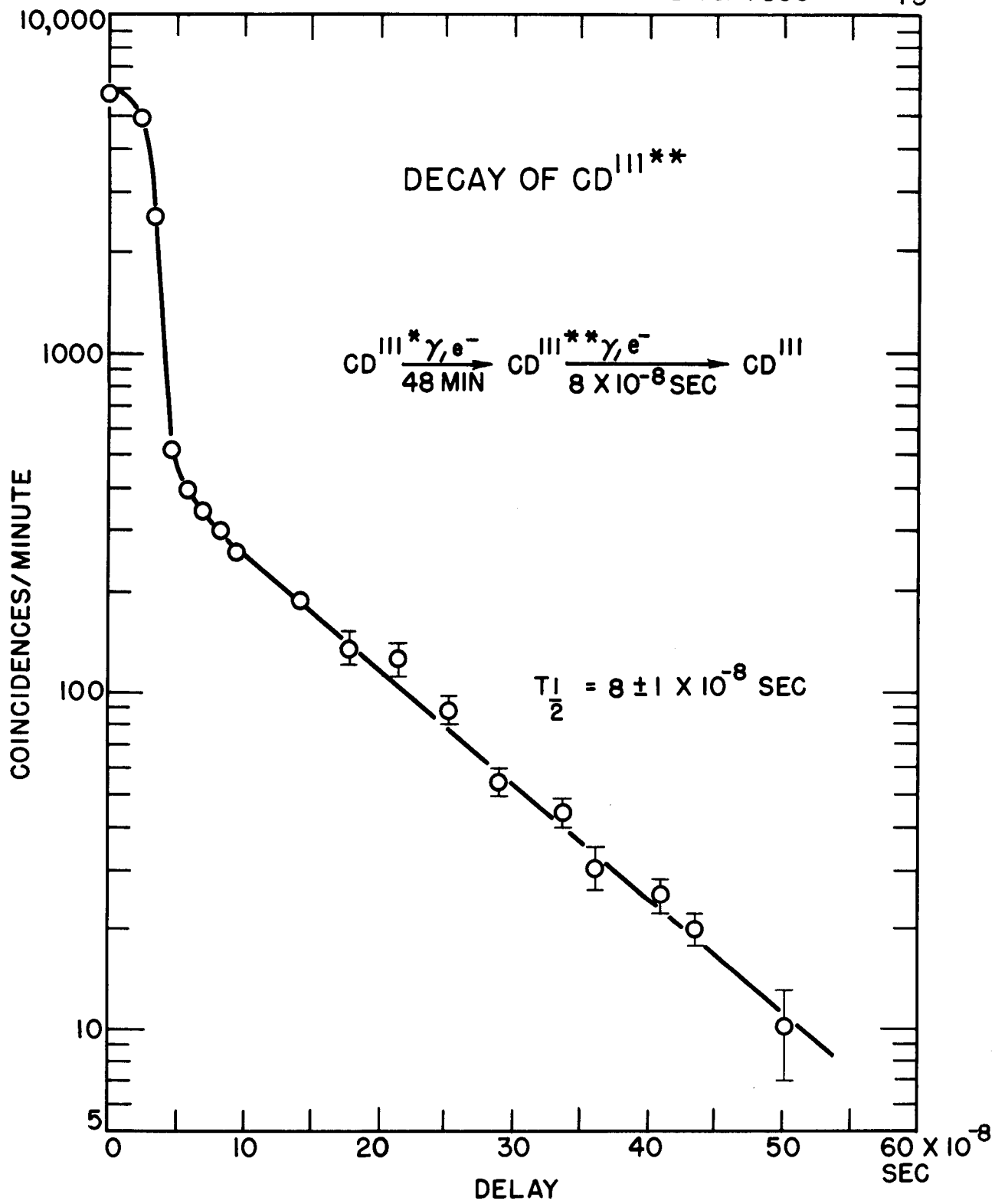

FIG. 21

THE NUMBER OF DELAYED COINCIDENCES AS A FUNCTION OF DELAY TIME

of Ag^{111} (7.5 da.) which decays by β^- were examined for delayed coincidences but none were observed above the expected random rate indicating that Ag^{111} decays predominantly to the ground state of Cd^{111}.

The delayed coincidence scintillation spectrometer was used to investigate the radiation resulting from the decay of the isomeric state. The lower curve of Fig. 22 shows the spectrum of the delayed radiation obtained by counting delayed coincidences in a small height interval as a function of pulse height. The solid curve represents the electron spectrum after subtracting the Compton electron distribution of the γ-ray from the gross spectrum. The K internal conversion electron line corresponds to a 247 kev transition. For comparison the upper curve shows the spectrum of the total radiation from Cd^{111} obtained by counting single counts. The internal conversion peak for the 247 kev transition is hardly visible. The broad peak at 30 units on the pulse height scale is the unresolved K and L internal conversion lines of the 148 kev transition from the decay of the 48 minute isomeric state.

A disintegration scheme for Ag^{111}, Cd^{111}, and In^{111}, which includes the results of magnetic spectrometer measurements by other authors,[20,21] is presented in Fig. 23. In effect, this was the first isotope in which two isomeric states have been observed. Since the observation of this case, Goldhaber et al. have observed a similar case

---

[20] F. Boehm, O. Huber, P. Marmier, P. Preiswerk, and R. Steffen, Helv. Phys. Acta 22, 69 (1949).

[21] A. C. Helmholz, R. W. Hayward, and C. L. McGinnis, Phys. Rev. 75, 1469A (1949).

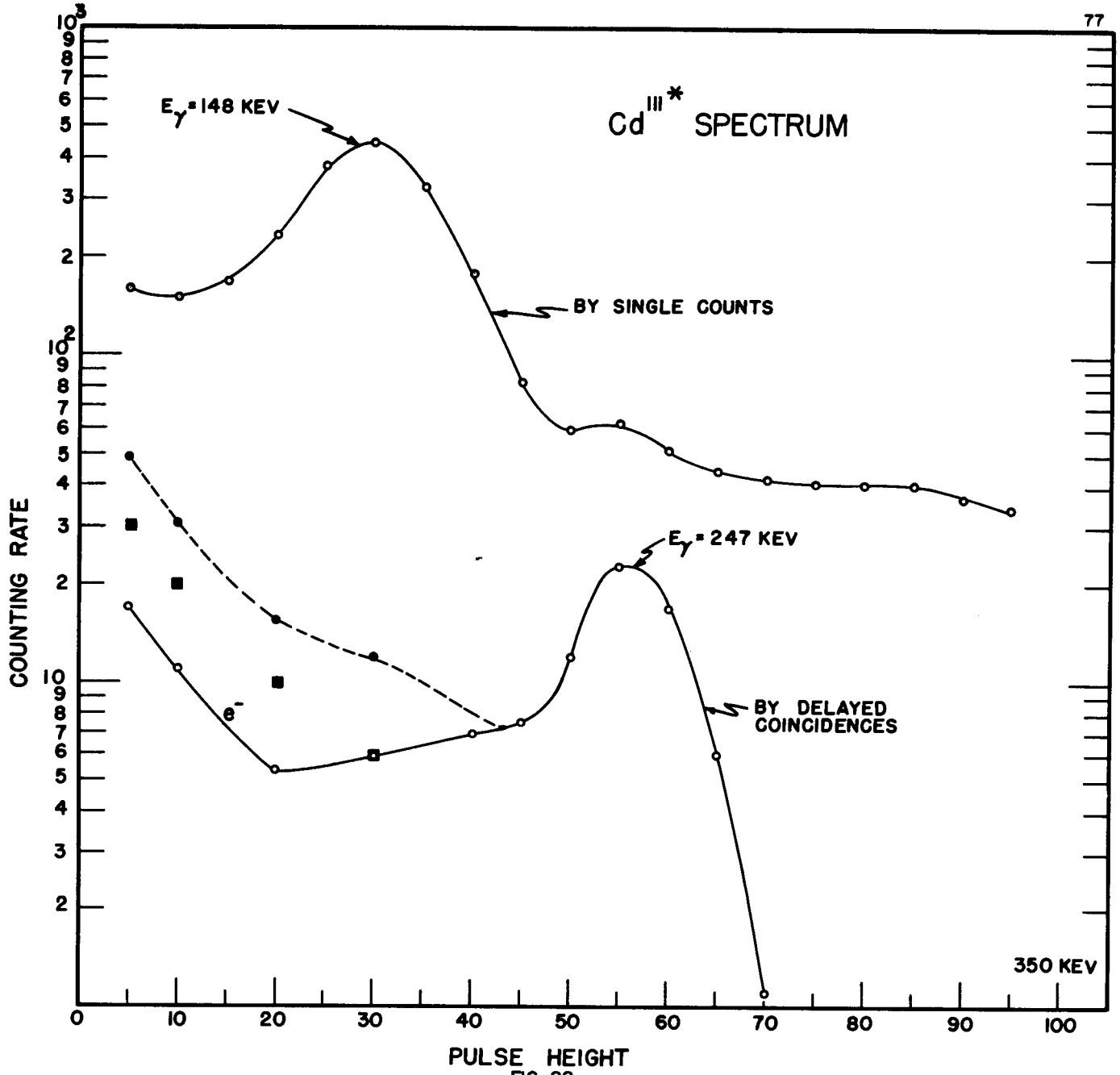

FIG. 22

PULSE HEIGHT DISTRIBUTION OF THE RADIATION FROM Cd^{III*}

UNCLASSIFIED
DWG. 7685

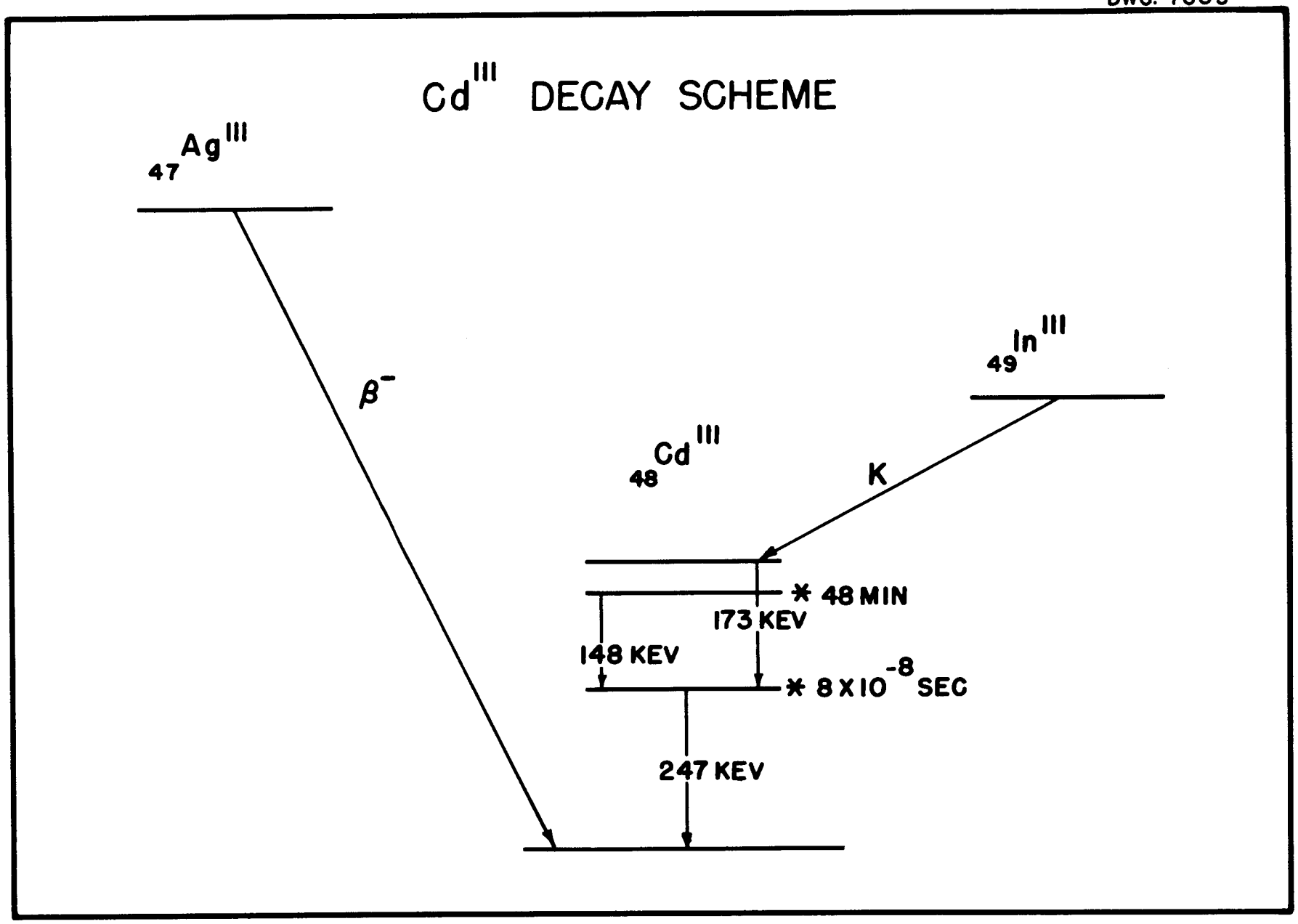

FIG. 23

A DISINTEGRATION SCHEME FOR Ag^{111}, Cd^{111}, AND In^{111}

in Pb^{204}. Axel and Dancoff[22] have classified the 48 minute isomeric state to be $\ell = 4$ forbiddenness on the basis of lifetime and energy of the transition. This forbiddenness corresponds to a $\Delta J = 3$ or 4 units of $\hbar$ of angular momentum depending on the parity of the initial and final states involved in the transition. Likewise on the basis of energy and lifetime the 8×10^{-8} sec. short-lived isomer falls between forbiddenness $\ell = 2$ and 3 but is slightly nearer $\ell = 3$ which requires $\Delta J = 2$ or 3 units of $\hbar$ of angular momentum. Since both Boehm and Helmholz have measured the internal conversion coefficients for the 247 and 173 kev transitions, it is possible to check on the ℓ value assignment by comparing the experimental data with theoretical K shell internal conversion coefficients.[23] Although the experimental values differ by a factor of two, the agreement with theoretical values appears to be best for a mixture of magnetic dipole and electric quadrupole radiation for both transitions. This means that both transitions are parity forbidden and $\ell = 2$. Since the lifetime of a state for γ-ray emission from the semiquantitative theory goes as $\left(\frac{137}{W}\right)^{2\ell+1}$, the initial level of the 173 kev transition should be metastable with a period larger than the 247 kev transition. However, no one has observed this state to be metastable. Since the x-rays resulting from the K capture decay of In^{111} are 23 kev, it is conceivable that previous experiments failed to detect the x-rays, in which case there is no evidence to indicate

---

[22] P. Axel and S. M. Dancoff, Phys. Rev. 76, 892 (1949).

[23] M. E. Rose, G. H. Goertzel, B. I. Spinrad, J. Harr, and P. Strong, Phys. Rev. 76, 1883 (1949). Tables of K shell internal conversion coefficients privately circulated.

that the initial state of the 173 kev transition is or is not metastable. In this survey In^{111} has not been investigated because it is not possible to prepare it by neutron activation.

There is one additional piece of information concerning the 173 and 247 kev transitions. Boehm and Walter[24] have measured the angular correlation of the successive γ-rays and their results indicate that an anisotropy exists. It appears that the angular momentum assignments of the three states are either 1/2, 3/2, and 5/2 or 1/2, 5/2, and 7/2 in the direction of increasing excitation. The experimental uncertainty in their experiment was of the order of $\sim 50\%$ and this measurement should be repeated. In any case their results indicate a forbiddenness $\ell = 2$ for both transitions. Another point of interest is that the anisotropy is not destroyed even though the intermediate state is metastable. Normally the lifetime of intermediate state must be short compared to the period of precession of the nuclear moment in the magnetic field arising from the orbital electrons. In the case of Cd the normal atomic state is $^1S_0$ and therefore no h.f.s. splitting is expected. Thus, the anisotropy is not destroyed.

It appears that better experimental internal conversion coefficients are needed to determine the forbiddenness of the isomeric transition, and an angular correlation experiment should be done with greater precision to yield the assignment of the angular momenta of the states.

Ta^{181*} (10^{-8} sec. and 2.2×10^{-5} sec.)

---

[24] F. Boehm and M. Walter, Helv. Phys. Acta 22, 378 (1949).

In effect, the first short-lived isomer to be found[25] by the method of delayed coincidences was an excited state of Ta^{181}. More recently a second metastable state in Ta^{181} with a half-life of 1.1×10^{-8} sec. was observed by Barber.[3] This result has been confirmed and the half-life measured is in good agreement with the value above.

Though numerous authors have investigated Hf^{181}, there is no general agreement as to the disintegration scheme. A majority of the investigators have, however, interpreted their data to support a level scheme first proposed by Chu and Wiedenbeck[26] and amended recently by Cork et al.[27] However, Deutsch and Hedgran[28] have obtained results from a delayed coincidence spectrometer that seemed to rule out the decay scheme of Chu and Wiedenbeck. In Fig. 24 level scheme A is the proposed energy level scheme by Chu and Wiedenbeck and level scheme B is one proposed on the basis of experimental results to be presented below.

Both the radiation preceding and following the decay of the 22 μsec. and the 10^{-8} sec. isomeric states have been measured with the delayed coincidence scintillation spectrometer. The spectrum of the radiation preceding the 22 μsec. metastable state appears to be a simple β-ray distribution unaccompanied by γ-radiation or internal conversion electrons. This supports previous conclusions on the preceding

---

[25] S. DeBenedetti and F. K. McGowan, Phys. Rev. 70, 569 (1946).

[26] K. Y. Chu and M. L. Wiedenbeck, Phys. Rev. 75, 226 (1949).

[27] J. M. Cork, A. E. Stoddard, W. C. Rutledge, C. E. Branyan, and J. LeBanc, Phys. Rev. 78, 299 (1950).

[28] M. Deutsch and A. Hedgran, Phys. Rev. 79, 400 (1950).

UNCLASSIFIED
DWG. 9854

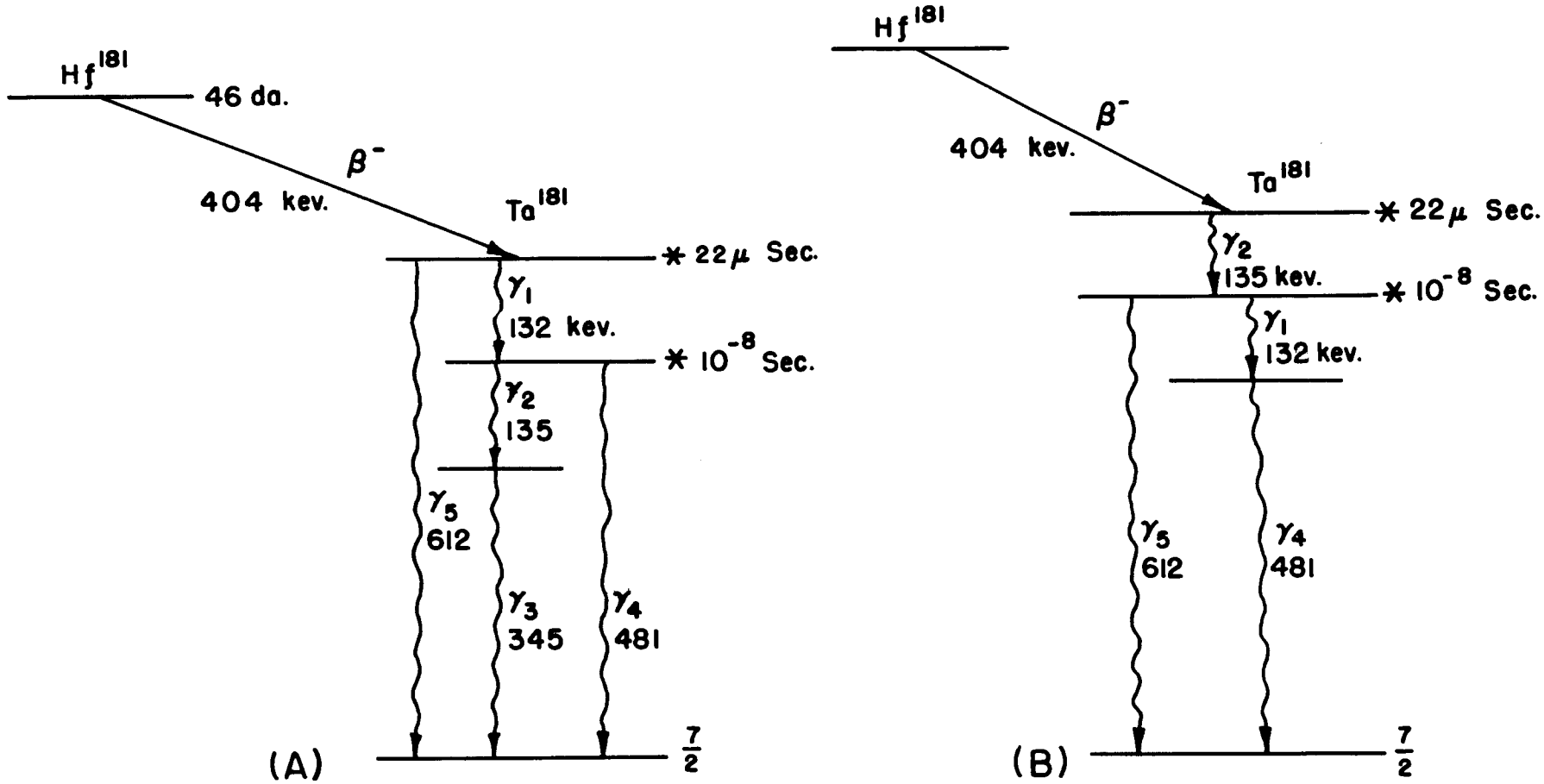

LEVEL SCHEMES FOR Ta^{181}

FIG. 24

DISINTEGRATION SCHEMES FOR Hf^{181}

radiation. Fig. 25 shows the spectrum of the radiation that follows the decay of the 22 μsec. metastable state. In this case the 132 kev radiation is not resolved from the 135 kev radiation. Thus, the K and (L + M) peaks in the internal conversion electron spectrum represent the sum of the internal conversion of γ_1 and γ_2. From the area under the peaks one obtains the ratio of $(K_1 + K_2)$ to $(L_1 + M_1 + L_2 + M_2)$ to be 1.4 ± 0.2. The spectrum of the γ-rays above 150 kev shows clearly that the 481 kev transition follows the 22 μsec. period but it is not clear whether any 345 kev radiation follows the decay of the 22 μsec. metastable state.

Since the radiation preceding the 22 μsec. metastable state is unaccompanied by γ-radiation, the 10^{-8} sec. metastable state must lie below the 22 μsec. level. A study of the radiation preceding and following the 10^{-8} sec. period should yield additional information concerning the level scheme of Ta^{181}. Fig. 26 shows the internal conversion electron spectrum of the radiation announcing the formation of the 10^{-8} sec. state. The K and (L + M) peaks correspond to the internal conversion electron lines of γ_2. The ratio of K_2 to $(L_2 + M_2)$ obtained from the area under the peaks is 0.5 ± 0.1. On the basis of lifetime, energy, and K to (L + M) ratio the transition is probably $el(2)^3$-pole radiation. Fig. 27 shows the lower energy spectrum of the radiation following the 10^{-8} period taken with the same source and geometrical conditions as the spectrum of the preceding radiation. The K and (L + M) peaks of curve (2) correspond to the internal conversion electron lines of γ_1. The ratio of K_1 to $(L_1 + M_1)$ from the area under the peaks is 6 ± 1. On the basis of lifetime, energy, and K to (L + M) ratio the transition is probably a combination of $el(2)^2$-pole and $mag(2)^1$-pole radiation. Also,

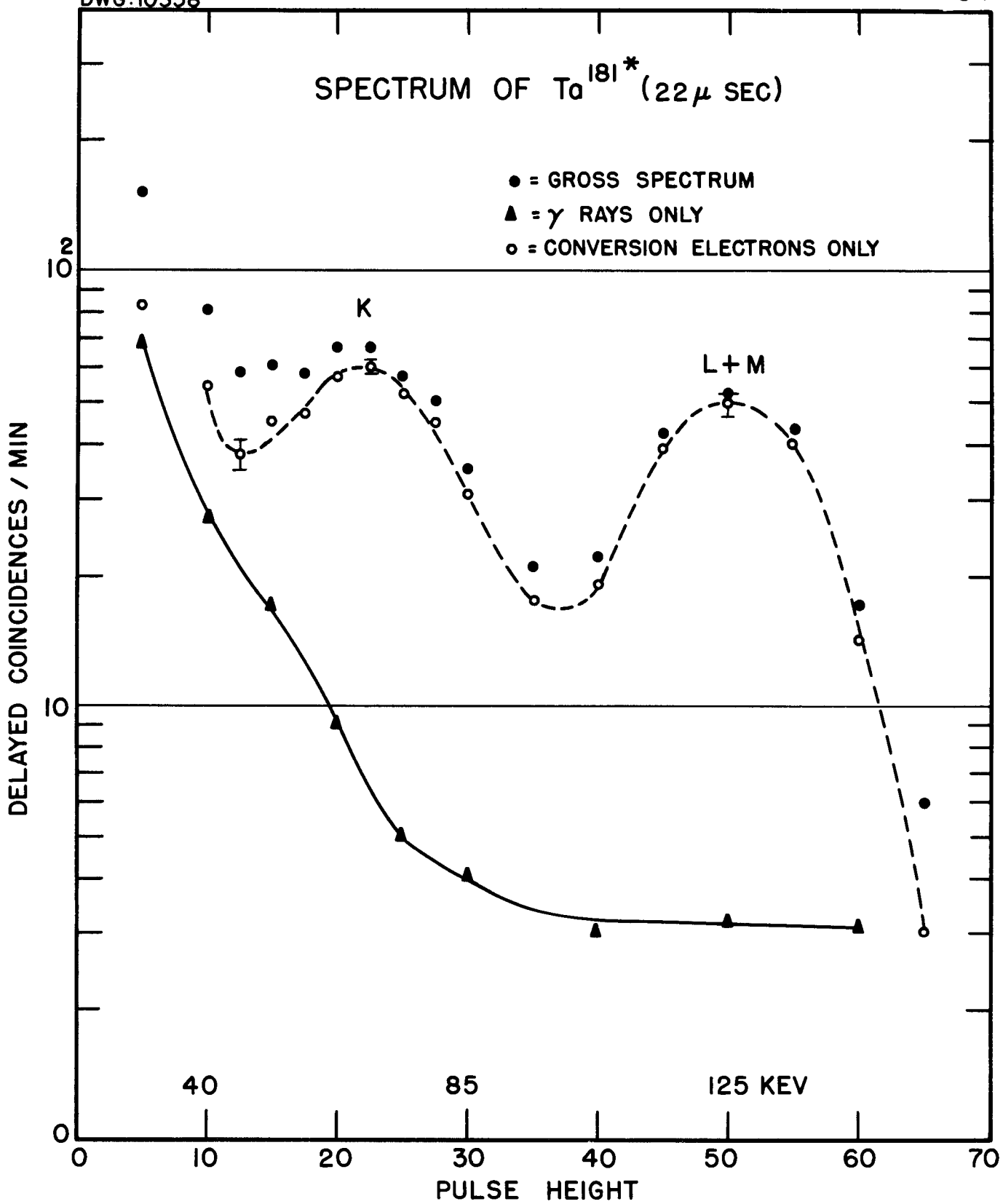

FIG. 25
PULSE HEIGHT DISTRIBUTION OF RADIATION FOLLOWING THE DECAY OF Ta^{181*} (22 μ sec.)

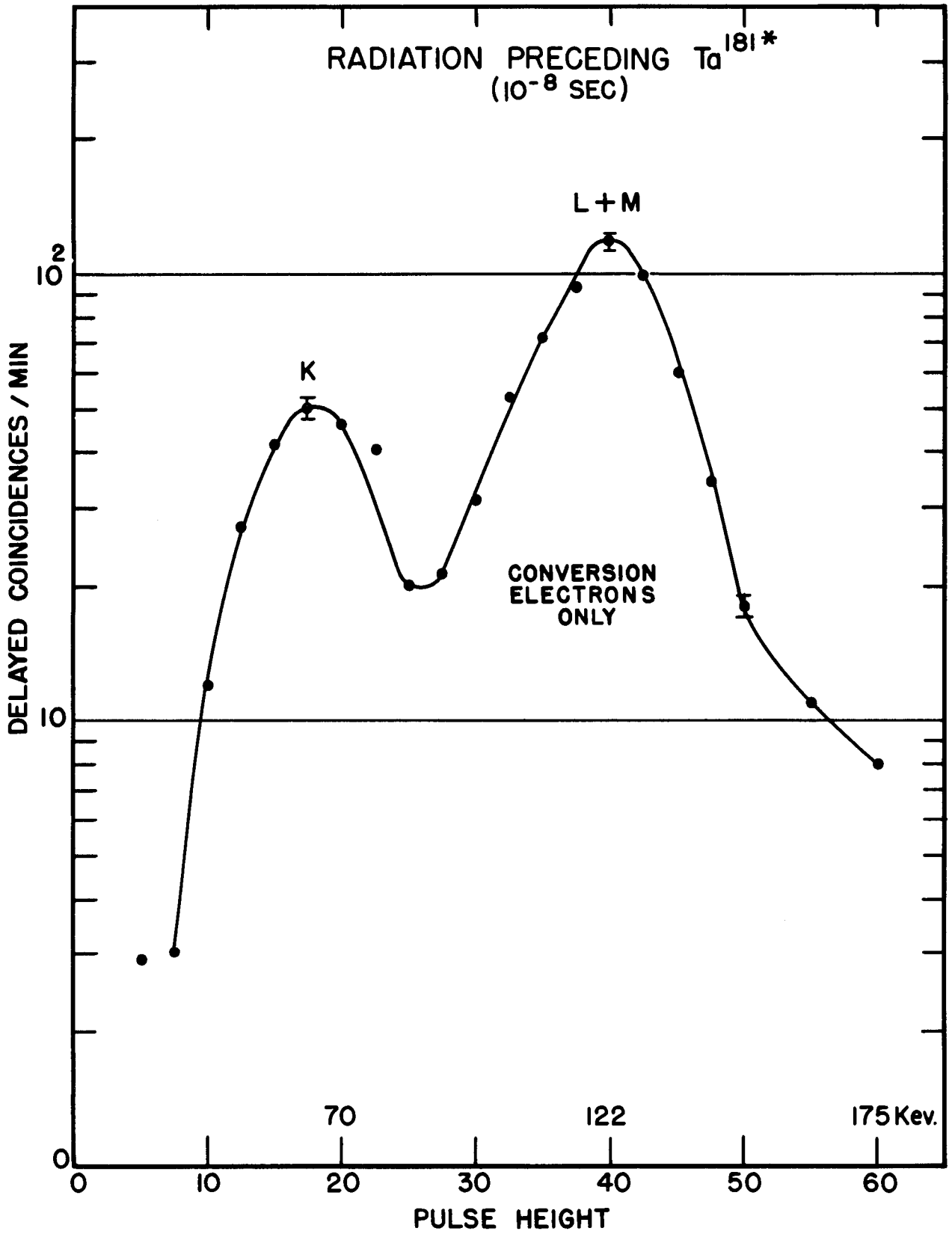

FIG. 26

PULSE HEIGHT DISTRIBUTION OF RADIATION PRECEDING Ta^{181*} (10^{-8} sec.)

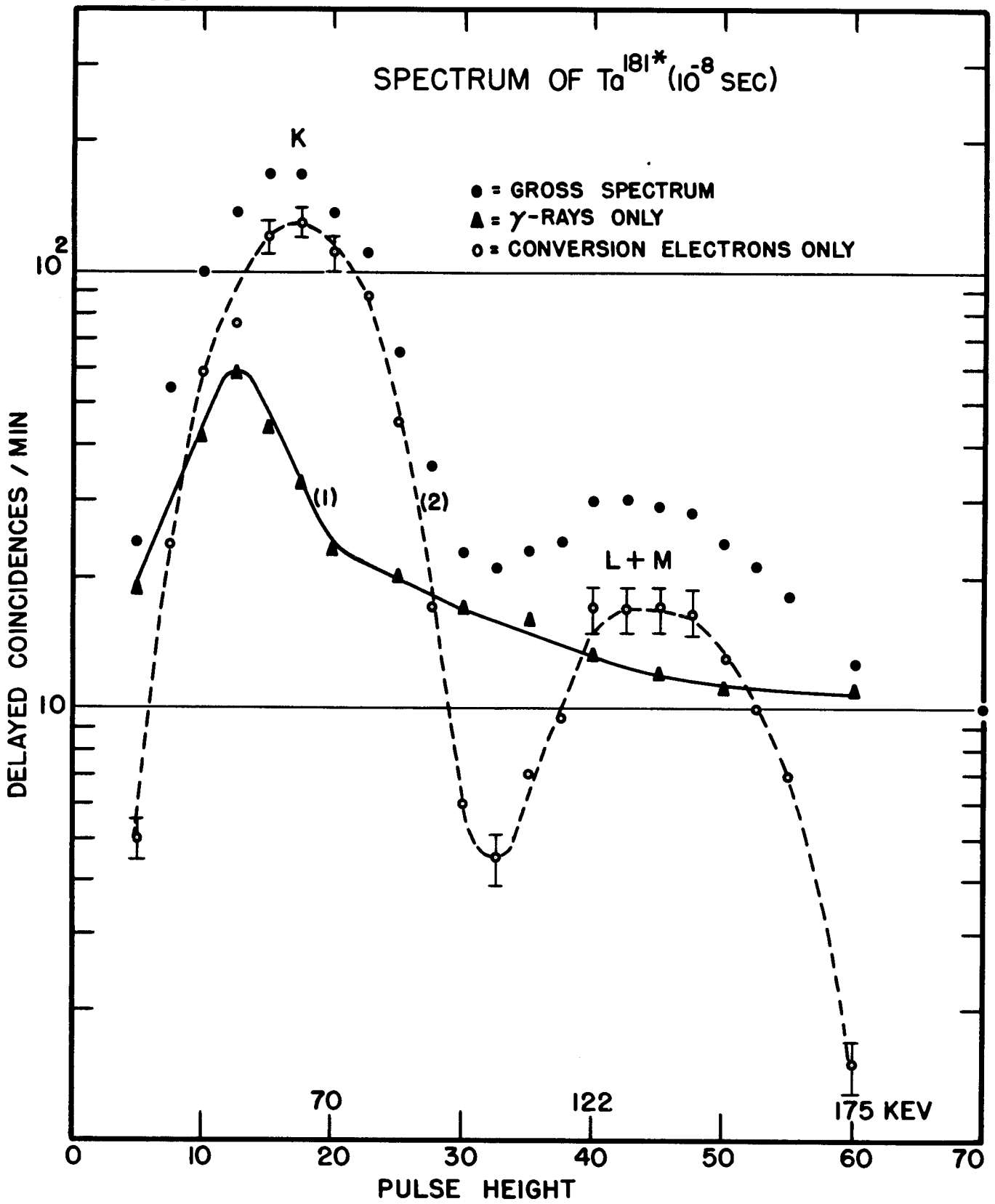

FIG. 27
PULSE HEIGHT DISTRIBUTION OF LOWER ENERGY RADIATION FOLLOWING THE DECAY OF Ta^{181*} (10^{-8} sec.)

from Fig. 26 and 27 it is possible to obtain the ratio of $(K_1 + K_2)$ to $(L_1 + M_1 + L_2 + M_2)$ from the area under the peaks. The value obtained in this manner is 1.4 which is in good agreement with the direct measurement from the spectrum of the radiation following the 22 μsec. period.

The higher energy spectrum of the radiation following the 10^{-8} sec. period is shown in Fig. 28. The peak at 420 kev corresponds to the unresolved K and L internal conversion electron lines of the 481 kev transition. Curve (2) is the Compton recoil electron distribution of the γ-radiation. The endpoint of the distribution at 315 kev is attributed to 481 kev γ-radiation. Between 125 to 225 kev the Compton recoil electron distribution was carefully examined many times for the possible presence of 345 kev γ-radiation following the 10^{-8} sec. period. In some cases it was difficult to rule out a possible 10 to 15% branching by the route of the 135 kev and 345 kev transitions of level scheme A. However, the data shown in Fig. 28, which were taken under slightly better conditions, appear to be a distribution for a single γ-ray. This was shown to be the case by comparing this distribution with a Compton distribution obtained from the 411 kev γ-radiation following the β-decay of Au^{198}.

Chu and Wiedenbeck have determined the number of conversion electrons emitted in the various transitions per β-disintegration. In the case of γ_1 and γ_2 these fractions are 0.56 and 0.22 for K shell internal conversion. Thus, if the branching through the 135 kev and 345 kev transitions was 15%, then the number of conversion electrons from K shell conversion per initial state formed of the 135 kev transition is

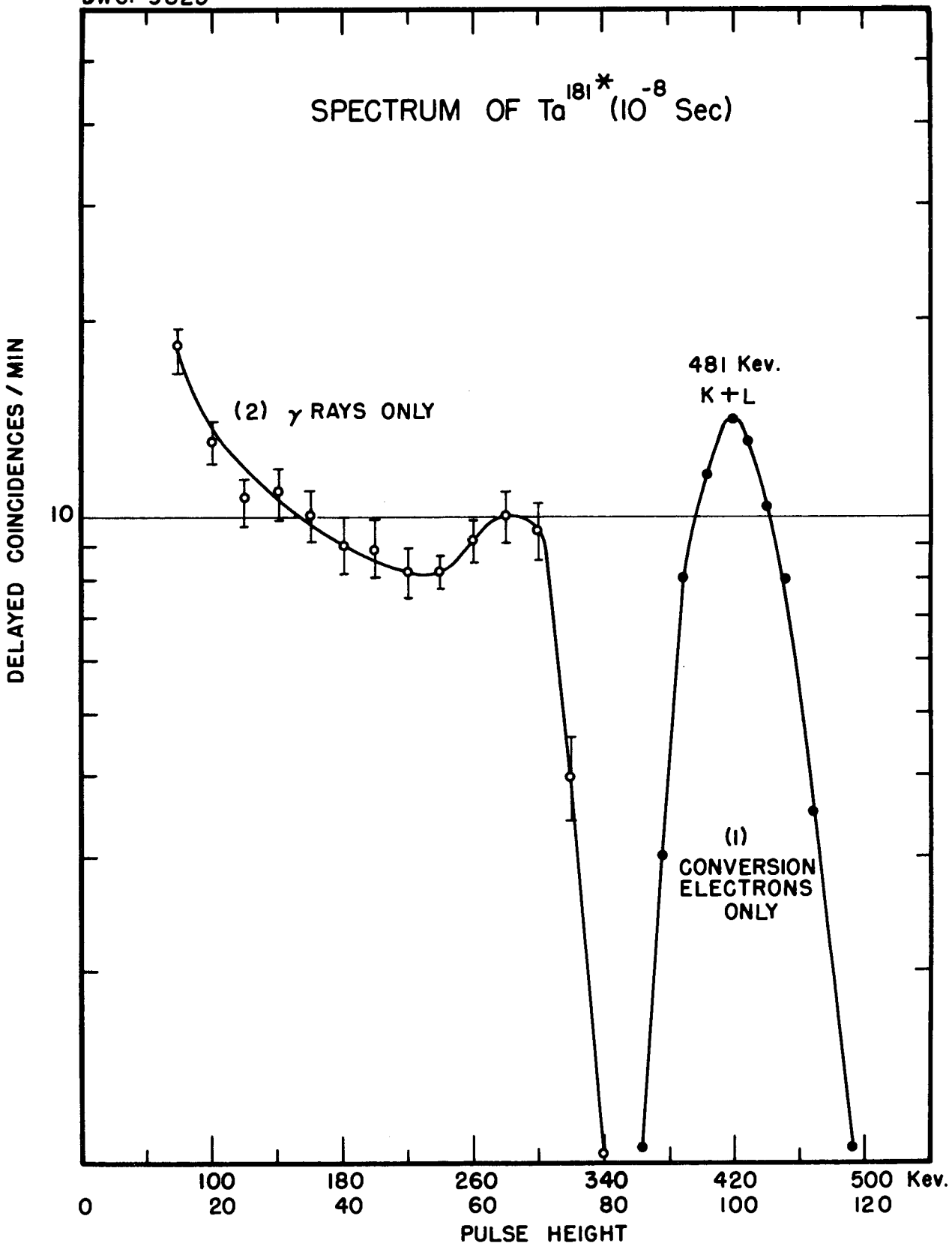

FIG. 28

PULSE HEIGHT DISTRIBUTION OF HIGHER ENERGY RADIATION FOLLOWING THE DECAY OF Ta^{181*} (10^{-8} sec.)

about 1.5. This is absurd. Thus, one is forced to the conclusion that the 345 kev transition is not related to the β-decay of Hf^{181}.

From the standpoint of lifetime and energy of the transition following the 10^{-8} sec. period, level scheme A is consistent only if the 481 kev transition corresponds to forbiddenness $\ell = 3$ and the 135 kev transition to forbiddenness $\ell = 2$. As a check on the assignment of forbiddenness for the 481 kev transition there are the Chu and Wiedenbeck data on the amount of internal conversion in the K shell. This value is .025 which has been corrected for a possible 85% branching. The theoretical values[23] are .045 for $el(2)^3$-pole and .165 for $mag(2)^2$-pole. On the other hand the theoretical values are .017 for $el(2)^2$-pole and .060 for $mag(2)^1$-pole. Therefore, the assignment of forbiddenness $\ell = 3$ is probably incorrect on the basis of the internal conversion coefficient data. The lower multipole order assignment lends support in favor of level scheme B. The 481 kev transition is probably electric quadrupole radiation and the 132 kev transition is probably the 10^{-8} sec. isomeric transition corresponding to forbiddenness $\ell = 2$.

In addition to the 46 day Hf^{181} activity Burson et al.[29] have observed a 5.5 hour period presumedly belonging to Hf. From coincidence absorption measurements of both Hf activities these workers concluded that the 46 day level in Hf^{181} is an isomeric state and that part of the β-disintegrations of the 5.5 hour period lead to the 10^{-8} sec. metastable state. If these conclusions were correct, the 10^{-8} sec. metastable state should be observed following the β-decay of the 5.5 hour

---

[29] S. B. Burson and K. W. Blair, Phys. Rev. 78, 89 (1950).

period. No delayed coincidences were observed above the random rate to follow this 5.5 hour period. This result does not conclusively rule out that the 46 day level is an isomeric state in Hf^{181} but does rule out a β-component of the 5.5 hour period leading to the 10^{-8} sec. metastable state of Ta^{181}.

$$_{32}Ge^{72*} \ (2.9 \times 10^{-7} \text{ sec.})$$

The existence of the short-lived isomeric state of Ge^{72} was confirmed.[1] The value of the half-life was found to be $(2.9 \pm 0.6) \times 10^{-7}$ sec. This value is somewhat different from that previously reported and probably more accurate.

Several authors[30,31] have investigated the β- and γ-ray spectra of Ga^{72} (14 hr.). The β-ray spectrum is found to be highly complex. A conversion line occurring in about .5% of the disintegrations is observed at .70 Mev in the β-ray spectra but not in the photoelectron spectrum of the γ-rays. This indicates that the .70 Mev transition is probably totally converted. Bowe et al. attributed the isomeric transition in Ge^{72} to this transition. If this were an ordinary radiative transition, the internal conversion coefficient would be $\sim$.002. Thus, the .70 Mev isomeric transition must be a $0 \longrightarrow 0$ transition with no parity change and, therefore, totally converted. Since Ge^{72} is an even-even isotope, it seemed probable that the .70 Mev transition is a

---

[30] Allen C. G. Mitchell, D. J. Zaffarano, B. D. Kern, Phys. Rev. 73, 1424 (1948).

[31] S. K. Haynes, Phys. Rev. 74, 423 (1948).

transition to the ground state of Ge^{72}. However, the analysis of the β-ray groups of Ga^{72} has not indicated a level at .70 Mev above the ground state. For this reason the radiation announcing the formation of the isomeric state and the radiation resulting from the decay of the metastable state were examined with the delayed coincidence scintillation spectrometer.

The spectrum of the delayed conversion electrons indicates clearly that the 0.70 Mev transition is the isomeric transition. Since the metastable state is formed in about 0.5% of the disintegrations of Ga^{72}, it is immediately apparent that no detailed spectrum of the beta ray leading to the metastable state could be obtained.

Owing to the low intensity only the integral distributions of the Compton electron spectra of the γ-rays were examined in the preceding and delayed radiation. The data indicate that no γ-radiation is present in the preceding radiation and that there is probably γ-radiation in the delayed radiation. It is probable that this γ-radiation is in cascade with the isomeric transition. This places the $0 \longrightarrow 0$ transition between two high energy levels which must have opposite parity of the ground state of Ge^{72}. Otherwise, the high energy $0 \longrightarrow 0$ transitions to the ground state would compete strongly with the 0.70 Mev transition.

$$Re^{187*} \ (5.5 \times 10^{-7} \text{ sec.})$$

The existence of the short-lived isomeric state of Re^{187}[32] was confirmed. The value of the half-life was found to be $(5.5 \pm 0.5) \times$

---

[32] S. DeBenedetti and F. K. McGowan, Phys. Rev. 71, 380 (1947).

10^{-7} sec. This value is somewhat different from that previously reported and is probably more accurate.

Re^{187*} is known to follow the β-decay of 24 hr. W^{187}. The β-spectrum of W^{187} consists of two components of 1.318 and 0.627 Mev maximum energy and intensities 23 and 77% respectively, accompanied by a rather large number of conversion lines.[33] Levy finds 6 γ-rays with energies 133, 204, 478, 615, 680, and 767 kev. As previously reported, DeBenedetti and McGowan showed that the isomeric state follows the lower energy component of the β-spectrum. Some delayed coincidences, not numerous enough to permit the measurement of an absorption curve, were observed after absorbing all the preceding β-rays, indicating that some γ-rays are present in the preceding radiation.

Measurements of the preceding radiation with the delayed coincidence scintillation spectrometer indicate that the 1.33 Mev β-group does not announce the formation of the metastable state in agreement with previous results. The spectrum of electromagnetic radiation in the preceding radiation indicates clearly that only the 478 kev γ-ray is present.

Fig. 29 shows the spectrum of the radiation following the decay of Re^{187*}. Curve (1) is the spectrum of the electromagnetic radiation, indicating that no γ-rays above 150 kev follow in cascade with the decay of Re^{187*}. Curve (2) is the internal conversion electron spectrum. The two conversion peaks, K and (L + M), correspond to a γ-ray with an energy of 133 kev. The ratio of K shell conversion to (L + M) shell

---

[33] P. W. Levy, "Radiations from 24 Hr. W^{187}," ORNL 312 (March, 1949).

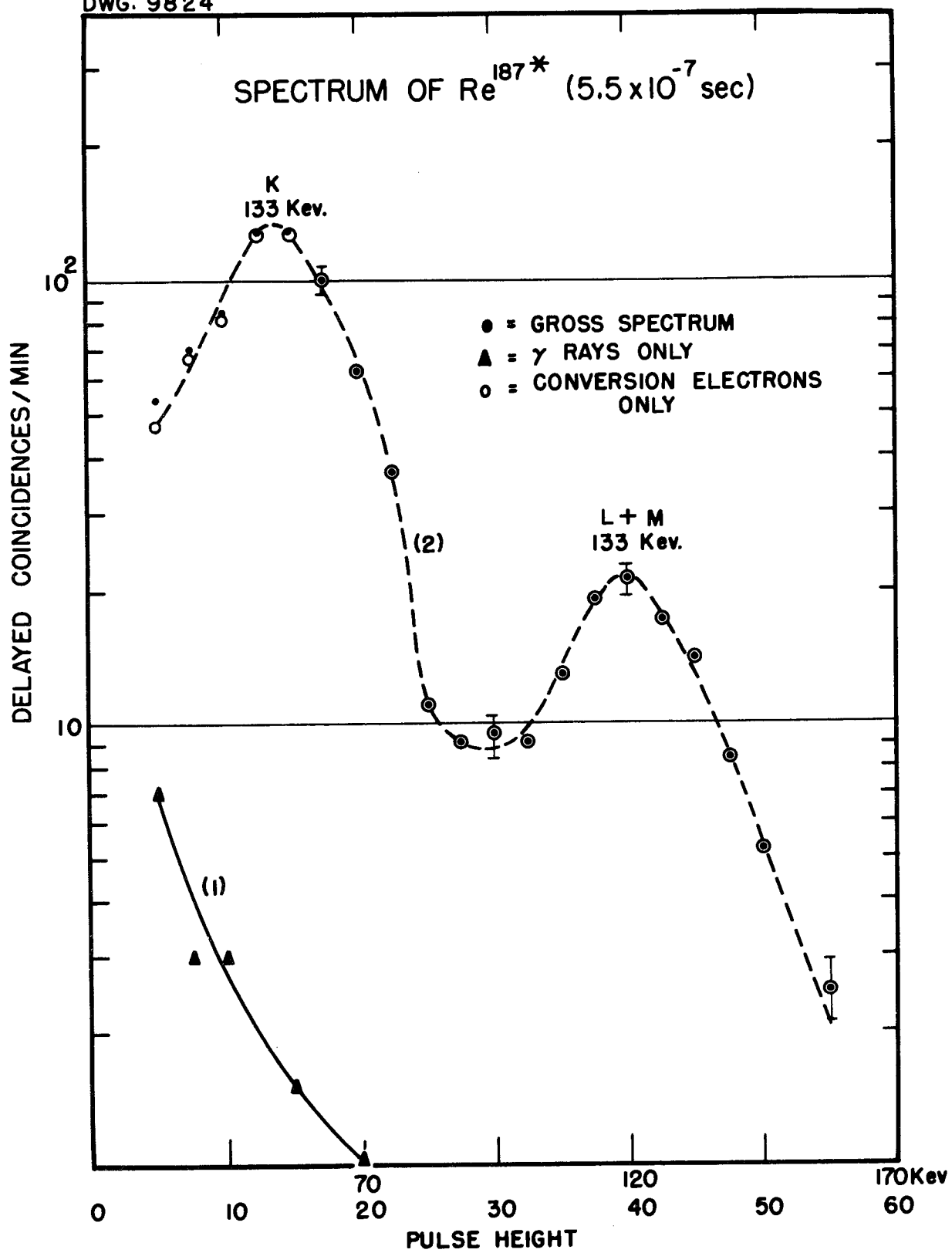

FIG. 29

PULSE HEIGHT DISTRIBUTION OF RADIATION FOLLOWING THE DECAY OF Re^{187*}

conversion obtained from the areas under the peaks is 5 ± 1.

Though many authors[34] have investigated W^{187}, there is no general agreement as to the disintegration scheme. The energy difference between the β-ray groups is 690 kev. The disintegration by the way of the metastable state indicates that the 133 kev transition is preceded by a 478 kev γ-ray and the .627 Mev. β-ray group. An additional γ-ray transition with an energy 60 to 70 kev is needed to account for the energy difference of the β-ray groups. A γ-ray of this energy cannot be excluded from these experiments because the scintillation spectrometer would not be able to distinguish between the γ-ray and the K x-ray of 59 kev.

$$Tm^{169*} \ (7.0 \times 10^{-7} \text{ sec.})$$

The existence of the short-lived isomeric state[35] of Tm^{169} was confirmed. The value of the half-life was found to be $(7.0 \pm 0.5) \times 10^{-7}$ sec. This value is somewhat different from that previously reported and probably more accurate.

Tm^{169*} is known to follow the 33 day Yb^{169} activity which decays by K-capture. The internal conversion electron and the photoelectron spectra of the γ-rays have been measured recently by several investigators.[36,37] Jensen et al. find 9 γ-rays with energies between 94 and

---

[34] C. L. Peacock and R. G. Wilkinson, Phys. Rev. 74, 297 (1948).

[35] F. K. McGowan and S. DeBenedetti, Phys. Rev. 73, 1269 (1948).

[36] E. N. Jensen, L. J. Laslett, R. T. Nichols, W. W. Pratt, Phys. Rev. 79, 243A (1950).

[37] J. M. Cork, H. B. Keller, W. C. Rutledge, and A. E. Stoddard, Phys. Rev. 78, 95 (1950).

308 kev and Cork et al. find 8 γ-rays. Both investigators report γ-ray energies of 94, 110, 131, 178, 198, and 308 kev. In addition Jensen reports γ-ray energies of 120, 144, and 160 kev. It will be shown from the results of the delayed coincidence spectrometer that the 120 and 144 kev γ-rays were probably misinterpreted by improper assignment of internal conversion lines from K or L shell conversion. Cork et al. observed a γ-ray energy of 63 kev which Jensen did not report and an internal conversion line corresponding to a γ-ray energy of 118 kev if K shell conversion or 68 kev if L shell conversion. The delayed coincidence spectrometer data indicate that the interpretation should be a 68 kev γ-ray.

Fig. 30 shows the spectrum of the radiation announcing the formation of the metastable state of Tm^{169}. It is evident from curve (1), which is the spectrum of γ-rays, that the metastable state is preceded by a 68 kev γ-ray. The peak corresponds to a complete dissipation of the γ-ray energy by several Compton scatterings within the phosphor. Curve (2) is the internal conversion electron spectrum after subtraction of the "γ-ray only" from the gross spectrum. The conversion lines at 35 and 85 kev are interpreted as due to conversion in the K and L shell of the 94 kev γ-ray.

The spectrum of the radiation following the decay of the metastable state in Tm^{169} is shown in Fig. 31. Curve (1) is the spectrum of the unconverted γ-rays with very little detail to aid in the identification of the γ-ray energies. Likewise, curve (2) is the spectrum of internal conversion electrons with very little detail. The fact that the energy distribution is more or less continuous up to 225 kev is

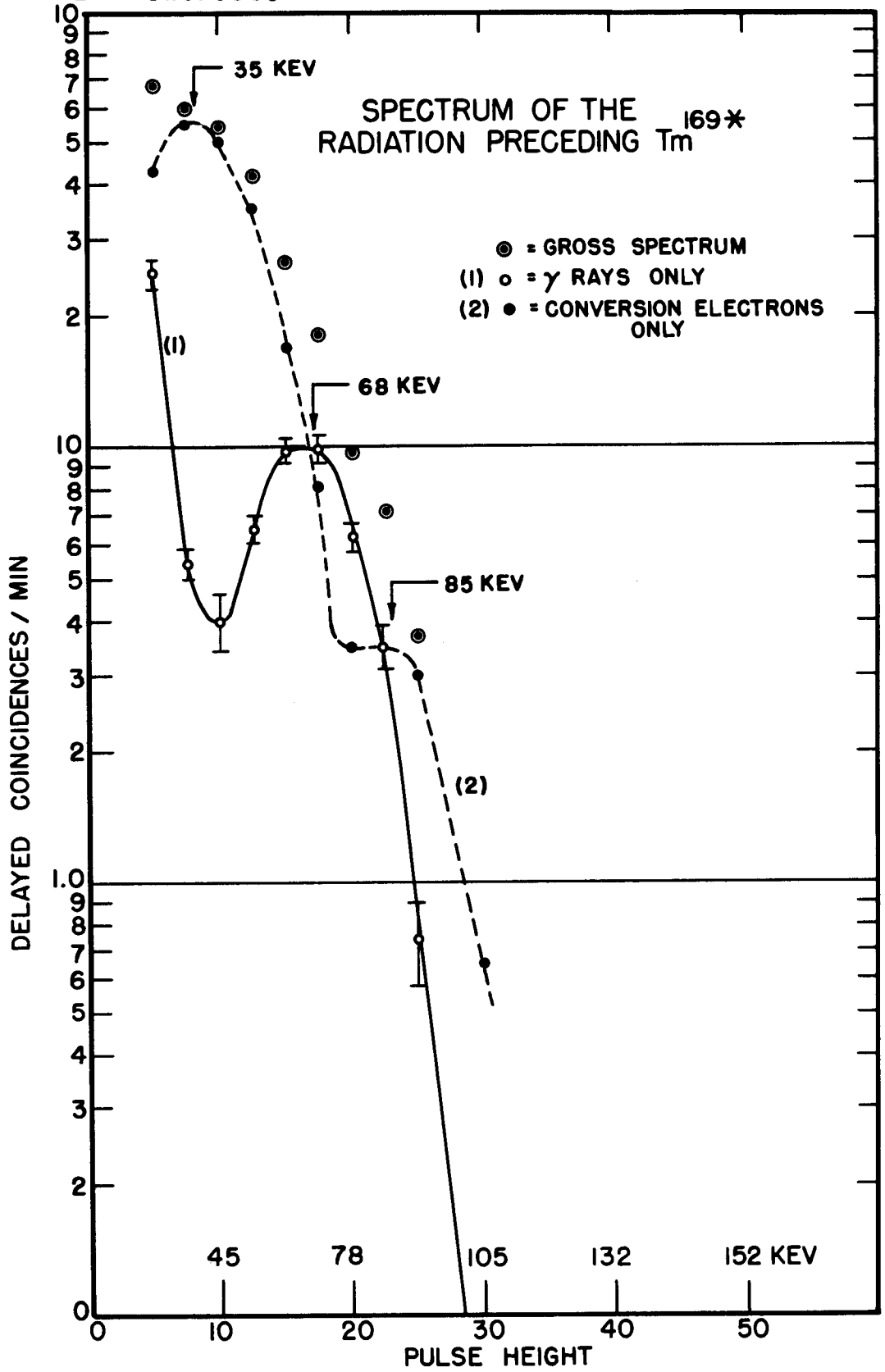

FIG. 30

PULSE HEIGHT DISTRIBUTION OF RADIATION PRECEDING Tm^{169*}

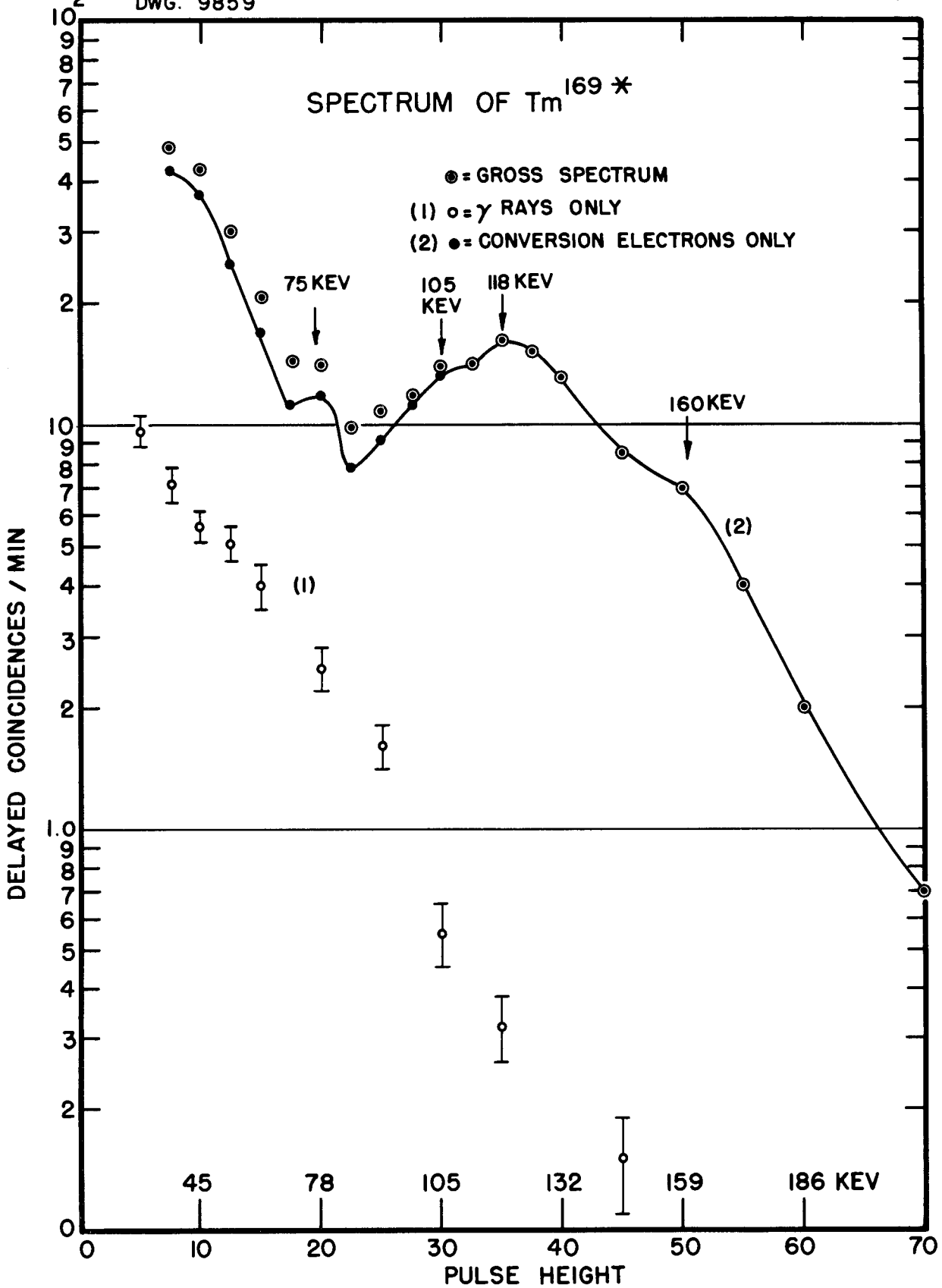

FIG. 31
PULSE HEIGHT DISTRIBUTION OF RADIATION FOLLOWING DECAY OF Tm^{169*}

indicative of either several γ-ray branches from the metastable state or several γ-rays in cascade following the decay of the metastable state. The former appears plausible because from the work of Jensen et al. and Cork et al. there are a number of combinations of γ-ray energies that add up to 308 kev. The assignment of the partially resolved internal conversion lines is not certain but it is possible to ascribe them in terms of internal conversion in either the K or L shell of γ-rays with energies 110, 131, 178, and 198 kev. These same γ-rays appear to be strongly internally converted from Jensen's data. A disintegration scheme consistent with the data is presented in Fig. 32. The three branches of γ-ray transitions from the metastable state to the ground state of Tm^{169} are rather peculiar. It is difficult to explain why the cascade branches compete favorably with the γ-ray of 308 kev, because the 110, 178, and 198 kev transitions are strongly converted, and therefore of high polarity.

A careful investigation of the internal conversion lines from Tm^{169} by means of a delayed coincidence spectrometer with high resolution is needed in order to elucidate these points.

Hg^{198*}?

Independently from this work and essentially at the same time, MacIntyre[38] used the method of delayed coincidences for the study of short-lived isomers. An excited state in Hg^{198} with a half-life 2.3×10^{-8} sec. was observed following the well known beta decay of Au^{198}

---

[38] W. J. MacIntyre, Phys. Rev. 76, 312 (1949).

UNCLASSIFIED
DWG. 9858

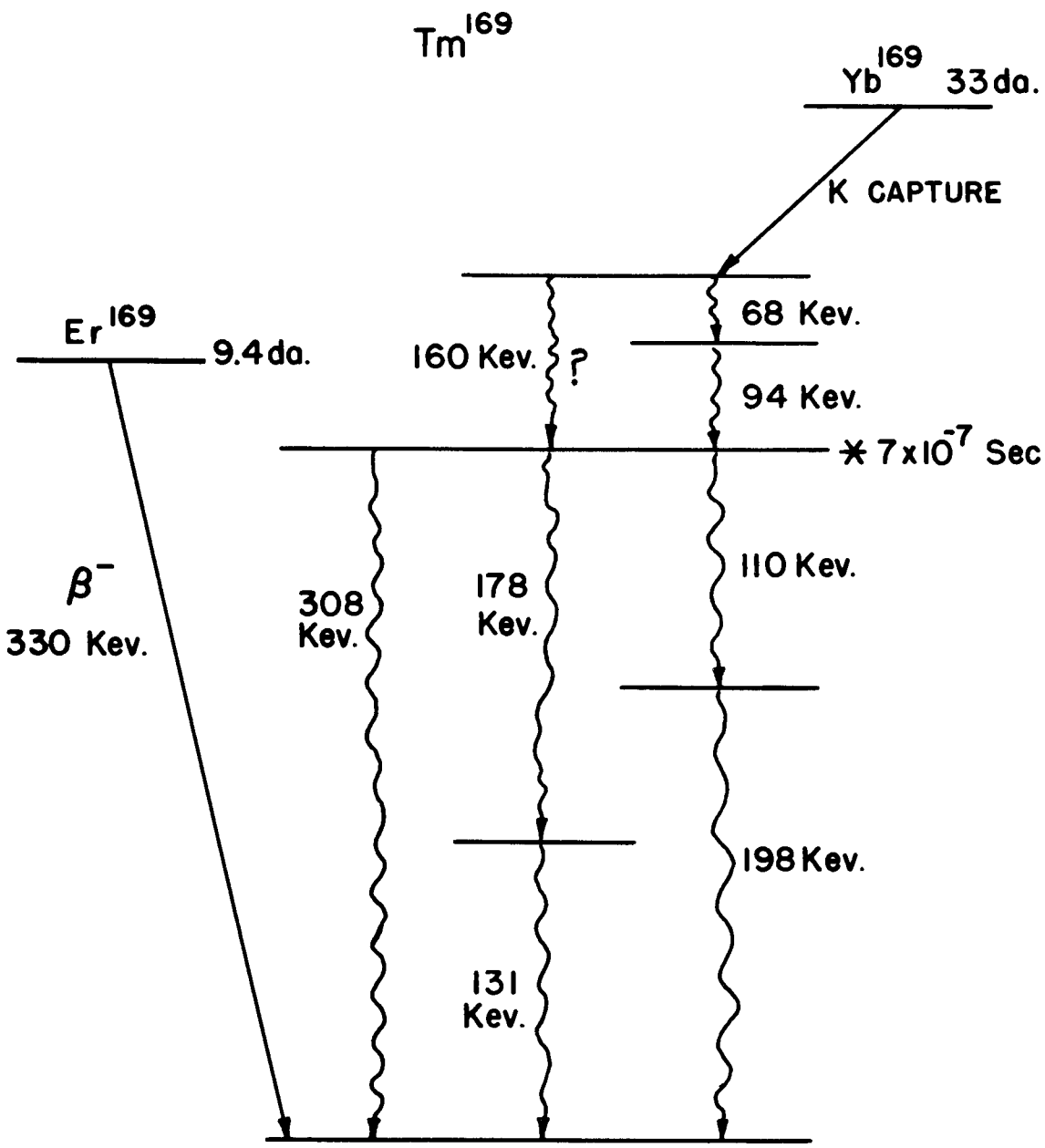

FIG. 32
DISINTEGRATION SCHEME FOR Tm^{169}

(2.7 da.) by MacIntyre. Since this result contradicted previous findings with Au^{198} at Oak Ridge National Laboratory, the delayed coincidence experiment on Au^{198} was repeated with better coincidence resolution for prompt events.

Fig. 33 curve (1) shows the resolution curve for essentially β-γ coincidences when a 560 mg/cm^2 lucite absorber is placed between the source and the detector for delayed radiation. Since a relatively good geometry of 15 and 30% was used, it was necessary to determine the number of coincidences due to two Compton scatterings of a single γ-ray exciting both channels. For this purpose a source of Cs^{137} (33 yr.) is convenient because the 661 kev γ-ray following the β-decay is not coincident with the beta ray. Curve (2) of Fig. 33 shows the number of coincidences after subtraction of the random coincidence rate as a function of delay time due to two Compton scatterings of the γ-ray. Since this contribution is only $\sim$ 2% of the coincidences obtained from Au^{198}, this proves that the data obtained for curve (1) are β-γ coincidences. From geometrical considerations (i.e. 4.5% of the γ-rays entering the phosphor were counted) the observed coincidence rate at zero delay is equal the computed rate provided the β- and γ-rays are coincident in time.

The leading and trailing edge of curve (1) indicates that the half-life of the 411 kev excited state in Hg^{198} is less than 3×10^{-9} sec. Similar results have been reported by Deutsch et al.[9] and Bell et al.[39] for an upper limit of the half-life of the excited state in Hg^{198}.

---

[39] R. E. Bell and H. E. Petch, Phys. Rev. 76, 1409 (1949).

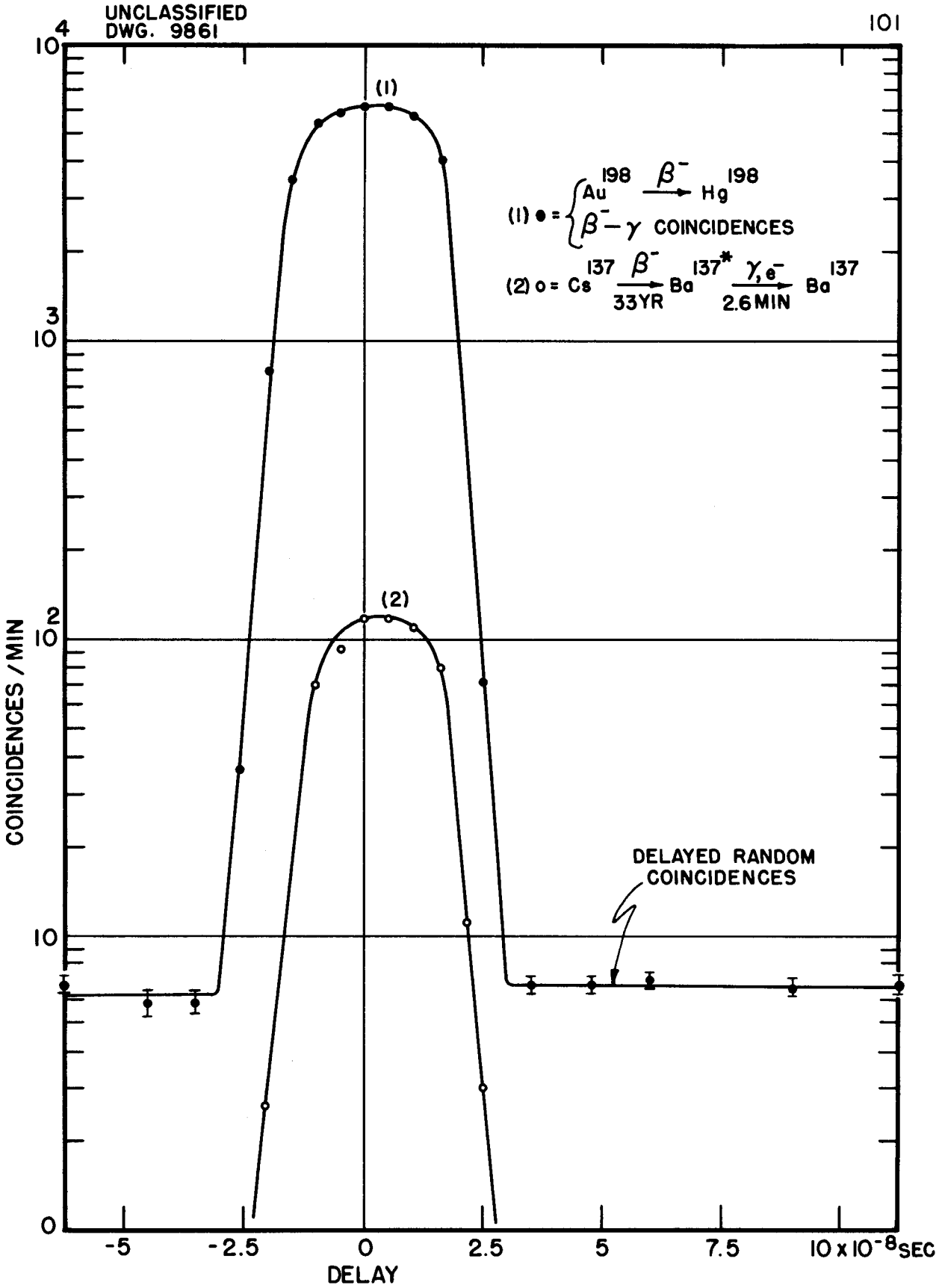

FIG. 33
RESOLUTION CURVE OF β-γ COINCIDENCES FROM Au^{198}

The present observations are difficult to reconcile with MacIntyre's results.

A group[40] at Washington University have suggested that the activity of Au^{198}, in addition to 2.7 day period, decays with a 4 hour period. This group also observed that the 4 hour activity led to a metastable state with a half-life of $(4 \pm 1) \times 10^{-8}$ sec. This observation could account for the failure of some observers to find the short-lived state following the decay of Au^{198}. To check this point, samples of Au were examined for the 4 hour period and delayed coincidences immediately after a short exposure to neutron irradiation in the reactor. Neither the 4 hour period nor the short-lived metastable state was observed in the samples. The Washington group, however, claims that the above observations were detected with samples irradiated in the Oak Ridge reactor.

---

[40] P. S. Jastram, W. Konneker, and M. R. Cleland, Phys. Rev. 79, 243A (1950).

CHAPTER VII

DISCUSSION OF RESULTS

In this chapter a general discussion of all the short-lived isomers of nuclei observed to date is given. The data that have been reported for the short-lived isomers are collected in Table V. A comparison of experimental lifetimes with the predicted estimates, a prevalence of short-lived isomers in odd mass nuclei with Z odd, and a correlation of the negative results with nuclear shell structure is presented.

Comparison of Experimental Lifetimes with the Predicted Estimates

A comparison can be made between the experimentally determined lifetimes and those predicted by equation (6). Fig. 34 is a graph of log τ_γ as a function of log W where the lines are drawn in for $\ell = 2$, 3, 4, and 5 with $\rho = 3.3$. The observed lifetime of each short-lived isomer is exhibited as a point on the graph. The evidence for groupings is very slight. The dependence of the lifetime on energy, at least in many cases, is certainly not as is predicted by the theoretical estimate. However, the observed lifetime will be less than the estimated lifetime for gamma ray emission because of the competing decay process of internal conversion which tends to increase the total transition rate. If the total internal conversion coefficient is known, one may convert τ_{exp} to τ_γ for each isomer by equation (8).

In most cases the experimental internal conversion coefficients are not available. Therefore, it is necessary to estimate the total

TABLE V

DATA FOR THE SHORT-LIVED ISOMERS

Isomer	$(T_{1/2})_{exp}$ (sec.)	Energy E_γ (kev)	$(N_K/N_L)_{exp}$	Internal Conversion Coefficient $(\alpha)_{exp}$	Probable Forbiddenness (l)	Total Conversion Coefficient (Estimated)	$\tau_\gamma \rho^{2l}$
$_{26}Fe^{57}$ [a]	1.1×10^{-7}	14			2	~ 300	8.2×10^{-4}
$_{48}Cd^{111}$	8×10^{-8}	247	5 ± 1	$\alpha_K = .03$ $\alpha_L = .006$	2 or 3?	.04	5.0×10^{-6}
$_{63}Eu^{153}$ [b]	3×10^{-9}	103			2	~ 2	8.7×10^{-7}
$_{68}Er^{166}$ [c]	1.7×10^{-9}	80		$\alpha_L \sim .4$	2	$\sim .8$	3.2×10^{-7}
$_{69}Tm^{169}$	7.0×10^{-7}	Several γ's 110 to 308 kev			2 and 3	---	---
$_{69}Tm^{171}$	2.5×10^{-6}	112		1.3?	3	1.3	5.4×10^{-3}
$_{70}Yb^{170}$ [d]	1.6×10^{-9}	84	.14	$\alpha_K = .08$ $\alpha_L = .55$	2	.8	3.1×10^{-7}
$_{71}Lu^{177}$	1.3×10^{-7}	150	3 ± 1		2? or 3	~ 5	7.7×10^{-4}
$_{73}Ta^{181}$	2.2×10^{-5}	135	0.5		3	$\alpha_3 \sim 4$	1.1×10^{-1}
$_{73}Ta^{181}$	1.1×10^{-8}	132	6 ± 1		2	$\beta_1 \sim 2$	3.9×10^{-6}
$_{75}Re^{187}$	5.5×10^{-7}	133	5 ± 1		2? or 3	~ 8	5.7×10^{-3}
$_{77}Ir^{191}$	5.7×10^{-9}	65			2	~ 1	1.4×10^{-6}
$_{79}Au^{197}$ or $_{80}Hg^{197}$	7×10^{-9}	135	<1	$\alpha_K \sim .53$	2	~ 2	2.8×10^{-6}
$_{82}Pb^{204}$	3×10^{-7}	374	2	$\sim .05$	3	$\sim .05$	4.2×10^{-4}
$_{32}Ge^{72}$	2.9×10^{-7}	700			$0 \longrightarrow 0$ Transition		---

[a] M. Deutsch and W. E. Wright, Phys. Rev. 77, 139 (1950).

[b] F. K. McGowan, Phys. Rev. 80, 482 (1950).

[c] F. K. McGowan, Phys. Rev. 80, Dec. 1 (1950).

[d] R. E. Bell and R. L. Graham, Phys. Rev. 78, 490 (1950).

[e] A. W. Sunyar, D. E. Alburger, G. Friedlander, M. Goldhaber, G. Goldhaber, Phys. Rev. 78, 326 (1950).

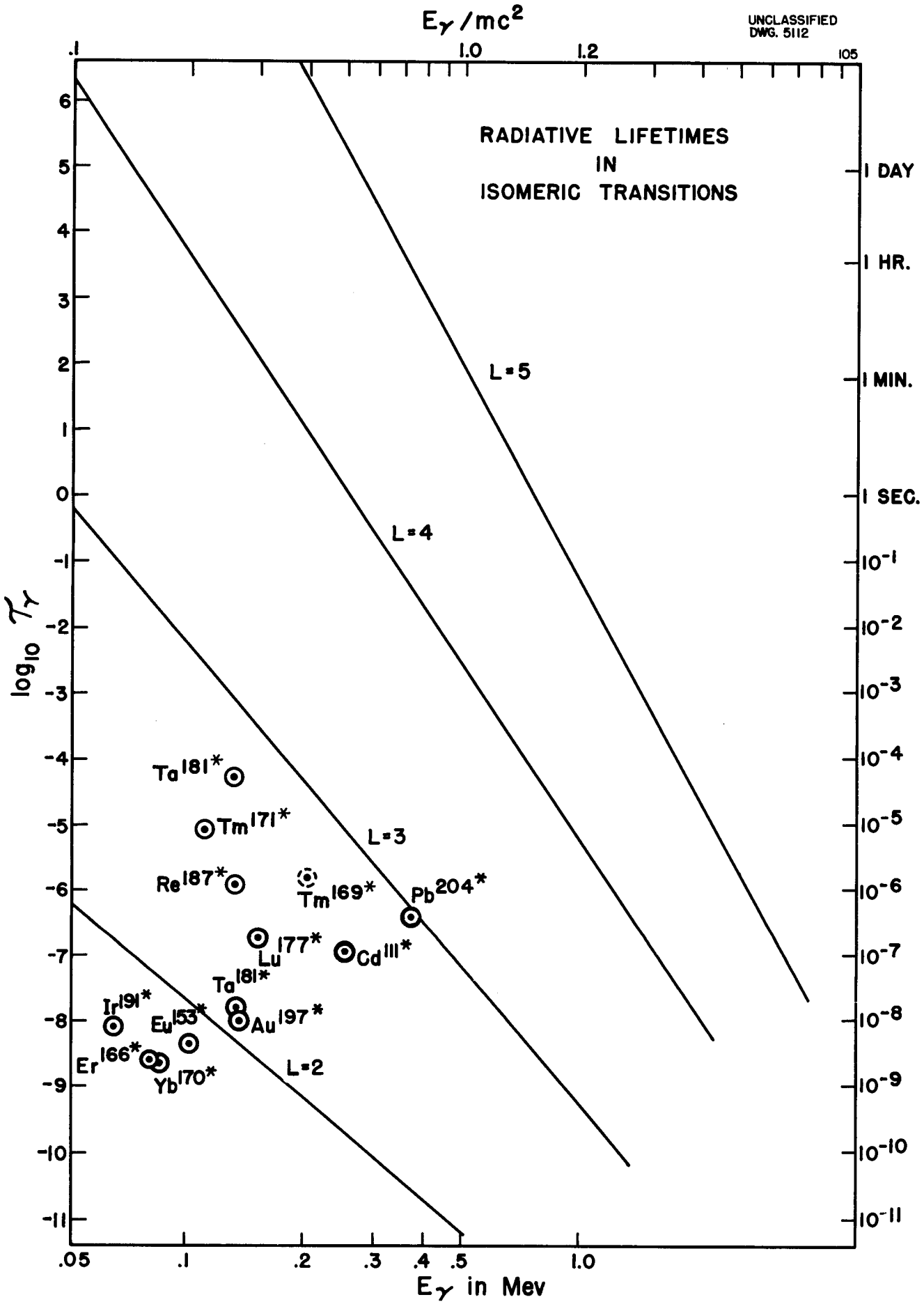

FIG. 34

VALUES OF LOG τ_γ AS A FUNCTION OF LOG W

internal conversion coefficients. Table V contains a tabulation of existing data for 15 known short-lived isomers. Some of the data include results from other laboratories which have been cited in Chapter VI. The assignment of probable forbiddenness ℓ was made on the basis of Fig. 34. However, for cases where the experimental internal conversion coefficient is known, the ℓ-value assignment was made by comparing the experimental internal conversion coefficient with theoretical values.[1] The total internal conversion coefficient was estimated using the $(N_K/N_L)_{exp}$, the probable forbiddenness assignment, the energy of the isomeric transition, and Rose's relativistic K shell internal conversion coefficients for electric and magnetic multipole. In the case of extremely different values between electric and magnetic conversion coefficients, an intermediate value was selected quite arbitrarily. With these estimates for the conversion coefficient τ_{exp} has been converted to τ_γ by equation (8). The last column of Table V is the product $\tau_\gamma \rho^{2\ell}$, where ρ is the nuclear radius in units of e^2/mc^2. The value of the nuclear radius was taken as $r = 1.5\ A^{1/3} \times 10^{-13}$ cm.

A more quantitative comparison of $(\tau_\gamma)_{exp}$ with theoretical estimates should be possible by taking account of the value $\rho^{2\ell}$ for each isomer. That is, equation (6) indicates that the product $\tau_\gamma \rho^{2\ell}$ depends only on the energy of the isomeric transition. Fig. 35 shows the short-lived isomers on a plot of log $(\tau_\gamma \rho^{2\ell})$ as a function of log W. The theoretical estimates for $\ell = 2$, 3, and 4 are drawn in for

---

[1] M. E. Rose, G. H. Goertzel, B. I. Spinrad, J. Harr, and P. Strong, Phys. Rev. 76, 1883 (1949). Tables of K shell internal conversion privately circulated.

UNCLASSIFIED
DWG. 8462

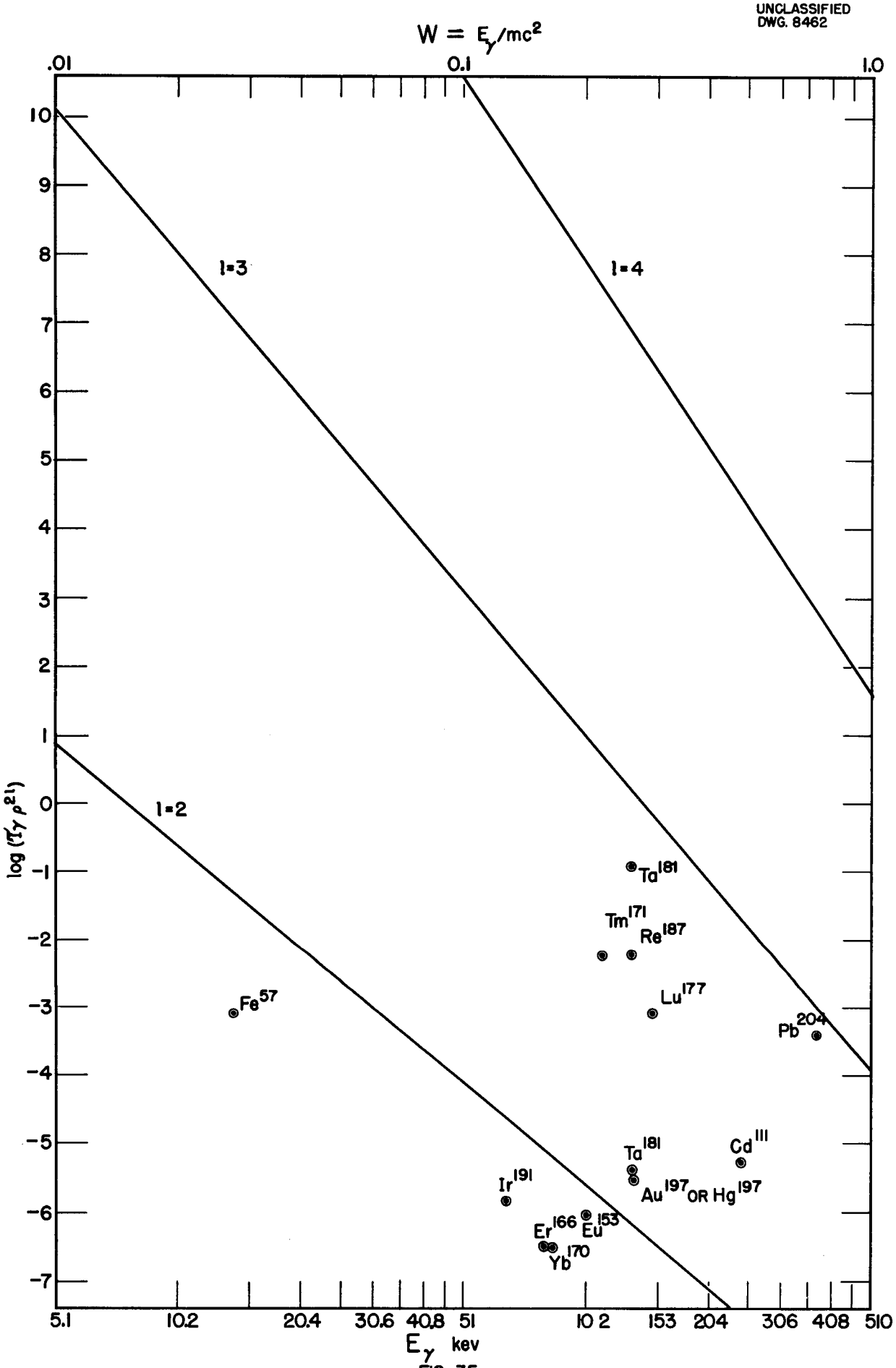

FIG. 35
VALUES OF LOG ($\tau_\gamma \rho^{2\ell}$) AS A FUNCTION OF LOG W

comparison with experiment. The agreement between the $\ell = 2$ and $\ell = 3$ lines and the experimental points is certainly not good. In fact, the fluctuations are all below the line $\ell = 3$ and, in particular, Tm^{171}, Re^{187}, Lu^{177}, and Cd^{111} fall well outside the predicted lines by a factor of nearly 1000. A similar classification by Axel and Dancoff[2] of 60 isomers indicated agreement between the $\ell = 4$ and $\ell = 5$ lines and the experimental points. The points all fall within the anticipated factor of 100 of the predicted lines.

One might consider a reassignment of ℓ for the most doubtful cases, such as Lu^{177}, Tm^{171}, or Re^{185}. The reassignment to $\ell = 2$ group would decrease $\tau_\gamma \rho^{2\ell}$ at most by a factor of 50. These changes would obviously not fit the predicted line $\ell = 2$. For forbiddenness $\ell = 2$ or 3 any error in the estimate of the conversion coefficient would not introduce a factor of more than 10 in the correction factor for the conversion of τ_{exp} to τ_γ. Thus, it appears that equation (6) fails to predict the lifetime for gamma ray emission of forbiddenness $\ell = 2$ or 3.

It is interesting to note that the 4 short-lived isomeric transitions occurring in Ta^{181}, Re^{187}, and Hg^{197} have essentially the same energy but widely different half-life and $N_K/(N_L + N_M)$. Until the relativistic L shell internal conversion coefficients become available, no definite conclusions can be made regarding the multipole order and the electric and magnetic character of the radiating multipoles. However, there is evidence from results of the two isomeric transitions in Hg^{197} that the ratio of K shell conversion to L shell conversion may not

---

[2] P. Axel and S. M. Dancoff, Phys. Rev. 76, 892 (1949).

provide a means of fixing the multipole order uniquely. In Hg^{197} the 165 kev isomeric transition with a 23 hr. half-life is followed by a 134 kev transition with a 7×10^{-9} sec. half-life. The ratios $N_K/(N_L + N_M)$ are 0.31 and 0.29 respectively.[3] On the basis of their lifetime and their energy these isomeric states would fall in the classification $\ell = 5$ and $\ell = 2$.

Prevalence of Short-Lived Isomers in Odd Mass Nuclei with Z Odd

Feenberg and Hammack,[4] Nordheim,[5] and Mayer[6] in their development of nuclear shell structure have pointed out that for nuclei with odd mass number isomerism appears to occur in well defined "lakes" extending from $(Z \text{ or } N)_{odd} = 39$ to 49 and $(Z \text{ or } N)_{odd} = 63$ to 81. The prevalence of isomerism in these "lakes" is understood by the competition of orbits within one group (protons or neutrons). The isomeric states appear at odd particle numbers which are not too far below those for completed shells at 50 and 82. The interpretation of the phenomenon is generally explained by the not infrequent appearance of new orbits before the completion of the preceding shell. If the competing orbits give rise to adjacent states with sufficiently different angular momenta, isomerism occurs.

---

[3] H. Frauenfelder, O. Huber, A. De-Shalit, and W. Zunti, Phys. Rev. 79, 1029 (1950).

[4] E. Feenberg and K. C. Hammack, Phys. Rev. 75, 1877 (1949).

[5] L. W. Nordheim, Phys. Rev. 75, 1894 (1949).

[6] M. G. Mayer, Phys. Rev. 75, 1969 (1949).

The isomeric transitions for $63 \leq (Z \text{ or } N)_{odd} \leq 81$ are listed in Table VI. The number of short-lived isomers ($T_{1/2} < 10^{-2}$ sec.) in this "lake" is 9, out of a total of 11 observed thus far in nuclei with odd mass number. Eight of these occur in nuclei with Z odd. In the case of the long-lived isomers 17 occur in nuclei with N odd and only one occurs with Z odd. This coincidence could be a mere accident, but perhaps there is a difference in the order of neutron levels $63 \leq N_{odd} \leq 81$ and proton levels $63 \leq Z_{odd} \leq 77$. Such a difference in level order is not noticeable in the "magic numbers" and thus far has been disregarded in single particle computations. An inspection of Table II shows that of the odd mass nuclei investigated only 17% have N odd. One might conclude that the correlation is not significant because most nuclei investigated have Z odd. However, there are numerous examples (13) of nuclei with N odd where the parent nucleus decays either directly to the ground state or to an excited state already known to be metastable with a long period. For this reason many nuclei with N odd were not investigated. In view of this the correlation is probably still significant.

No such correlation exists for the "lake" $(Z \text{ or } N)_{odd} = 39$ to 49. In the first place no short-lived isomers have been observed in this "lake". Secondly, of the 18 long-lived isomers in the "lake", 9 occur in nuclei with Z odd and 9 occur in nuclei with N odd.

In order to interpret points concerning the position in the isotopic chart of short-lived isomers, it might be well to consider briefly the ordering of the states as proposed by Mayer[6] and Feenberg and Hammack.[4] The order of the levels in a square well are 1s, 2p, 3d, 2s,

TABLE VI

ISOMERS FOR $(Z \text{ or } N)_{odd} = 63$ to 81

Z or N	Odd Particle	Isomer	E_γ(kev)	$T_{1/2}$
63	n	Cd^{111}	148	48 min.
	n	Cd^{111}	247	8×10^{-8} sec.
	p	Eu^{153}	103	3×10^{-9} sec.
65	n	Cd^{113}?		2.3 min.
67	n	Sn^{117}	152	15 da
	n	Cd^{115}		43 da
69	n	Sn^{119}	69	245 da
	n	Te^{121}	82	140 da
	p	Tm^{169}	110 to 308	7.0×10^{-7} sec.
	p	Tm^{171}	113	2.5×10^{-6} sec.
71	n	Te^{123}	88	90 da
	p	Lu^{177}	150	1.3×10^{-7} sec.
73	n	Te^{125}	110	58 da
	n	Xe^{127}	125	75 sec.
	p	Ta^{181}	135	2.2×10^{-5} sec.
	p	Ta^{181}	132	1.1×10^{-8} sec.
75	n	Te^{127}	88	90 da
	p	Re^{187}	133	5.5×10^{-7} sec.
77	n	Te^{129}	106	30 da
	n	Ba^{133}	276	40 hr.
	n	Xe^{131}	165	12 da
	p	Ir^{191}	65	5.7×10^{-9} sec.
79	n	Te^{131}	177	1.2 da
	n	Ba^{135}	290	28 hr.
	p	Au^{197}	278	7.5 sec.
81	n	Ba^{137}	661	2.5 min.
	n	Xe^{135}	520	15 min.

4f, 3p, 5g, 4d, 6h, 3s, 5f, 7i, 4p, etc. Mayer inverts the 3s and 6h and also the 4p and 7i. The energies of these levels are close together in the square well. If a strong spin-orbit coupling, increasing with angular momentum, is assumed, a level scheme with the "magic numbers" 20, 50, 82, and 126 occurring at the place of the spin-orbit splitting is obtained. The shell grouping is as follows:

$$(1s)^2,\ (2p)^6,\ (2s)^2,\ (3d)^{10},\ \underset{20}{}\ 4f_{7/2},\ \underset{28}{}\ 4f_{5/2},\ \underset{34}{}\ 3p_{3/2},\ 3p_{1/2},\ \underset{40}{}\ 5g_{9/2},\ \underset{50}{}$$

$$5g_{7/2},\ \underset{58}{}\ 4d_{5/2},\ \underset{64}{}\ 4d_{3/2},\ \underset{68}{}\ 3s_{1/2},\ 6h_{11/2},\ \underset{82}{}\ 6h_{9/2},\ 5f_{7/2},\ 5f_{5/2},\ 4p_{3/2},$$

$$4p_{1/2},\ 7i_{13/2},\ \underset{126}{}$$

where the total number of particles up to and including each orbit is given directly below.

It does not seem unreasonable that the competing orbits $3s_{1/2}$ and $6h_{11/2}$ could possibly account for the long-lived isomers of Table VI. For the short-lived isomeric transitions changes of angular momentum of 1, 2, or 3 units of $\hbar$ are necessary. One might possible consider $3s_{1/2}$, $4d_{3/2}$, and $4d_{5/2}$ as competing orbits for changes of angular momentum of 1 and 2 units of $\hbar$. At Z = 71 and 73 the ground states of Lu^{175} and Ta^{181} which have spin 7/2 would require a $g_{7/2}$ orbit. Although there is no g orbit occurring at these proton numbers in Mayer's scheme, such an orbit competing with $3s_{1/2}$ or $4d_{3/2}$ orbits would give rise to changes of angular momentum of 3 and 2 units of $\hbar$.

In the scheme of Feenberg and Hammack, the arrangement consists

in a pushing up of orbits with small angular momentum and radial nodes within the nucleus, such as the 2s, 3p, and 4d, which progresses more and more for heavier nuclei. A qualitative explanation for this tendency is given by the repulsive action of the Coulomb forces on protons, which will cause a decrease in density of nuclear matter at the center of heavy nuclei. Islands of isomerism occur with the crossing or close spacing of energy levels in the shell model when large angular momentum differences exist. The closed shells of neutrons and protons are as follows:

$$(1s)^2,\ (2p)^6,\ \underset{10}{(2s)^2},\ \underset{20}{(3d)^{10}},\ (4f)^{14},\ \underset{50}{(5g)^{18}},\ (6h)^{22},\ \underset{82}{(4d)^{10}},$$

where certain levels (2s, 3p, and 4d) drift upward with increasing N or Z.

In the interval 51 to 60 there is a filling of the 4d shell and is filled completely before the inversion of the 6h and 4d levels takes place. Between 61 and 82 the 2s, 3p, and 4d levels drift upward and cross over during the filling of 6h shell giving rise to possible closely spaced paired configurations.

$$\left[60\ \text{shell}\right] \begin{bmatrix} (6h)^{2n}\ (2s)^1 \\ (6h)^{2n+1} \end{bmatrix} \begin{matrix} \text{even parity} \\ \text{odd parity,} \end{matrix}$$

$$\left[60\ \text{shell}\right]\ (3p)^6 \begin{bmatrix} (6h)^{2n}\ (2s)^1 \\ (6h)^{2n+1} \end{bmatrix} \begin{matrix} \text{even parity} \\ \text{odd parity,} \end{matrix}$$

$$\left[60\ \text{shell}\right] \begin{bmatrix} (6h)^{2n}\ (2p)^1 \\ (6h)^{2n+1} \end{bmatrix} \begin{matrix} \text{odd parity} \\ \text{odd parity,} \end{matrix}$$

$$\left[50 \text{ shell}\right] \quad \begin{bmatrix} (4d)^{9}\ (6h)^{2n+2} \\ (4d)^{10}\ (6h)^{2n+1} \end{bmatrix} \begin{matrix} \text{even parity} \\ \text{odd parity,} \end{matrix}$$

$$\left[50 \text{ shell}\right] \quad \begin{bmatrix} (6h)^{2n}\ (4d)^{1} \\ (6h)^{2n+1} \end{bmatrix} \begin{matrix} \text{even parity} \\ \text{odd parity.} \end{matrix}$$

These paired configurations provide a large choice of states which generate the initial and final states of an isomeric transition. The many isomeric transitions between $63 \leq (Z \text{ or } N)_{odd} \leq 81$ may be correlated with the above configurations.

Correlation of Negative Results with Nuclear Shell Structure

A reasonable explanation can be given for the negative results listed in Table II of Chapter V on the basis of the shell models mentioned in the preceding section. For Z_{odd} = 21 to 37 four isotopes were investigated for metastable states. Three of these nuclei have spin 7/2 and the other has spin 3/2. The competing orbits being filled in this region are $4f_{7/2}$, $4f_{5/2}$, and $3p_{3/2}$ in Mayer's scheme. Since the difference in angular momentum between states resulting from these orbits is small, isomeric states are not expected. On the basis of the scheme by Feenberg and Hammack, no isomerism is expected in this region if 2s level does not overtake the 4f before the completion of the 4f shell.

For Z_{odd} = 39 to 49 five isotopes were investigated for short-lived metastable states. The competing orbits in Mayer's scheme in this region are $3p_{1/2}$ and $5g_{9/2}$ and the difference in angular momentum

between the states is 4 units of $\hbar$ which accounts for the occurrence of only long-lived isomers in this region. The crossovers occurring during the filling of the 5g shell are the 2s and 3p levels in the scheme of Feenberg and Hammack. These crossovers introduce several possibilities for configurations involved in isomerism at $(Z \text{ or } N)_{odd} = 39$ to 49. These configurations are

$$\begin{bmatrix} (3p)^4 \ (5g)^1 \\ 3p^5 \end{bmatrix} \begin{matrix} \text{even parity} \\ \text{odd parity,} \end{matrix}$$

$$\begin{bmatrix} (2p)^5 \ (5g)^2 \\ (2p)^6 \ (5g)^1 \end{bmatrix} \begin{matrix} \text{odd parity} \\ \text{even parity,} \end{matrix}$$

$$\begin{bmatrix} (5g)^{2n} \ (3p)^1 \\ (5g)^{2n+1} \end{bmatrix} \begin{matrix} \text{odd parity} \\ \text{even parity,} \end{matrix}$$

$$\begin{bmatrix} (5g)^{2n} \ (2s)^1 \\ (5g)^{2n+1} \end{bmatrix} \begin{matrix} \text{even parity} \\ \text{even parity.} \end{matrix}$$

These paired configurations do not, however, exclude the occurrence of short-lived isomers.

Between $Z_{odd} = 51$ and 61 six isotopes were investigated for metastable states. Two of these nuclei have spin 7/2 and two have spin 5/2. The competing orbits are $5g_{7/2}$ and $4d_{5/2}$ in Mayer's scheme and the difference in angular momentum between states is 1 unit of $\hbar$. Thus, no short-lived isomers are expected to occur in this region except possibly extremely low energy transitions. In the scheme of Feenberg and Hammack, the 4d shell is being filled and is probably filled completely

before the inversion of the 6h and 4d levels takes place. Since the 2s and 3p levels crossover during the filling of 5g shell, it appears that no competing orbits occur in this region which is in agreement with the fact that no isomers have been observed.

CHAPTER VIII

CONCLUSIONS

The prevalence of isomerism in the region $63 \leq (N \text{ or } Z)_{odd} \leq 81$ is fairly well established. The number of short-lived isomers in this region is 9, out of a total of 11 observed in odd mass nuclei. In this region it appears that the long-lived isomers occur in nuclei with N odd and the short-lived isomers occur in nuclei with Z odd. Though this state of affairs could be a mere accident, an interpretation of this correlation may help to decide the preferred configurations for neutrons and protons in this region.

Of the 15 short-lived isomers tabulated in Table V, the first excited state is metastable in 8 cases and in 5 cases the metastable state occurs at higher excited states. The position of the metastable state for the remaining 2 cases has not been determined.

Since numerous workers have searched for short-lived isomers with half-lives between 10^{-8} and 10^{-3} sec., one cannot escape the impression that isomerism occurs less frequently for forbiddenness $\ell = 2$ or 3 than for $\ell = 4$ or 5. One must keep in mind though that the short-lived isomeric transitions observed to date cover a relatively narrow band of energy. It is conceivable at transition energies less than 100 kev that isomerism will occur in the region 10^{-3} to several seconds for forbiddenness $\ell = 3$. On the other hand for $\ell = 2$ and the same transition energies the estimated lifetimes are in the millimicrosecond region. Many more short-lived isomers should be observed in this region because quadrupole transitions should occur as a rule rather than

the exception in nuclear radiative transitions. The extension of the method of delayed coincidences to measure time intervals in the region of 10^{-9} sec. has already yielded several new results; namely, Yb^{170} (1.6×10^{-9} sec.),[1,2] Eu^{153} (3×10^{-9} sec.),[2] and Er^{166} (1.7×10^{-9} sec.).[3] This extension has been made possible through the use of wide band distributed amplifiers, scintillation spectrometer, and improved methods of analysis of delayed coincidence resolution curves.

Although the energy and half-life of these short-lived isomers and in some cases the ratio of K shell conversion to (L + M) shell conversion are known, an unique assignment of the multipole orders and the magnetic and electric nature of the radiating multipoles is not possible. Even when the theoretical L shell internal conversion coefficients become available it is rather unlikely that the K/L ratio alone will fix the assignment in every case. The most urgently needed data are precise measurements of the absolute internal conversion coefficients. There are, of course, the possible directional correlation experiments between gamma-quanta emitted in successive nuclear transitions. In some cases comparison of experiment[4] with theory[5] has yielded consistent assignments of the angular momentum quantum numbers of the nuclear states involved and multipole orders of the gamma radiation

---

[1] R. E. Bell and R. L. Graham, Phys. Rev. 78, 490 (1950).

[2] F. K. McGowan, Phys. Rev. 80, 482 (1950).

[3] F. K. McGowan, Phys. Rev. 80, Dec. 1 (1950).

[4] E. L. Brady and M. Deutsch, Phys. Rev. 78, 558 (1950).

[5] D. R. Hamilton, Phys. Rev. 58, 122 (1940).

emitted. Of the short-lived isomers listed the cascade of 173 and 247 kev gamma rays in Cd^{111} following the K capture decay of In^{111} is the only promising case for a directional correlation experiment. The case of Pb^{204} has already been done by Goldhaber and coworkers.[6] In the case of Ta^{181} and Hg^{197} a likely experiment is the directional correlation of successive conversion electrons where the intermediate state is metastable with a lifetime $\sim 10^{-8}$ sec. The extension of the general theory of directional correlation to successive conversion electrons has been treated by Ling.[7] Because of some unknown parameters in the internal conversion angular distribution functions, Ling was unable to present explicit numerical results. Also, a high degree of experimental precision probably would be necessary to uniquely determine angular momentum quantum numbers and parity of the nuclear states involved. However, with the development of the delayed coincidence scintillation spectrometer as described it appears that this precision may be possible. A directional correlation experiment between the cascade conversion electrons of the 135 and 132 kev transitions in Ta^{181} and the 165 and 134 kev transitions in Hg^{197} would be feasible. Rose has pointed out that theoretical numerical results could be obtained for individual cases if the need arises.

---

[6] A. W. Sunyar, D. Alburger, G. Friedlander, M. Goldhaber, and G. Scharff-Goldhaber, Phys. Rev. 79, 181 (1950).

[7] D. S. Ling, Jr., Ph.D. Thesis, University of Michigan (1948).

BIBLIOGRAPHY

BIBLIOGRAPHY

Axel, P., and S. M. Dancoff. "Classification of Nuclear Isomers," Physical Review 76, 892 (1949).

Barber, W. C. "Short-Lived Isomers of Ta^{181}," Physical Review 80, 332 (1950).

Bay, Z. "Calculation of Decay Times from Coincidence Experiments," Physical Review 77, 419 (1950).

Bell, P. R., S. DeBenedetti, and J. E. Francis, Jr. "A Fast Coincidence Circuit with Pulse Height Selection," Physical Review 72, 160 (1947).

Bell, R. E., and H. E. Petch. "Upper Limit for the Lifetime of the 411-Kev Excited State of Hg^{198}," Physical Review 76, 1409 (1949).

Bell, R. E., and R. L. Graham. "Measurement of a Millimicrosecond Half-Life in Yb^{170}," Physical Review 78, 490 (1950).

Bethe, H. A. "Nuclear Physics. B. Nuclear Dynamics, Theoretical," Review of Modern Physics 9, 226 (1937).

Binder, D. "Analysis of Delayed Coincidence Counting Experiments," Physical Review 76, 856 (1949).

Boehm, F., O. Huber, P. Marmier, P. Preiswerk, and R. Steffen. "Die Knoversion der Gammastrahlen des In^{111}," Helvetica Physica Acta 22, 69 (1949).

Boehm, F., and M. Walter. "Richtungsverteilung der $\gamma\gamma$ - Koinzidenzen beim In^{111}," Helvetica Physica Acta 22, 378 (1949).

Bothe, W., and W. Gentner. Naturwiss 25, 284 (1937).

Bowe, J. C., M. Goldhaber, R. D. Hill, W. E. Meyerhof, and O. Sala. "Short-Lived Metastable State in an Even-Even Nucleus: Ge^{72}," Physical Review 73, 1219 (1948).

Brady, E. L., and M. Deutsch. "Angular Correlation of Successive Gamma-Rays," Physical Review 78, 558 (1950).

Burson, S. B., and K. W. Blair. "A Proposed Decay Scheme for Hf^{181}," Physical Review 78, 89 (1950).

Cork, J. M., A. E. Stoddard, W. C. Rutledge, C. E. Branyan, and J. Le Blanc. "Radioactivity of Hafnium," Physical Review 78, 299 (1950).

Cork, J. M., H. B. Keller, W. C. Rutledge, and A. E. Stoddard. "Reinterpretation of the Electron Spectra of Radioactive Ytterbium and Tantalum," Physical Review 78, 95 (1950).

Chu, K. Y., and M. L. Wiedenbeck. "Radiations from Hf^{181}," Physical Review 75, 226 (1949).

DeBenedetti, S., and F. K. McGowan. "A Metastable State of 22 Microseconds in Ta^{181}," Physical Review 70, 569 (1946).

DeBenedetti, S., and F. K. McGowan. "A Metastable State of Half-Life about 10^{-6} Second in Re^{187}," Physical Review 71, 380 (1947).

DeBenedetti, S., and F. K. McGowan. "Short-Lived Isomers of Nuclei," Physical Review 74, 728 (1948).

DeBenedetti, S., F. K. McGowan, and J. E. Francis, Jr. "Self-Delayed Coincidences with Scintillation Counters," Physical Review 73, 1404 (1948).

Deutsch, Martin, and Arne Hedgran. "Radioactivity of Hf^{181}," Physical Review 79, 400 (1950).

Deutsch, Martin, and D. T. Stevenson. "Nuclear Lifetime for a Quadrupole Transition in Cd^{111}," Physical Review 76, 184 (1949).

Deutsch, Martin, and W. E. Wright. "Lifetimes of Excited States of Au^{197}, Fe^{57}, Cd^{111}, Hg^{198}, and Tl^{203}, "Physical Review 77, 139 (1950).

Feenberg, E., and K. C. Hammack. "Nuclear Shell Structure," Physical Review 75, 1877 (1949).

Fierz, M., "Zur Theorie der Kapillarschwingungen eines Flüssigkeitstropfens," Helvetica Physica Acta 16, 365 (1943).

Frauenfelder, H., O. Huber, A. De-Shalit, and W. Zunti. "Decay of Hg^{197}," Physical Review 79, 1029 (1950).

Hamilton, D. R. "On Directional Correlation of Successive Quanta," Physical Review 58, 122 (1940).

Haynes, S. K. "Beta- and Gamma-Spectra of Gallium Irradiated by Slow Neutrons," Physical Review 74, 423 (1948).

Hebb, M. H., and E. Nelson. "Internal Conversion of Gamma Radiation in the L Shell," Physical Review 58, 486 (1940).

Helmholz, A. C., R. W. Hayward, and C. L. McGinnis. "Radio Activities of Ag^{111}, Cd^{111}, and In^{111}," Physical Review 75, 1469A (1949).

Heitler, W. "On the Radiation Emitted by a Multipole and its Angular Momentum," Proceedings of the Cambridge Philosophical Society 32, 112 (1936).

Huber, O., R. Steffen, and F. Humbel. "Anregungs-Niveaux des Au^{197}--Kerns," Helvetica Physica Acta 21, 192 (1948).

Jastram, P. S., W. Konneker, and M. R. Cleland. "The Doubtful Decay of Au^{198}," Physical Review 79, 243A (1950).

Jensen, E. N., L. J. Laslett, R. T. Nichols, and W. W. Pratt. "Disintegration of Yb^{169}," Physical Review 79, 243A (1950).

Jordan, W. H., and P. R. Bell. "A General Purpose Linear Amplifier," Review of Scientific Instruments 18, 703 (1947).

Jordan, W. H. and P. R. Bell. "Scintillation Counters," Nucleonics 5, 30 (1949).

Kelley, G. G. "High Speed Oscilloscope," Physics Division Quarterly Progress Report, ORNL 366, 29 (June, 1949).

Kelley, G. G. "A High Speed Synchroscope," Review of Scientific Instruments 21, 71 (1950).

Konopinski, Emil J. "Beta-Decay," Review of Modern Physics 15, 209 (1943).

Langer, Lawrence M. "Beta-Spectra of Cl^{38}," Physical Review 77, 50 (1950).

Levy, P. W. "Radiations from 24 hr. W^{187}," ORNL 312 (March, 1949).

Ling, D. S., Jr. "The Theory of Angular Correlations Involving Internal Conversion Electrons," Ph.D. Thesis, University of Michigan, 1948.

Lowen, I. S. "Lifetimes of Nuclear Levels with Respect to Electric Multipole Radiation," Physical Review 59, 835 (1941).

MacIntyre, W. J. "Measurement of a 2.3×10^{-8} Second Metastable State in Hg^{198}," Physical Review 76, 312 (1949).

Madansky, Leon, and M. L. Wiedenbeck. "Measurement of the Decay Time of Short-Lived Metastable States," Physical Review 72, 185 (1947).

Mayer, Maria G. "On Closed Shells in Nuclei II," Physical Review 75, 1969 (1949).

McGowan, F. K. "Metastable State of Half-Life 13×10^{-8} Sec. in $_{71}Lu^{177}$," Physical Review 76, 1730 (1949).

McGowan, F. K. "7×10^{-9} Sec. Isomeric State in $_{79}Au^{197}$," Physical Review 77, 138 (1950).

McGowan, F. K. "5.7×10^{-9} Sec. Isomeric State in $_{77}Ir^{191}$," Physical Review 79, 404 (1950).

McGowan, F. K. "A 3×10^{-9} Sec. Isomeric State in $_{63}Eu^{153}$," Physical Review 80, 482 (1950).

McGowan, F. K. "A 1.7 x 10^{-9} Sec. Isomeric State in $_{68}Er^{166}$," Physical Review 80, (December 1, 1950).

McGowan, F. K., and S. DeBenedetti. "Short-Lived Isomers in Tm^{169} and Tm^{171}," Physical Review 73, 1269 (1948).

Mitchell, Allan C. G., Daniel J. Zaffarano, and Bernard D. Kern. "Beta- and Gamma-Rays of Ga^{72}," Physical Review 73, 1424 (1948).

Morton, G. A., and J. A. Mitchell. "Performance of 931-A Type Multiplier as a Scintillation Counter," Nucleonics 4, 16 (1949).

Newton, T. D. "Decay Constants from Coincidence Experiments," Physical Review 78, 490 (1950).

Nordheim, L. W. "On Spins, Moments, and Shells in Nuclei," Physical Review 75, 1894 (1949).

Nordheim, L. W. "β-Decay and the Nuclear Shell Model," Physical Review 78, 294 (1950).

Peacock, C. L., and R. G. Wilkinson. "Disintegration of Scandium^{46}, Gold^{198}, and Tungsten^{185,187}," Physical Review 74, 297 (1948).

Rose, M. E. "Nuclear Isomerism and Internal Conversion," Theoretical Nuclear Physics Lecture Notes, 148 (1947).

Rose, M. E., G. H. Goertzel, B. I. Spinrad, J. Harr, and P. Strong. "K-Shell Internal Conversion Coefficients," Physical Review 76, 1883 (1949). Tables of K-Shell Internal Conversion Coefficients privately circulated.

Saxon, D. "The Beta-Spectra of W^{185} and Os^{193}," Physical Review 74, 1264A (1948).

Seaborg, G. T., and I. Perlman. "Table of Isotopes," Review of Modern Physics 20, 585, 630 (1948).

Segre, Emilio, and A. C. Helmholz. "Nuclear Isomerism," Review of Modern Physics 21, 271 (1949).

Stanley, J. P., H. Gellman, and B. A. Griffith. "Internal Conversion in the L_I-Shell," Physical Review 80, 866 (1950).

Stratton, Julius Adams. Electromagnetic Theory (New York and London: McGraw-Hill Book Company, 1941), p. 424.

Sunyar, A. W., D. Alburger, G. Friedlander, M. Goldhaber, and G. Scharff-Goldhaber. "Isomerism in Pb^{204} and Memory in Angular Correlation," Physical Review 79, 181 (1950).

Tralli, N., and I. S. Lowen. "Magnetic Multipole Internal Conversion," Physical Review 76, 1541 (1949).

Van Name, F. W. "Measurement of the Radioactive Decay Constant of ThC' Using a Coincidence Method," Physical Review 75, 100 (1949).

von Weizsacker, C. F. Naturwiss 24, 813 (1936).